
**The auditory cortex of the bat *Phyllostomus
discolor*: Functional organization and
processing of complex stimuli.**

**Dissertation
der Fakultät für Biologie
der Ludwig-Maximilians Universität
München**

**Vorgelegt von
Susanne Hoffmann**

am 02. März 2009



1. Gutachter: Prof. Dr. Gerd Schuller
 2. Gutachter: PD Dr. Lutz Wiegrebe
- Tag der mündlichen Prüfung: 23.06.2009

Contents

ZUSAMMENFASSUNG	V
------------------------	----------

SUMMARY	VII
----------------	------------

GENERAL INTRODUCTION	1
-----------------------------	----------

<u>1. PSYCHOPHYSICAL AND NEUROPHYSIOLOGICAL HEARING THRESHOLDS IN THE BAT <i>PHYLLOSTOMUS DISCOLOR</i></u>	5
---	----------

1.1 ABSTRACT	5
1.2 INTRODUCTION	6
1.3 METHODS	7
1.3.1 PSYCHOPHYSICS	7
1.3.1.1 Experimental animals	7
1.3.1.2 Experimental setup	7
1.3.1.3 Acoustic stimuli	8
1.3.1.4 Training procedure	8
1.3.2 NEUROPHYSIOLOGY	9
1.3.2.1 Surgery	9
1.3.2.2 Recording procedure	10
1.3.2.3 Data analysis	10
1.4 RESULTS	11
1.4.1 PSYCHOPHYSICS	11
1.4.2 NEUROPHYSIOLOGY	12
1.5 DISCUSSION	14
1.5.1 COMPARISON WITH NEUROPHYSIOLOGICAL DATA OF OTHER PHYLLOSTOMID BATS	16
1.5.2 COMPARISON WITH BEHAVIORAL AUDIOGRAMS OF OTHER PHYLLOSTOMID BATS	17
1.6 ACKNOWLEDGEMENTS	19

<u>2. THE AUDITORY CORTEX OF THE BAT <i>PHYLLOSTOMUS DISCOLOR</i>: LOCALIZATION AND ORGANIZATION OF BASIC RESPONSE PROPERTIES</u>	21
--	-----------

2.1 ABSTRACT	21
2.1.1 BACKGROUND	21
2.1.2 RESULTS	21

2.1.3 CONCLUSIONS	22
2.2 BACKGROUND	22
2.3 RESULTS	23
2.3.1 AUDITORY RESPONSES IN THE CORTEX OF <i>PHYLLOSTOMUS DISCOLOR</i>	23
2.3.2 NEUROANATOMY	25
2.3.3 BASIC NEURONAL RESPONSE PROPERTIES	29
2.3.4 REPRESENTATION OF NEURONAL RESPONSE PROPERTIES IN CORTICAL FIELDS	32
2.4 DISCUSSION	36
2.4.1 COMPARISON WITH THE AUDITORY CORTEX OF OTHER BATS	36
2.4.2 INFLUENCE OF ANESTHESIA AND MULTI UNIT RECORDINGS ON RESPONSE PATTERNS	37
2.4.3 PARCELLATION OF THE AUDITORY CORTEX IN <i>P. DISCOLOR</i>	38
2.5 CONCLUSIONS	40
2.6 METHODS	41
2.6.1 EXPERIMENTAL ANIMALS	41
2.6.2 ANESTHESIA AND SURGICAL PREPARATION	41
2.6.3 STEREOTAXIC PROCEDURE AND VERIFICATION OF RECORDING SITES AND CORRELATION WITH NEUROARCHITECTURAL FEATURES	41
2.6.4 ACOUSTIC STIMULI AND RECORDING OF NEURONAL RESPONSES	42
2.6.5 DATA ANALYSIS	44
2.7 ACKNOWLEDGEMENTS	45
<u>3. A NEURAL CORRELATE OF STOCHASTIC ECHO IMAGING</u>	47
3.1 ABSTRACT	47
3.2 INTRODUCTION	47
3.3 MATERIALS AND METHODS	48
3.3.1 ANIMALS	48
3.3.2 PSYCHOPHYSICS	49
3.3.3 NEUROPHYSIOLOGY	50
3.4 RESULTS	51
3.4.1 PSYCHOPHYSICS	51
3.4.2 NEUROPHYSIOLOGY	52
3.4.3 COMPARISON OF PSYCHOPHYSICS AND NEUROPHYSIOLOGY	56
3.5 DISCUSSION	57
3.6 ACKNOWLEDGEMENTS	61
<u>4. AN AREA SENSITIVE TO APPARENT ACOUSTIC MOTION IN THE AUDITORY CORTEX OF THE BAT <i>PHYLLOSTOMUS DISCOLOR</i></u>	63
4.1 ABSTRACT	63
4.2 INTRODUCTION	64
4.3 METHODS	65
4.3.1 EXPERIMENTAL ANIMALS AND SURGICAL PREPARATION	65
4.3.2 STEREOTAXIC PROCEDURE AND VERIFICATION OF RECORDING SITES	65

4.3.3 ACOUSTIC STIMULATION USED FOR DETERMINATION OF BASIC NEURONAL RESPONSE PROPERTIES	66
4.3.4 TWO-TONE STIMULI (APPARENT HORIZONTAL ACOUSTIC MOTION)	66
4.3.5 RECORDING OF NEURAL RESPONSES	69
4.3.6 DATA ANALYSIS	70
4.3.6.1 Basic response properties	70
4.3.6.2 Response properties to dynamic two-tone stimulation	70
4.4 RESULTS	73
4.4.1 MOTION INSENSITIVE UNITS	74
4.4.2 MOTION SENSITIVE UNITS	77
4.4.3 REPRESENTATION OF MOTION SENSITIVITY AT THE CORTICAL SURFACE	82
4.4.4 BASIC RESPONSE PROPERTIES OF MOTION SENSITIVE AND INSENSITIVE UNITS IN THE PDF	84
4.4.5 MOTION SPECIFIC RESPONSE PROPERTIES OF MOTION SENSITIVE AND INSENSITIVE UNITS IN THE PDF	84
4.5 DISCUSSION	86
4.5.1 COMPARISON TO OTHER STUDIES	86
4.5.2 MOTION SENSITIVITY	87
4.5.3 INHIBITION BY DYNAMIC STIMULATION	89
4.6 ACKNOWLEDGEMENTS	90
GENERAL DISCUSSION	91
THE PARCELLATION OF THE PHYLLOSTOMUS AC IN COMPARISON TO OTHER BATS	93
FUNCTIONAL ROLE OF DIFFERENT AUDITORY CORTICAL SUBFIELDS IN BATS	94
OUTLOOK	97
REFERENCES	99
LIST OF ABBREVIATIONS	113
LIST OF FIGURES	115
LEBENS LAUF	117
DANKSAGUNG	119
EHRENWÖRTLICHE ERKLÄRUNG	121

Zusammenfassung

Als auditorischer Kortex wird der Teil des Neokortex bezeichnet, der Neurone enthält, die auf akustische Reize antworten. Er stellt die höchste Ebene der Verarbeitung akustischer Information in der aufsteigenden Hörbahn dar. Die in dieser Arbeit zusammengefassten Studien untersuchten den auditorischen Kortex der Fledermaus *Phyllostomus discolor* mit Hilfe einfacher sowie komplexer akustischer Reize. Innerhalb der Experimente wurden unterschiedliche Methoden verwendet (z.B. Psychophysik und Neuroanatomie). Der Schwerpunkt der Arbeit liegt jedoch auf der elektrophysiologischen Untersuchung des auditorischen Kortex.

Das erste Kapitel beschäftigt sich mit einer Studie, die den Hörbereich von *P. discolor* anhand neuronaler Hörschwellen und Verhaltenshörschwellen untersuchte. Die Ergebnisse dieser Studie zeigen, dass akustische Reize mit einer Frequenz zwischen 4 und 100 kHz von *P. discolor* wahrgenommen werden konnten. Die niedrigsten Hörschwellen wurden im hochfrequenten Bereich über 35 kHz gemessen. Das verdeutlicht die hohe Sensitivität des Hörsystems von *Phyllostomus* gegenüber Frequenzen im Ultraschallbereich, die z.B. in den Echoortungslauten dieser Tiere enthalten sind. Die neuronalen Hörschwellen sowie die Verhaltenshörschwellen von *P. discolor* lagen in einem Bereich, der auch bei anderen Fledermausarten beobachtet wurde.

Das zweite Kapitel beschreibt eine Studie, die durchgeführt wurde, um den auditorischen Kortex von *P. discolor* zu lokalisieren, seine Grenzen zu bestimmen und ihn in einzelne Bereiche zu unterteilen. Neurone, die eine Antwort auf akustische Reizung zeigten wurden lateral im caudalen Teil des Neokortex gefunden. Anhand neuroanatomischer und neurophysiologischer Kriterien konnte dieser Kortexbereich in vier größere Felder unterteilt werden. Die zwei ventral gelegenen Felder zeigten eine tonotope Organisation und scheinen der „Kernregion“ des auditorischen Kortex anzugehören. Das posteriore ventrale Feld zeigte Eigenschaften, die denen des primären auditorischen Kortex anderer Säugetiere ähnlich sind. Das anteriore ventrale Feld hingegen scheint das anteriore auditorische Feld des Säugerkortex darzustellen. Die zwei dorsal gelegenen Felder zeigten keine klare tonotope Organisation sondern beinhalteten Neurone, die vorrangig auf hohe Frequenzen über 45 kHz antworteten. Da die dominanten Harmonischen des Echoortungslautes von *P. discolor* diesen Frequenzbereich umfassen, scheinen das anteriore und das posteriore dorsale Feld besonders in Verarbeitungsprozesse der durch Echoortung gewonnenen Information involviert zu sein.

Das dritte und das vierte Kapitel beschreiben Experimente, die die kortikale Verarbeitung der echoortungs-relevanten akustischen Parameter Echorauhigkeit und akustische Bewegung untersuchten. Die Echorauhigkeit ist eine Meßgröße, die die zeitlichen Fluktuationen der

Einhüllenden eines Signals beschreibt und die besonders wichtig für die Diskrimination komplexer Strukturen wie z.B. Büsche oder Bäume ist. Bäume mit großen Blättern produzieren rauere Echos als Bäume mit kleinen Blättern oder Nadeln. Wie in Kapitel drei beschrieben, haben die neurophysiologischen Experimente zu dieser Studie eine Neuronenpopulation im anterioren Teil des auditorischen Kortex aufgedeckt, die Echorauhigkeit in ihrer Antwortrate kodierten. Die Antwort dieser Neurone konnte mit dem psychophysikalischen Diskriminationsvermögen von *P. discolor* in Beziehung gesetzt werden.

In dem in Kapitel vier beschriebenen Experiment, wurden Reintonpaare verwendet, um Echos von einem sich bewegenden Objekt oder von einem stationären Objekt welches von einer Fledermaus angefliegen wird zu simulieren. Im posterioren dorsalen Feld des auditorischen Kortex von *P. discolor* wurde eine bewegungssensitive Neuronenpopulation gefunden, die stark faszilitierend auf dynamische Stimulation im Vergleich zu statischer Stimulation antwortete. Ein Teil dieser bewegungssensitiven Neurone konnte das dynamische azimuthale rezeptive Feld bei kleinen zeitlichen Abständen zwischen den zwei Reintönen des dynamischen Reizes auf kleine Areale im frontalen Bereich fokussieren. Die Antwort dieser Neurone scheint für das aktive Nachverfolgen eines Zielobjektes während einer Annäherung durch die Fledermaus wichtig zu sein.

Die in dieser Arbeit präsentierten Ergebnisse zeigen, dass der auditorische Kortex von *P. discolor* in mindestens vier funktionell unterschiedliche Felder unterteilt werden kann. Diese Unterteilung deutet auf die gesonderte Verarbeitung ökologisch- und verhaltensrelevanter Echoparameter hin.

Summary

The auditory cortex is the acoustically responsive part of the neocortex and represents the highest level of processing of the ascending auditory pathway. The experiments described in this thesis were designed to study the auditory cortex of the microchiropteran bat *Phyllostomus discolor* with both, simple and complex acoustic stimuli. During the experiments, different methods were used (e.g. psychophysics and neuroanatomy), but the main focus was laid on the electrophysiological examination of the auditory cortex.

The first chapter covers a study that investigated the hearing range of *P. discolor* by measuring neural and behavioral audiograms in this species. This study shows that acoustic stimuli at frequencies between 4 and 100 kHz could elicit either a neuronal or behavioral response in *P. discolor*. Lowest thresholds were found in the high frequency range above 35 kHz indicating the high sensitivity of the auditory system of *P. discolor* to ultrasonic sounds as for example contained in echolocation calls. However, electrophysiologically and psychophysically determined hearing thresholds lay in the range of thresholds known for other bat species.

The second chapter describes a study that determined the location, extend, and subdivision of the auditory cortex of *P. discolor*. The area that contained acoustically responsive neurons was laterally positioned at the caudal part of the neocortex. Within this area four major cortical subfields could be distinguished based on neuroanatomical and neurophysiological criteria. The two ventral fields were tonotopically organized and were assumed to belong to the “core” region of the auditory cortex. The posterior ventral field showed properties similar to that found in the primary auditory cortex of other mammals, whereas, the anterior ventral field seems to resemble the anterior auditory field of the mammalian auditory cortex. The two dorsally located subfields did not show a clear tonotopy, but contained neurons, which were mainly responsive to high frequencies above 45 kHz. As the dominant harmonics of the echolocation call of *P. discolor* cover this high frequency range, the anterior and posterior dorsal fields seem to be strongly involved in processing of information obtained from echolocation.

The third and fourth chapter describes experiments that investigated the cortical processing of sound parameters relevant for echolocation: echo roughness and acoustic motion. Echo roughness as a measure for the temporal envelope fluctuation of a signal is especially important for the discrimination of complex targets like trees and bushes. Broad leaved trees produce echoes with a higher degree of roughness compared to small leafed trees, e.g. conifers. The neurophysiological experiment described in chapter three revealed a population of cortical neurons in the anterior part of the auditory cortex, which encoded echo roughness

in their response rate. The response of these neurons could be correlated to the behaviorally measured discrimination performance of *P. discolor*.

In the experiment described in chapter four, pairs of pure tones were used to simulate either echoes from an object moving in azimuth or echoes from a stationary object encountered by a bat during approach. In the posterior dorsal field of the auditory cortex of *P. discolor* a population of motion sensitive neurons was found, which showed strong response facilitation to dynamic stimuli in contrast to static stimulation. In a subset of motion sensitive neurons the dynamic azimuthal response range was focused to small areas in the frontal field at short temporal intervals between the two components of the dynamic stimuli. The response of these neurons might be important for the tracking of targets during an approach by the bat.

The results presented in this thesis reveal that the auditory cortex of *P. discolor* is functionally parcellated into at least four different fields. This parcellation seems to reflect the segregated processing of behaviorally and ecologically important echo parameters within specialized areas of the auditory cortex.

General introduction

The general objective of this thesis was to functionally characterize different subfields of the auditory cortex (AC) in the bat *Phyllostomus discolor*. Microchiropteran bats use echolocation to navigate and forage in complete darkness. They emit ultrasonic calls and listen to the modified echoes reflected from nearby obstacles or prey. This process of “active hearing” is special to microbats and cetaceans, whereas most other mammals rely mainly on “passive hearing”.

The temporal and spectral structure of the echolocation calls used by different bat species is adapted to the specific habitat and foraging behavior of the species (Neuweiler 1990). Long-duration constant-frequency (CF) echolocation calls are used by bats that mainly hunt flying insects in dense foliage (CF/FM-bats, e.g. *Rhinolophus rouxi* and *Pteronotus parnellii*), exploiting the small amplitude- and frequency-modulations imprinted by the wing beats of the insect on the CF component of their calls (Schuller 1984). FM-bats that preferentially hunt insects in open space like *Myotis lucifugus* and *Eptesicus fuscus* use short-duration frequency-modulated (FM) calls yielding good ranging accuracy (Simmons et al. 1979). *P. discolor* belongs to the microchiropteran family *Phyllostomidae*. It uses short FM echolocation signals for orientation and shows a mainly frugivorous foraging behavior. Although it once in a while enriches its diet with small insects living at the collected fruits, it never actively hunts flying insects.

The basic structure and function of the microchiropteran auditory system follows in general the mammalian plan. The ability of many bat species to process spectral or temporal information with extreme accuracy shows up in neural overrepresentation of specific parameters. Also brain structures mediating auditory control of motor, e.g. vocal activity are more conspicuous than in non-echolocating mammals (for review: Covey 2005). Neuroanatomical specializations associated with echolocation may originate in the cochlea and lower brainstem and may be traceable throughout the ascending auditory pathway (Vater et al. 1985; Zook and Leake 1989; O'Neill 1995; Covey 2005). Functional specializations related to echolocation, as e.g. neurons preferentially responding to combinations of echolocation call and echo, can be observed from the auditory midbrain to the AC of bats (Suga and Horikawa 1986; Schuller et al. 1991; Tanaka et al. 1992; Wenstrup and Grose 1995; Wenstrup et al. 1999). The functional specializations of the AC are highly species-specific, and show considerable differences among bat species.

The AC is the acoustically responsive part of the neocortex and represents the highest level of processing of the ascending auditory pathway. Rather complex auditory information processing is supposed to take place at this level (Nelken 2008). In CF/FM-bats such as

P. parnellii and *R. rouxi*, the AC has been intensely studied (O'Neill and Suga 1982; Suga et al. 1987; Radtke-Schuller and Schuller 1995; Radtke-Schuller 2001). Although, FM-bats constitute the majority of echolocating bat species, data on anatomical and neurophysiological properties and on the function of subfields of the AC in FM-bats are comparably rare (Wong and Shannon 1988; Dear et al. 1993; Esser and Eiermann 1999). *P. discolor* was chosen as experimental animal in order to study the functional organization of different auditory cortical fields in a frugivorous FM-bat.

The range of frequencies and intensities an animal can hear is described by the audiogram and the frequency/intensity plane above. Audiograms can be evaluated behaviorally or as neural audiograms at different levels of the auditory pathway. In the bat *P. discolor*, neural audiograms were measured quantitatively in the inferior colliculus (IC) and the AC, and additionally, a behavioral audiogram was established during the first series of experiments.

It is well known, that the AC in different animals consists of a varying number of subfields in mostly species-specific arrangement. These subfields are characterized by cytoarchitectural features of the neurons, the afferent connections from thalamic structures and the efferent target structures, as well as by the physiological response properties of their neurons. In general, auditory cortical subfields are assigned to either the “core” or “belt” region (nomenclature adopted from Pandya and Sanides 1973). Subfields of the core region such as the primary auditory field (AI) and the anterior auditory field (AAF) represent the region where main afferent auditory input reaches the AC. Thus, AI and AAF receive strong connections from the ventral division of the medial geniculate body (MGB) of the thalamus (Andersen et al. 1980; Radtke-Schuller 2004), which in turn gets afferent input from the central nucleus of the IC. In addition, both core areas show tonotopic organization of opposed gradients that reflect the cochlear frequency representation. In contrast, subfields of the belt region are usually less tonotopically organized, and they receive their inputs mainly from the dorsal nucleus of the medial geniculate body (Andersen et al. 1980; Radtke-Schuller et al. 2004). In the second series of experiments, the AC of *Phyllostomus* was subdivided into different subfields using the measure of general neurophysiological characteristics of the neurons, as well as differences in neuroanatomical features. This basic delimitation of fields served as foundation for the third and fourth study where functional properties in the subfields could be specified in detail, and subfields could be investigated regarding their contribution to processing of complex temporal and spatial tasks.

The neural encoding of echo roughness in the AC of *Phyllostomus* was subject of the third study. Roughness of an echo signifies the temporal fluctuations of the envelope of sound pressure in the echo and contains information representing an “acoustic image” of the echo source. The acoustic image of an object can be represented by the sum of the reflections upon ensonification with an acoustic impulse, and thus be described by its impulse response (IR). The echolocating bat emits an ultrasonic signal with a defined spectro-temporal composition.

When the echolocation call impinges on an object it is convolved with the IR of the object and reflected back to the bat. If the bat's auditory system can extract and analyze the imprinted IR from the modified sonar emission the bat has access to an acoustic image of the ensonified object. In a behavioral study it has been shown that *P. discolor* is able to discriminate and classify echoes generated with IRs of different roughness (Grunwald et al. 2004). The identification of natural objects (e.g. landmarks for orientation) by classification of their echoes is supposed to facilitate navigation within a complex environment. In addition, as a fruit tree with relatively few but large leaves produces echoes with higher roughness, than a conifer with numerous small leaves, recognition of foliage types based on roughness may facilitate the bat's decision whether to approach a certain tree to collect fruits or not. Up to now, neural processing of echo roughness has not been studied.

This reasoning motivated the third series of experiments in which a neural correlate of statistical echo analysis, i.e. neural coding of echo roughness, was found in the AC of *P. discolor*. Additionally, the behavioral threshold for auditory-object discrimination based on echo roughness was determined.

As stationary events are comparably rare during a bat's life, whereas detection and locating of moving targets is most important, the responses of auditory cortical neurons to apparent acoustic motion stimuli were examined in the fourth series of investigations. Unlike in the visual system where motion is represented already at the sensory level of the retina, the perception of acoustic motion is more complex. The position of an echo source in the bat's body centered space is computed from interaural differences in intensity and arrival time, and also the spectrum differences at both ears give cues for direction. Due to the pulse like emission pattern of the echolocation calls, the bat obtains a stroboscopic view of its environment. The temporal resolution of the perceived dynamic scene depends on the rate of sonar emissions.

A change in spatial position of a target relative to the bat whether induced by motion of the target or by movements of the bat itself, causes a change in interaural parameters between successive echoes reflected from the moving target. These differences of interaural parameters between successive echoes should provide the bat with the necessary information to evaluate the momentary position of a target and to eventually track it.

Several behavioral studies show the ability of bats to flexible adapt call emission to the dynamic conditions of prey catching on the wings, which requires an accurate dynamic interplay between auditory processing of spatial cues and motor control for vocalization and flight. For example, *E. fuscus* remarkably increases the rate of emitted echolocation calls (4 to 200 pulses per second) when approaching a target in order to increase information flux (Griffin et al. 1960). Furthermore, it actively centers its sonar beam axis onto a selected target by turning the head or body when tracking a target during approach (Ghose and Moss 2003). These studies indicate that the auditory system in bats can process spatial information on target position fast enough to provide the vocal-motor system with the appropriate control signals.

The present research (fourth study series) shows that a subset of neurons in the AC of the frugivorous FM-bat *P. discolor* is indeed capable to encode fast azimuthal movements. Cortical neurons that exhibit enhanced activity when stimulated with sounds moving in azimuth are not uniformly scattered over cortical subfields but cluster to a circumscribed posterior location in a dorsal subfield.

Dorsally positioned non-primary auditory cortical subfields seem to have a strong involvement in processing of echo-information, a view, supported by two major points: First, neurons responding best to frequencies within the range of the dominant harmonics of the echolocation call are overrepresented, and second, neurons showing behaviorally relevant functional properties like sensitivity to echo roughness and enhanced responses to specific acoustic motion stimuli are aggregated in these subfields.

The evaluation of the specificity for echolocation of certain subfields of the AC in *Phyllostomus* may serve as a first step for future investigations regarding e.g. auditory feedback for vocal-motor control or object discrimination by echolocation.

1. Psychophysical and neurophysiological hearing thresholds in the bat *Phyllostomus discolor*

This study was published in 2008 by Susanne Hoffmann, Leonie Baier*, Frank Borina*, Gerd Schuller, Lutz Wiegrebe and Uwe Firzloff in the Journal of Comparative Physiology A: Neuroethology, Sensory, Neural, and Behavioral Physiology (Vol. 194, pp. 39-47, * = contributed equally).*

The psychophysical experiment was designed and implemented by Lutz Wiegrebe. The training of the animals, the acquisition and analysis of psychophysical data was done by Leonie Baier. The neurophysiological experiment for studying the IC was designed and implemented by Frank Borina and Lutz Wiegrebe. Frank Borina performed the neurophysiological recordings in the IC and analyzed the data. The neurophysiological experiment for studying the AC was designed by Uwe Firzloff, and implemented by Uwe Firzloff and myself. The acquisition of neurophysiological data in the AC was done by Uwe Firzloff and me. I did the analysis of the cortex-data. Gerd Schuller provided the equipment for both neurophysiological setups. The paper was written and proofread, respectively, by Uwe Firzloff and myself, and Lutz Wiegrebe and Gerd Schuller.

1.1 Abstract

Absolute hearing thresholds in the spear-nosed bat *Phyllostomus discolor* have been determined both with psychophysical and neurophysiological methods. Neurophysiological data has been obtained from two different structures of the ascending auditory pathway, the inferior colliculus and the auditory cortex. Minimum auditory thresholds of neurons are very similar in both structures. Lowest absolute thresholds of 0 dB SPL are reached at frequencies from about 35 to 55 kHz in both cases. Overall behavioral sensitivity is roughly 20 dB better than neural sensitivity. The behavioral audiogram shows a first threshold dip around 23 kHz but threshold was lowest at 80 kHz (-10 dB SPL). This high sensitivity at 80 kHz is not reflected in the neural data. The data suggests that *P. discolor* has considerably better absolute auditory thresholds than estimated previously. The psychophysical and neurophysiological data is compared to other phyllostomid bats and differences are discussed.

1.2 Introduction

Up to now, behavioral auditory thresholds have been measured in several bat species belonging to the neotropical family Phyllostomidae: *P. discolor* (Esser and Daucher 1996), *Phyllostomus hastatus* (Koay et al. 2002; Bohn et al. 2004), *Carollia perspicillata* (Koay et al. 2003), and *Artibeus jamaicensis* (Heffner et al. 2003). Bats of this family utter broadband, multi-harmonic and downward frequency-modulated (FM) echolocation calls and are therefore described as FM-bats. In general, the audiograms of these bats are broadly V-shaped with a region of maximal sensitivity (ca. 0 dB SPL threshold) in the low frequency range. The slope of threshold curves is much steeper at the high frequency side than that at the low frequency side. In contrast to the audiogram of the constant frequency (CF) bat *Rhinolophus ferrumequinum* (Long and Schnitzler 1975), which shows a narrowly tuned additional threshold minimum in the range of the dominant harmonic of the echolocation call, the audiograms of FM-bats show no obvious specializations for echolocation behavior.

Phyllostomus discolor is a medium sized species of the subfamily *Phyllostominae*. The omnivorous bat is widely distributed in Central and South America. In its natural environment, it has to navigate through highly structured surroundings using echolocation for orientation. It emits brief (<3 ms), broadband, multiharmonic and downward frequency-modulated sweeps. The fundamental frequency of the echolocation calls is modulated around 20 kHz, but most energy is contained in the frequency range between 40 and 90 kHz. Maximum sound pressure levels up to 86 dB SPL were measured in a stationary bat at a distance of 10 cm in front of the mouth (Rother and Schmidt 1982). Due to these low intensity echolocation calls, *P. discolor* as well as other phyllostomid bats is described as “whispering bat”. In contrast, echolocation calls of insectivorous bats are generally louder, e.g. *Myotis lucifugus* (Grinnell and Griffin 1958).

Furthermore, *P. discolor* uses a rich repertoire of social calls for species-specific communication. These directive calls (e.g. mother-infant communication) cover a frequency range from 11 to 54 kHz (Esser and Schmidt 1990). In contrast to high-frequency echolocation calls, these low frequency social calls reach a higher maximum sound pressure level (up to 110 dB SPL) and are longer in duration (about 50 ms). Based on their physical structure, social calls seem to be adequate for long distance communication whereas low intensity echolocation calls appear to be used for near distance exploration of the environment (Esser and Daucher 1996).

The behavioral audiogram of *P. discolor* as determined by Esser and Daucher (1996) is roughly W-shaped and depicts two regions of maximal sensitivity divided by a high threshold region at 55 kHz. Threshold minima of about 20 dB SPL are reached at low frequencies between 15 and 35 kHz and at high frequencies around 85 kHz. Thus, compared to behavioral audiograms of other FM-bats, some differences are obvious: data by Esser and Daucher (1996) suggests that overall auditory thresholds of *P. discolor* are relatively high. Moreover, a second region of maximal sensitivity at high frequencies, even more sensitive than that around 20 kHz, has not been found in other phyllostomid bats.

P. discolor has often been used as an animal model for behavioral and physiological research in the mammalian auditory system (Esser and Schmidt 1990; Esser and Kiefer 1996; Esser and Lud 1997; Grunwald et al. 2004; Wittekindt et al. 2005; Firzlaff et al. 2006; Schuchmann et al. 2006; Firzlaff et al. 2007). In order to correctly design and carry out studies on the auditory system of *P. discolor*, basic information about its hearing ability is necessary. Therefore, we re-determined the behavioral hearing thresholds of this species. This data is compared to neurophysiologically measured best frequency (BF) thresholds of single neurons and small neuronal clusters in the inferior colliculus (IC) and the auditory cortex (AC) of *P. discolor*.

1.3 Methods

1.3.1 Psychophysics

1.3.1.1 Experimental animals

Four adult male *P. discolor* were trained to perform the behavioral experiment. The bats originated from a breeding colony in the Department II of the Ludwig-Maximilians University in Munich. Experimental training sessions were performed at five days a week. During these days, the bats received food (a mixture of banana pulp, infant milk powder and honey) only as a reward for successful training inside the setup. On the two resting days of the week the bats were fed with fruits as well as meal worms (larvae of *Tenebrio molitor*). Thus the animals' body weight could be kept between 30 and 40 grams which roughly corresponds to the naturally occurring body weight of 29.5 to 31.5 g (Goodwin and Greenhall 1961). Animals had free access to water at all times.

1.3.1.2 Experimental setup

The bats were trained in a three-alternative forced-choice (3AFC) setup (see Fig. 1.1 for a schematic view). Its design was very similar to a 2AFC paradigm which has been used before in psychophysical experiments with *P. discolor* (Grunwald et al. 2004; Firzlaff et al. 2006; Schuchmann et al. 2006). The experimental setup was located inside a sound-proof and echo-reduced chamber which was illuminated by a red light bulb. The walls and ceiling of the experimental maze consisted of wire mesh and the floor was covered with cloth. Three channels branched off three sides of a pentagonal chamber with an angle of 72° between the midline of the channels. Each channel housed a broad-band, ultrasonic loudspeaker (EAS10 TH800D, Technics, Secaucus, USA) and a computer-controlled feeder at its end. The starting position of the animal was located at the centre of the pentagonal chamber. The minimum distance between the starting position and the feeder was 30 cm. The feeder started pumping banana pulp out of a syringe when the bat interrupted a light barrier in front of the feeder. The maze could be watched from above via an infrared camera.

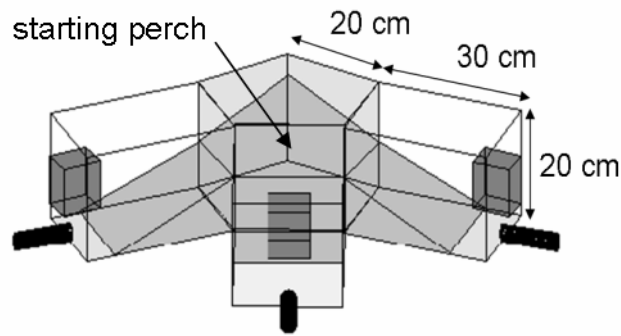


Fig. 1.1 Schematic drawing of the 3AFC setup used for the psychophysical experiments. The dark grey boxes represent the loudspeakers. The black tubes represent the feeders. The angle between the midline of two channels was 72° .

1.3.1.3 Acoustic stimuli

The stimuli were band-pass filtered noise with a duration of 500 ms (including 10 ms raised-cosine rise/fall time) The -3 dB bandwidth was $\pm 10\%$ of the centre frequency; the slope of the filters was 24 dB per octave. Stimuli were presented at a period of 1 s. Thresholds were obtained for eight centre frequencies equally spaced along a logarithmic frequency axis between 4.5 and 80 kHz (4.5, 6.8, 10.3, 15.5, 23, 35, 53, and 80 kHz). Thus, the highest presented frequency was about 88 kHz. Unfortunately, we could not play back band-pass noise with the next higher centre frequency, 120 kHz. The bandwidth of this stimulus would have reached up to 132 kHz which is well beyond the Nyquist frequency of our D/A converter (see below). For all centre frequencies, the sound pressure level at the starting position was calibrated for the three loudspeakers separately.

All stimuli were computer generated and converted by a real-time processor (RP2.1, Tucker Davis Technologies, Gainesville, USA). The sampling rate was set to the maximum for this device, 196 kHz. The stimuli were attenuated using a programmable attenuator (PA5, Tucker Davis Technologies, Gainesville, USA), amplified by a power amplifier (iP900, LAB. Gruppen, Kungsbacka, Sweden) and a high-power passive end attenuation of 40 dB. Then, stimuli were switched to one of the three speakers with a custom-made, computer-controlled passive switch located outside the experimental chamber. Due to the passive end attenuation, background noise was very low.

1.3.1.4 Training procedure

In the 3AFC paradigm, the bats were trained to crawl towards the loudspeaker which emitted a sequence of band-pass noise stimuli at a centre frequency of 23 kHz. The playback stopped

if any light-barrier was interrupted, but at the latest after 20 seconds. Correct decisions were rewarded with food from the computer-controlled feeders. Once a stable level of correct choices (>70 %) had been established by a particular bat, the collecting of threshold data started. To determine the auditory threshold for a particular centre frequency, psychometric functions were obtained for stimulus attenuations varied in steps of 5 dB. Each point of the psychometric functions is based on at least 30 decisions. A sigmoid function was fitted to the psychometric function and the 47 % correct value of this fit was taken as threshold. A numerical simulation of the 3AFC paradigm with 30 trials per point showed that this value corresponds to a $p < 0.05$.

1.3.2 Neurophysiology

Neurophysiological data from the IC and AC was recorded at both sides of the brain in six (three male, three female) and ten (five male, five female) adult *P. discolor*, respectively.

1.3.2.1 Surgery

For anaesthesia, a mixture of Medetomidin (Domitor®, Novartis, Mississauga, Canada), Midazolam (Dormicum®, Hoffmann-La Roche, Mississauga, Canada) and Fentanyl (Fentanyl-Janssen®, Janssen-Cilag, Neuss, Germany) was injected subcutaneously (MMF, 0.4, 4.0 and 0.04 µg/g body weight). During surgery, skin and muscles covering the upper part of the cranium were cut rostro-caudally along the midline and shifted aside laterally. The cranial bone was completely cleaned of remaining tissue and a metal rod (for fixation of the animal within the experimental apparatus) was fixed onto the bat's skull using light-curing dental cement (Charisma®, Heraeus Kulzer, Wehrheim Germany). In order to alleviate postoperative pain, an analgesic drug (2 µl/g body weight Meloxicam, Metacam®, Boehringer-Ingelheim, Ingelheim, Germany) was administered orally after full recovery of the bat.

A stereotaxic procedure was carried out in each bat to allow the pooling and comparison of all electrophysiologically measured data within one and among different experimental animals. A detailed description of this procedure, i.e. the determination of brain orientation and reconstruction of recording sites has been already published elsewhere (Schuller et al. 1986). To be able to lower the recording electrode into the brain regions of interest, small holes of about 500 µm in diameter were drilled into the animal's skull covering the area of interest and the dura was perforated. For verification of recording sites, electrolytic lesions were made into the brain and additionally pharmacological markers were applied. At termination of the experiment, a transcardial perfusion and subsequent histological processing of the brain, allowed the reconstruction of the position of recording sites in standardized brain atlas coordinates (Nixdorf, Fenzl, Schweltnus, unpublished data).

1.3.2.2 Recording procedure

All experiments were conducted in a heated (ca. 36°C), electrically shielded and anechoic chamber. Each recording session lasted typically four hours and was repeated on four days a week for about six weeks. At the beginning of each session, the bat was anaesthetized using MMF (see above). Throughout each experimental session the animal was provided with oxygen.

Acoustic search stimuli were 20 ms pure tones. The stimuli were presented via custom-made ultrasonic earphones (Schuller 1997) with a flat frequency response (± 3 dB between 10 and 100 kHz). Once a single neuron or small neuronal cluster (unit) was detected, its best frequency (BF: frequency at which auditory threshold is lowest), was determined audiovisually. In addition, for most units the frequency response area (FRA) was determined in more detail. Pure tone stimuli (20 ms duration, 2 ms rise/fall time), in various frequency and level combinations were presented either binaurally or only contralaterally if inhibition of the ipsilateral ear was too strong. These stimuli were computer generated (Matlab® 6.1, Mathworks, Natick, USA), D/A converted at a sampling rate of 260 kHz (RX6, Tucker Davis Technologies, Gainesville, USA) and attenuated (PA5, Tucker Davis Technologies, Gainesville, USA).

For stimulation of IC-units, all frequency-intensity combinations were presented pseudo-randomly with five repetitions and a repetition period of 150 ms. The recording window started at stimulus onset and lasted for 100 ms. For stimulation of AC-units, all frequency-intensity combinations were presented pseudo-randomly with ten repetitions and a repetition period of 500 ms. The recording window started 10 to 50 ms before stimulus onset and lasted for 450 ms.

Responses from units in the IC and AC were recorded extracellularly using either borosilicate glass electrodes (#1B100F-3, WPI, Sarasota, USA) filled with 2 M NaCl and 4 % pontamine sky blue (3 to 8 M Ω impedance), carbon fibre microelectrodes (Carbostar-1, Kation Scientific, Minneapolis, USA; 0.4 to 0.8 M Ω impedance) or glass insulated tungsten microelectrodes (Alpha Omega GmbH, Ubstadt-Weiher, Germany, 1 to 2 M Ω impedance). Action potentials were amplified using conventional methods, A/D converted (RX5, Tucker Davis Technologies, Gainesville, USA, sampling rate: 25 kHz), recorded and threshold discriminated using Brainware (Tucker Davis Technologies, Gainesville, USA).

1.3.2.3 Data analysis

Computer programs used for data analysis were written in Matlab® (Matlab® 6.1, Mathworks, Natick, USA). Spike responses were displayed as peristimulus-time histogram (PSTH, 1 ms bin width). For the cortical recordings, an analysis window was set which started when the first bin exceeded the level of spontaneous activity and ended when the response reached spontaneous level again using visual criteria. The level of spontaneous activity was derived from the silent period preceding each stimulus onset. Recordings of IC

units were analyzed for the full length of the recording window as the spontaneous rate was generally low. The FRA of a unit was constructed by summing activity for each frequency-level combination within the given analysis window. Responses to different frequency-level combinations were considered to be significant if the spike rate exceeded 20 % of the maximum response to any frequency-level combination. BF and auditory threshold were directly determined from the FRA of the particular unit.

To calculate the auditory population thresholds for IC and AC, the units' BFs were classified into frequency bands with logarithmically spaced centre frequencies from 10.3 to 98.3 kHz in 0.3 octave steps, corresponding to the bandwidth used in the psychophysical experiments. For each of the 12 frequency bands, the mean threshold of the three most sensitive units was calculated and taken as the neural threshold to construct the neural audiogram.

1.4 Results

1.4.1 Psychophysics

Behavioral data was obtained from four adult male bats. Whereas two bats provided threshold data for seven different centre frequencies, one bat provided data for five centre frequencies and in one bat, auditory thresholds for only three centre frequencies could be determined. Due to the fact that it was not possible to obtain a complete set of data for each bat, mean thresholds for the eight tested centre frequencies were calculated from different numbers of animals. The mean threshold for the centre frequencies 4.5, 10.3, 15.5 and 80 kHz was calculated from the data of two bats, the mean threshold for the centre frequencies 6.8 and 35 kHz was calculated from the data of three bats and for the centre frequencies 23 and 53 kHz data was obtained from each bat and the mean threshold for these centre frequencies was thus calculated from the data of four bats. Thus, on average mean thresholds for the eight different centre frequencies were calculated from the data of three individuals. Mean thresholds of tested centre frequencies are in the range of -10.5 to 35.7 dB SPL.

Figure 1.2 depicts the average behavioral auditory thresholds of *P. discolor*; individual data is shown in Table 1.1 For centre frequencies between 4.5 and 23 kHz, the audiogram is characterized by a relatively fast decrease, starting with a mean threshold of 35.7 dB SPL at 4.5 kHz and reaching the first threshold dip at 23 kHz with an average threshold of -2.8 dB SPL. At a centre frequency of 35 kHz, the threshold increases to 2.8 dB SPL, but drops again with increasing centre frequency to form the second and more pronounced threshold minimum with a mean threshold of -10.5 dB SPL at a centre frequency of 80 kHz.

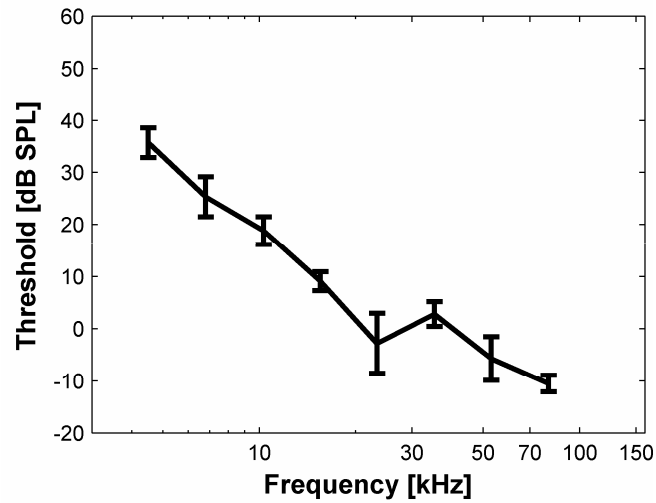


Fig. 1.2 Behavioral audiogram of *P. discolor*. The solid line represents the mean threshold values of four bats. Error bars indicate the standard error.

Centre frequency (kHz)	Bat 1	Bat 2	Bat 3	Bat 4	Mean
4.5		38.5	32.8		35.7
6.8		29.4	17.6	28.9	25.3
10.3		16.1	21.5		18.8
15.5		7.3	10.9		9.1
23	9.6	-1.2	-18.2	-1.2	-2.8
35		2.7	-1.2	7	2.8
53	0.3	1.3	-16.7	-7.7	-5.7
80	-8.9			-12.1	-10.5

Table 1.1 Behavioral threshold values in dB SPL determined from the psychometric functions of the four bats and mean values, respectively.

1.4.2 Neurophysiology

For maximal reliability of the data we excluded units with BFs exceeding the range of the flat frequency response of the earphones (10 to 100 kHz, see Methods) from further analysis. Thus, BF and neural threshold data was derived from 288 IC units and from 763 cortical units. Neural thresholds are shown as a function of unit BF in Fig. 1.3a and b for the IC and the AC, respectively.

For both the IC and AC units, BFs are in the frequency range of 10 to 100 kHz with most units having BFs above 50 kHz (IC: 60 %, AC: 75 %). Auditory thresholds of units in both IC and AC show a high variability but are in the same range. Units in the IC had thresholds of 0 to 78 dB SPL; units in the AC had thresholds of 0 to 82 dB SPL. Lowest thresholds of 0 dB SPL are reached in collicular units at the BF of 38 kHz and in cortical units at BFs between 46 and 52 kHz.

Minimum thresholds for the neural audiogram could be calculated for 11 frequency bands in both IC and AC. In both cases, the minimum value for the frequency band with the centre frequency of 10.3 could not be calculated because of the small number (<3) of recorded units with BFs in this frequency range (see Methods).

The neural audiogram from the IC is characterized by two regions of maximal sensitivity (Fig. 1.3a). The first threshold minimum (ca. 15 dB SPL) at 15 kHz is separated by a high-threshold region around 20 kHz (ca. 35 dB SPL) from a second threshold minimum at 35 kHz (0 dB SPL).

The neural audiogram from the AC is broadly V-shaped with a shallow ascending slope at low frequencies and a steeply ascending slope at high frequencies (Fig. 1.3b). Maximal sensitivity (0 dB SPL) is reached at 55 kHz. Whereas the ascending slope at the low frequency side shows a plateau at 15 kHz before increasing again, the slope at the high frequency side is constantly increasing.

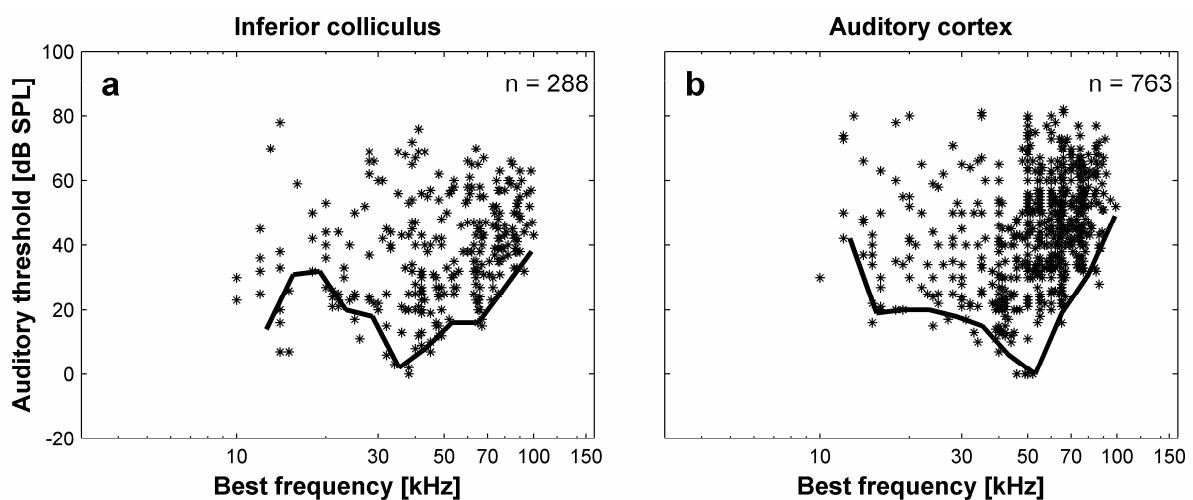


Fig. 1.3 Auditory thresholds of IC (a) and AC units (b) plotted as function of their best frequency. The solid lines represent the neurophysiologically determined audiograms of *P. discolor*. The audiograms are based on the mean values of the three lowest thresholds within 11 frequency bands.

1.5 Discussion

Both the behavioral and neural threshold data presented here indicate that hearing in the echolocating bat, *P. discolor* is quite sensitive with absolute thresholds down to zero dB SPL and below. A direct comparison of the current behavioral and neural audiograms is shown in Fig. 1.4 together with auditory thresholds estimated by Wittekindt et al. (2005) from measurements of distortion-product otoacoustic emissions (DPOAE).

The neural audiograms obtained from the IC and the AC show a high degree of similarity. In both cases, threshold minima are in the mid frequency range around 35 to 55 kHz where neural thresholds approach 0 dB SPL. As it is shown in Fig. 1.4, frequencies of this range are contained in both echolocation and communication calls of *P. discolor*. No special sensitivity peak in the frequency range where the echolocation calls are loudest (around 60 kHz) can be found, which is equally pronounced in both the neural audiograms of the IC and AC.

In the IC audiogram, an additional threshold minimum is seen at 15 kHz, which is only weakly reflected in the AC audiogram. This might be due to sampling biases, as the number of neurons recorded from the same frequency regions was not always the same in the IC and AC.

In the low and mid frequency range up to 55 kHz, the behavioral audiogram of *P. discolor* fits the neuronal audiograms quite well (see Fig. 1.4). In this frequency range, both the behavioral and the neural thresholds decrease with increasing frequency. However, the psychophysically determined thresholds are approximately 10 to 15 dB lower than the neural thresholds. This might be due to the influence of the anesthesia in the neurophysiological experiments (Evans and Nelson 1973; Gaese and Ostwald 2001). At a centre frequency of 23 kHz, the behavioral audiogram shows a small dip. This might be due to generalization of the training stimulus as the bat was trained by using a noise stimulus with a centre frequency of 23 kHz. However, the following facts weaken this hypothesis. At the one hand, for a centre frequency of 23 kHz, threshold data was obtained from all experimental animals. Thus, the large data set should result in a reduced standard error in comparison to other centre frequencies. But as one can see in Fig. 1.2, the error bars are largest at a centre frequency of 23 kHz which indicates that the inter-individual differences in auditory threshold were highest at this frequency. And at the other hand, the previous behavioral audiogram determined by Esser and Daucher shows a small dip at frequencies around 21 kHz too. Hence, the small dip at a centre frequency of 23 kHz in the present behavioral audiogram seems rather to be an attribute of the audiogram than a result of the training sessions. The largest difference between the behavioral and the neural audiograms is found in the high frequency range above 60 kHz: in the behavioral audiogram the threshold falls up to 80 kHz, whereas the neural thresholds rise in both the IC and the AC. This may be caused by a difference in body temperature between the anaesthetized and awake animals. As described by Ohlemiller & Siegel (1994) and Sendowski et al. (2006), a decrease in an animal's body temperature results in a larger threshold increase for high frequencies than for low frequencies. This is further supported by the DPOAE thresholds of *P. discolor* (Wittekindt et al. 2005), which also show higher

thresholds at higher frequencies compared to the behavioral audiogram (see Fig. 1.4). This study was carried out under the same conditions as the present electrophysiological study (anaesthetized animals, experimental chamber heated to 36°C). In consequence, DPOAE thresholds resemble the current neural audiograms more closely than the behavioral audiogram.

Due to technical limitations, behavioral thresholds for band-pass centre frequencies above 80 kHz were not obtained (sampling rate limited to 196 kHz, see Methods). Thus, it is unclear if the absolute minimum was reached at this frequency or whether the threshold would still further decrease at higher frequencies. However, it can be supposed that the threshold would steeply increase at frequencies above 80 kHz as it has been shown in the pure-tone measurements of Esser and Daucher (1996) and in the behavioral audiograms of other phyllostomid bats (see below).

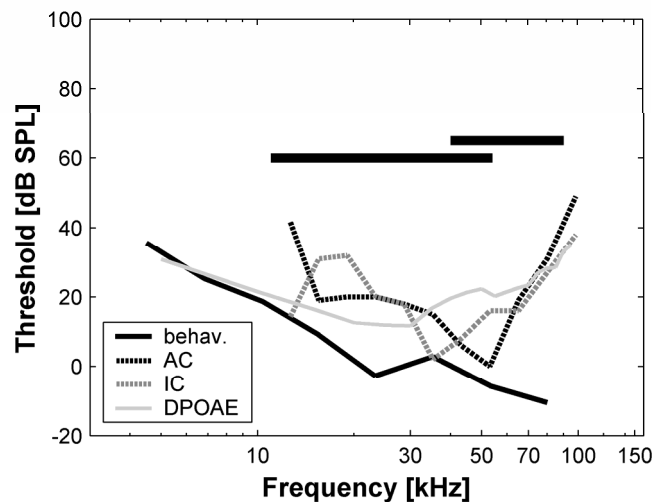


Fig. 1.4 Behavioral audiogram (solid black line), neural audiogram of cortical units (dotted black line), neural audiogram of collicular units (dotted grey line) and DPOAE threshold curve (solid light grey line, redrawn from Wittekindt et al. 2005) of *P. discolor*. Black horizontal bars indicate the frequency ranges of the communication (11-54 kHz) and echolocation (40-90 kHz) calls of this species.

1.5.1 Comparison with neurophysiological data of other phyllostomid bats

Figure 1.5 shows the neural audiograms of *P. discolor* and two other phyllostomid bats (*C. perspicillata* and *P. hastatus*). The shapes of the IC and AC audiograms of *P. discolor* are similar to the audiogram obtained from IC neurons of *P. hastatus* (Grinnell 1970) with slightly lower absolute thresholds in *P. discolor*. In contrast, the audiograms of *C. perspicillata* derived from recordings in the IC (Sterbing et al. 1994) and AC (Esser and Eiermann 1999) are strongly W-shaped. Especially the thresholds in the low frequency range of 15 to 30 kHz are lower in the audiograms of *C. perspicillata* compared to the neural audiograms of the present study. Furthermore, the AC audiogram of *C. perspicillata* is characterized by a very pronounced high-threshold region at 52 kHz which is also weakly indicated in the IC audiogram at slightly lower frequencies. In the present study this high-threshold range can neither be seen in the AC audiogram nor in the IC audiogram of *P. discolor*. Reasons for this difference might lie in the method of acoustic stimulation during neurophysiological recordings. Esser and Eiermann (1999), as well as Sterbing et al. (1994) used free field stimulation with condenser speakers placed at the contralateral side in the horizontal plane. In contrast, in the present study acoustic stimuli were presented via ear phones to the animal. Thus, influences of the bat's outer ear were completely excluded. Measurements of the head-related transfer functions of *P. discolor* (Firzlaff and Schuller 2003) demonstrated elevation dependent spectral notches around 55 kHz which were strongly influenced by the tragus of the outer ear. These spectral notches are mainly used by bats to determine the position of a sound source in elevation (Lawrence and Simmons 1982; Fuzessery 1996; Wotton and Simmons 2000; Chiu and Moss 2007). Thus, the high-threshold regions in the audiograms of *C. perspicillata* are most probably related to the influence of the outer ear and the tragus, which can not be seen when ear phones are used for acoustical stimulation. This is again supported by the measurements of the DPOAE thresholds in *P. discolor* (Wittekindt et al. 2005) which also exclude the influence of the outer ear. The DPOAE thresholds (see Fig. 1.4) also show no high-threshold region in the frequency range around 55 kHz.

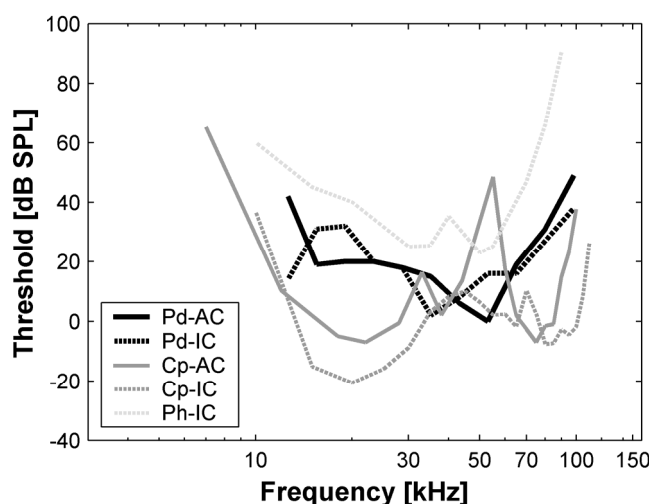


Fig. 1.5 Neural audiograms for three species of Phyllostomidae: cortical units of *P. discolor* (Pd-AC, solid black line), collicular units of *P. discolor* (Pd-IC, dotted black line), cortical units of *C. perspicillata* (Cp-AC, solid grey line, redrawn from Esser & Eiermann 1999), collicular units of *C. perspicillata* (Cp-IC, dotted grey line, redrawn from Koay et al. 2003) and collicular units of *P. hastatus* (Ph-IC, dotted light grey line, redrawn from Koay et al. 2002).

1.5.2 Comparison with behavioral audiograms of other phyllostomid bats

Figure 1.6 compares the behavioral audiograms of three different phyllostomid bats (*A. jamaicensis*: Heffner et al. 2003; *C. perspicillata*: Koay et al. 2003; *P. hastatus*: Koay et al. 2002) with the present behavioral audiogram of *P. discolor* and the audiogram measured by Esser and Daucher (1996). The present behavioral audiogram fits the audiograms of the other three phyllostomids in the low and mid frequency range up to 40 kHz well. At higher frequencies, thresholds inferred from the current audiogram are about 20 dB lower than in the other phyllostomids. A possible explanation for this difference might lie in the experimental design. In the present behavioral study, experimental animals were allowed to move their heads and ears freely while listening to the test tone. In the other studies, the animals were restrained in a fixed position and no movement of the head was possible (Koay et al. 2002; Koay et al. 2003; Heffner et al. 2003). As the directionality of hearing increases with increasing sound frequency (Firzlaflaff and Schuller 2003) sound detection in the high frequency range strongly depends on the position of head and ears relative to the sound source. The animals in the present study could improve sound detection in the high frequency range by movements of head and pinnae, whereas, in the studies of Koay et al. (2002), Koay et al. (2003) and Heffner et al. (2003) the restrained animals could not. Consequently, thresholds are higher in this frequency range. This is supported by personal observations of head and ear

movements of the bats in the present behavioral study. Movements during localization of a high test frequency were generally of a higher rate than during the localization of a low test frequency.

Most distinctive in Fig. 1.6 is the large difference of auditory threshold values between the present audiogram of *P. discolor* and the audiogram determined by Esser and Daucher (1996). The audiograms run roughly parallel but the audiogram of the present study is shifted towards lower sound intensities by 35 to 40 dB. Note, however, that also in the data by Esser and Daucher (1996), the lowest threshold was found at 80 kHz. As already suggested by Koay et al. (2003), the unusually high thresholds in the first experiment of Esser and Daucher (1996) may be mainly due to the difficulties in the discrimination task. For example, the bats in the study of 1996 had to crawl a distance of 1 m to reach the sound source and to get the food reward. In the present experiment, the task was simplified by reducing the distance between starting point and food reward to 30 cm.

A second difference between the previous and the present behavioral audiograms is the lack of the distinct high-threshold range around 50 kHz. This insensitive region is also very prominent in the behavioral audiogram of *C. perspicillata* (Koay et al. 2003). However, in the present behavioral audiogram of *P. discolor*, only a very shallow increase in threshold can be seen at 35 kHz. In addition, the behavioral audiograms of *A. jamaicensis* and *P. hastatus* (Koay et al. 2002; Heffner et al. 2003) also show only a weak threshold rise in the mid frequency range. As already discussed before, this high-threshold region might be caused by structural characteristics of the bat's outer ear. This view is further supported by the studies of Heffner et al. (2003) and Koay et al. (2003) in which the elevation dependency of the high-threshold region in the audiogram was shown. Differences in the spatial arrangement of loudspeaker and starting position of the bat as well as the degree of movability of the bats in the experimental set up most probably contribute to the strength of the high-threshold region in the mid frequency range in the behavioral audiograms of the different phyllostomid bats.

Third, in the present behavioral study, we stimulated with narrow-band noise signals instead of the classically used pure tones. On one hand, the narrow-band noise precludes the contamination of the behavioral audiograms by the fine structure of the audiogram, which has been observed in humans (Zwicker and Fastl 1990). This may be also important for the appearance of the spectral notch in the audiogram observed in other phyllostomid bats (see above). Supposedly, this notch is less pronounced with narrow-band stimulation than with pure-tone stimulation. On the other hand, the temporal envelope fluctuations introduced by the narrow-band noise may facilitate the localization of faint stimuli and thus the behavioral performance leading to lower thresholds.

In summary, both the behavioral and neural audiograms show that *P. discolor* has very good hearing in the low frequency range around 30 kHz, which is important for the detection and analysis of conspecific communication calls. The behavioral data also indicates a second frequency range with very low thresholds, which matches the spectral composition of *P. discolor* echolocation calls. This very high ultrasonic sensitivity may be adaptation to the relatively faint echolocation calls emitted by *P. discolor*. The fact that this second low-

threshold range is not seen in the neural audiograms may result from the anesthesia, which is known to affect high-frequency hearing more than low-frequency hearing.

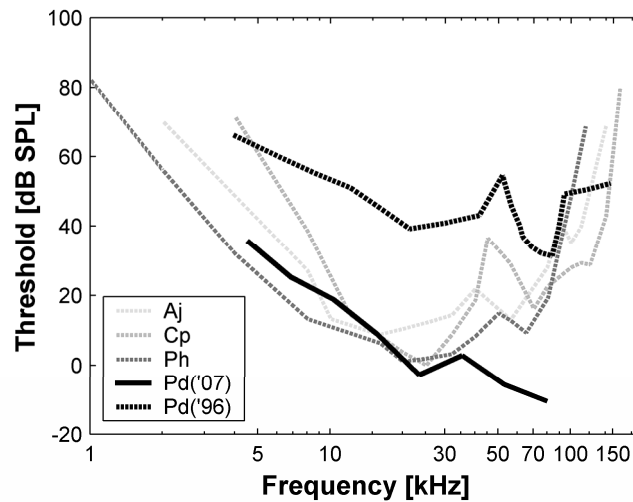


Fig. 1.6 Behavioral audiograms for four species of phyllostomid bats: *A. jamaicensis* (Aj, dotted light grey line, redrawn from Heffner et al. 2003), *C. perspicillata* (Cp, dotted grey line, redrawn from Koay et al. 2003), *P. hastatus* (Ph, dotted dark grey line, redrawn from Koay et al. 2002) and *P. discolor* (Pd('07), solid black line, current study, Pd('96), dotted black line, redrawn from Esser and Daucher 1996).

1.6 Acknowledgements

The authors wish to thank Susanne Radtke-Schuller for her help with reconstruction of recording sites, Claudia Schulte and Horst König for technical help and Britta Schwellnus for help during neurophysiological experiments.

All experiments were performed in agreement with the principles of laboratory animal care and under the regulations of the current version of German Law on Animal Protection (approval 209.1/211-2531-68/03 Reg. Oberbayern).

2. The auditory cortex of the bat *Phyllostomus discolor*: localization and organization of basic response properties

This study was published in 2008 by Susanne Hoffmann, Uwe Firzlaff, Susanne Radtke-Schuller, Britta Schwellnus and Gerd Schuller, in BMC Neuroscience (Vol. 9:65).

The neurophysiological experiment was designed and implemented by Uwe Firzlaff. The acquisition of neurophysiological data was done by Uwe Firzlaff, Britta Schwellnus and me. Uwe Firzlaff and I did the analysis of the data. Gerd Schuller provided the equipment for the neurophysiological setup. Susanne Radtke-Schuller performed the histological and neuroanatomical procedures and analyzed this data. The parts of the paper concerning the neuroanatomy were written by Susanne Radtke-Schuller and Gerd Schuller and the parts of the paper concerning the neurophysiology were written by Uwe Firzlaff, Gerd Schuller and me.

2.1 Abstract

2.1.1 Background

The mammalian auditory cortex can be subdivided into various fields characterized by neurophysiological and neuroarchitectural properties and by connections with different nuclei of the thalamus. Besides the primary auditory cortex, echolocating bats have cortical fields for the processing of temporal and spectral features of the echolocation pulses. This paper reports on location, neuroarchitecture and basic functional organization of the auditory cortex of the microchiropteran bat *Phyllostomus discolor* (family: Phyllostomidae).

2.1.2 Results

The auditory cortical area of *P. discolor* is located at parieto-temporal portions of the neocortex. It covers a rostro-caudal range of about 4800 μm and a medio-lateral distance of about 7000 μm on the flattened cortical surface.

The auditory cortices of ten adult *P. discolor* were electrophysiologically mapped in detail. Responses of 849 units (single neurons and neuronal clusters up to three neurons) to pure tone stimulation were recorded extracellularly. Cortical units were characterized and classified depending on their response properties such as best frequency, auditory threshold, first spike latency, response duration, width and shape of the frequency response area and binaural interactions.

Based on neurophysiological and neuroanatomical criteria, the auditory cortex of *P. discolor* could be subdivided into anterior and posterior ventral fields and anterior and posterior dorsal fields. The representation of response properties within the different auditory cortical fields was analyzed in detail. The two ventral fields were distinguished by their tonotopic organization with opposing frequency gradients. The dorsal cortical fields were not tonotopically organized but contained neurons that were responsive to high frequencies only.

2.1.3 Conclusions

The auditory cortex of *P. discolor* resembles the auditory cortex of other phyllostomid bats in size and basic functional organization. The tonotopically organized posterior ventral field might represent the primary auditory cortex and the tonotopically organized anterior ventral field seems to be similar to the anterior auditory field of other mammals. As most energy of the echolocation pulse of *P. discolor* is contained in the high-frequency range, the non-tonotopically organized high-frequency dorsal region seems to be particularly important for echolocation.

2.2 Background

During the last decade, the bat *P. discolor* has been used increasingly for psychophysical and neurophysiological studies of echolocation (Esser and Lud 1997; Grunwald et al. 2004; Fenzl and Schuller 2005; Firzlaff and Schuller 2007). *P. discolor* is medium-sized and forages for fruit, nectar, pollen and insects in a neotropical forest habitat. Its vocal emissions are brief (< three milliseconds), broadband multi-harmonic, downward frequency modulated (FM) echolocation pulses with a frequency range of about 40 to 90 kHz. In contrast, the rich repertoire of communication calls used for species-specific social interaction covers the lower frequency range from 11 to 54 kHz (Esser and Schmidt 1990; Hackel and Esser 1998). The responses of cortical neurons to complex stimuli relevant for echolocation in *P. discolor* have been compared to the behavioral performance of the bat (Firzlaff et al. 2006; Firzlaff et al. 2007). Therefore, it is important to gain knowledge of the detailed organization of the AC with respect to basic response properties.

The auditory cortex (AC) of mammals is composed of distinct fields, which can be characterized by physiological and cytoarchitectural features and their specific thalamo-cortical connections (for review see Clarey et al. 1992; Ehret 1997). The functional

organization of the AC in bats has been extensively studied physiologically in several species (e.g. *Pteronotus parnellii* (O'Neill and Suga 1982; Fitzpatrick et al. 1998b), *Rhinolophus spec.* (Ostwald 1984; Radtke-Schuller and Schuller 1995), *Eptesicus fuscus* (Dear et al. 1993; Jen et al. 2003), for review see (O'Neill 1995)). Among the best studied ACs so far are those of the mustached bat *P. parnellii* and the horseshoe bat, *Rhinolophus rouxi*, both belonging to the group of the so-called CF/FM-bats whose echolocation pulses consist of a constant frequency (CF) and a frequency modulated (FM) component. As common to all mammals studied so far, their ACs contain a tonotopically organized primary auditory field (AI) with the frequency gradient running from caudal to rostral. However, in both CF/FM-bats frequencies of the CF component of the calls are largely overrepresented in AI while frequencies of the FM component are only weakly represented (Suga and Jen 1976). The AI is surrounded by cortical regions with neurons that show facilitated responses to specific spectral and temporal combinations of the CF and FM parts of the different harmonics of the echolocation pulses. CF/FM-bats are rather specialized echolocators in that they hunt almost exclusively insects on the wings, whereas other bat species display more varied feeding ecology (insects, vertebrates, nectar, and fruits) and very commonly use short downward FM echolocation pulses often with several harmonic components. In these bats the functional specialization of the AC is often not so clearly apparent, but still cortical fields can be segregated based on neurophysiological criteria like best frequency (BF; frequency at which threshold is lowest) representation and response threshold (Wong and Shannon 1988; Dear et al. 1993). In the phyllostomid FM-bat *Carollia perspicillata* for example, two dorsal fields containing mainly neurons with BFs in the high-frequency range have been reported in addition to the tonotopically organized fields AI and anterior auditory field (AAF) (Esser and Eiermann 1999). In these high-frequency fields some neurons exhibited pulse-echo delay sensitivity as in CF/FM-bats (Hackel and Esser 1998), but without topographical organization. Except for a short autoradiographic labeling study (Esser 1995) the topography of the AC of *P. discolor* has not been studied. In general, the AC of only one other phyllostomid FM-bat, *C. perspicillata*, has been investigated, so far (Esser and Eiermann 1999). Therefore, the aim of the present study was to investigate neuroanatomical and neurophysiological properties of the AC of *P. discolor* in order to delineate its subdivisions.

2.3 Results

2.3.1 Auditory responses in the cortex of *Phyllostomus discolor*

As shown in Fig. 2.1A, units responding to acoustic stimuli are found at parieto-temporal portions of the neocortex of *P. discolor*. The distribution of neurophysiological recording sites defines the functional location of the bat's AC. External features roughly delineating the AC are the pseudocentral sulcus (McDaniel 1976), which is located at the rostro-dorsal border and the fissura rhinalis, which is located at the ventral border. The auditory cortical area covers a rostro-caudal distance of about 4800 μm and has a dorso-ventral extension of about 5100 μm

in the lateral view as shown in Fig. 2.1A. To obtain a realistic estimate of the cortical surface containing auditory units, the locations of the recorded units were projected on an unrolled and flattened surface projection along the medio-lateral coordinate (Fig. 2.1B, see Methods). In this projection, the lateral extension of the auditory responsive area is roughly 7000 μm .

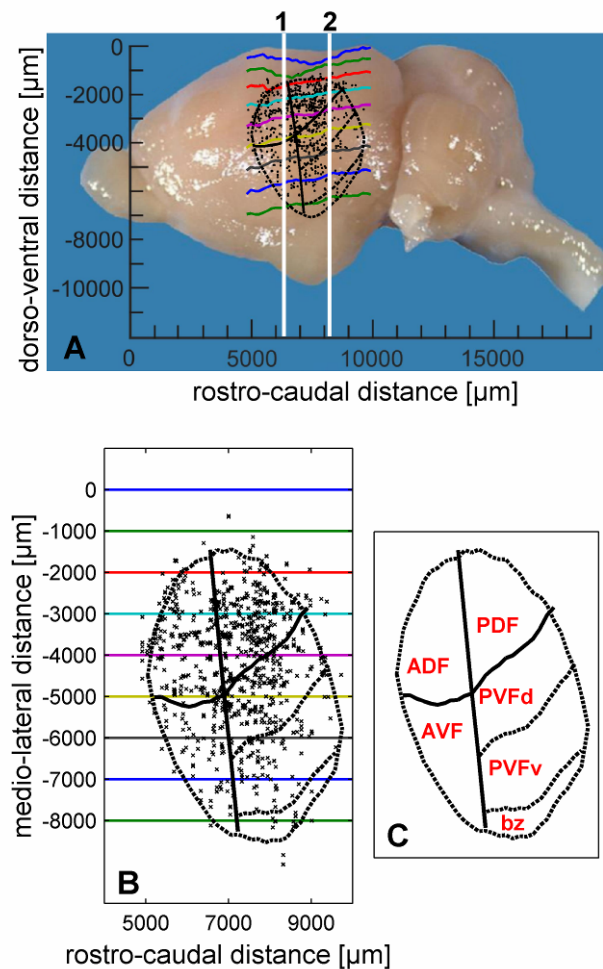


Fig. 2.1 Recording sites and subfields in the auditory cortex of *Phyllostomus discolor*. **A)** Lateral view of the *P. discolor* brain. Recording sites of all 849 units are indicated as black dots. Superimposed black outlines are neuroanatomically determined borders. Solid black lines represent reliable borders, whereas stippled black lines represent more variable borders. Rostro-caudal positions of frontal sections shown in Fig. 2.2 are indicated by the white vertical lines. Colored lines represent equal medio-lateral distances from the midline in 1000 μm steps as shown in the flattened cortical surface projection in Fig. 2.1B. **B)** Projection of recording sites (black crosses) and neuroanatomical borders (black lines) on an unrolled and flattened cortical surface. Lateral distances on the cortical surface are indicated in 1000 μm steps by corresponding colors as in the side view (2.1A). The origin used for the flattening process was fixed at 2000 μm lateral from the midline of the brain

(upper dark blue line). **C**) Schematic of the auditory cortical subfields: anterior dorsal field (ADF), posterior dorsal field (PDF), anterior ventral field (AVF) and posterior ventral field (PVF) with dorsal (PVFd), ventral (PVFv) parts and a border zone (bz) reconstructed on the flattened cortical surface. The neuroanatomically determined borders are indicated by black lines.

2.3.2 Neuroanatomy

In the area responsive to acoustic stimuli four major fields are recognized based on cyto- and myeloarchitectural features and zinc staining pattern, i.e. the anterior and posterior dorsal fields (ADF and PDF), an anterior ventral field (AVF) and a posterior ventral field (PVF). The PVF maybe further subdivided into a dorsal and a ventral part (PVFd and PVFv) and a border zone (PVFbz), due to minor modifications of the neuroarchitectural characteristics. The topographic position of these fields is depicted in Fig. 2.1C. Reliable borders of cortical fields are indicated by solid lines. Dashed lines represent the more variable outlines of the AC itself and for PVF possible anatomical subdivisions that are not corroborated by neurophysiological data of the study.

Frontal sections in Fig. 2.2 give showcase characteristics at two rostro-caudal levels (as indicated in Fig. 2.1A) to get a general idea of field differences. Total cortical thickness, relative thickness of the different layers, composition of cell types, cell density, content of myelinated fibers and zinc are considered as parameters for the distinction of the different fields. Cut-outs of frontal sections stained for cells (Nissl), myelinated fibers (Gallyas) and for zinc (sulphide/silver histochemical method) from the centers of the different cortical fields are mounted in Fig. 2.3 for detailed comparison.

Total cortical thickness varies between 1600 μm (ADF) and 1200 μm from dorso-rostral to ventro-caudal locations (PVFv) in the AC. Despite the high density of granular elements in layer III and IV of the dorsal fields, the cortical layers V and VI take more of the total thickness of the cortex. Therefore, they are addressed as parietal cortical fields. The ventral fields are thought to belong to the temporal cortex, as layers III and IV dominate layers V and VI in thickness although granular elements are sparse and the cell density is lower in layers III/IV compared to the dorsal fields.

Dorsal and ventral fields also differ with respect to layer I, which is generally thinner in the dorsal than in the ventral fields. The myelinated horizontal fibers in the superficial part of layer I form a narrow dense band in the dorsal fields, but a broader one in the ventral fields, which is paralleled by a nearly zinc-free stripe in the ventral fields.

The most characteristic features used for delimitation of cortical fields are described in detail as follows. ADF has the greatest cortical width that seems to be caused by a doubled layer V: layer V of the non-auditory cortical area dorsal to the AC seems to continue beneath layer V

of ADF (see frontal section stained for zinc in Fig. 2.2, left column, bottom, and Fig. 2.3, upper left panel, stars marking the two components of layer V).

In AVF, the rostral beginning coincides with the most caudal part of the claustrorocortex without a sharp border. The myelin content in AVF is comparably low, whereas the stain for zinc is generally intense (as is the stain in the rostrally adjacent claustrorocortex and the ventrally bordering perirhinal cortex). Even the paler staining band corresponding to layer IV is relatively dark.

The posterior fields are more homogeneous. Cortical width in PDF is smaller than in ADF and characteristic differences to the neighboring PVF are obvious at higher magnification (see Fig. 2.3). In the zinc stain, layer IV is narrower and more heavily stained in PDF than in PVF, whereas layer V is thicker and of higher staining intensity.

PVF has the most conspicuous wide and pale zinc staining band in layer IV, encompassing deep layer III. Layer V shows three subdivisions in the dorsal part (PVFd), whereas in the ventral part (PVFv) only two subdivisions are recognizable. Layer Vb, the most intense staining part of layer V is strikingly darker in PVFv. In PVFbz a gradual change of the characteristic features from PVF toward the ventrally adjacent perirhinal cortex takes place, e.g. the layered organization fades as well in the cell stain as in the zinc stain, and so do the myelinated fibers.

Layer IV appears as a pale band with the lowest staining intensity in the zinc stain and the staining intensity of layer IV varies characteristically between the fields. It is faint in layer IV of PDF, comparably lighter in ADF, relatively dark in AVF and faintest in PVF.

Layer IV (and deep layer III) contains a high number of granular elements in the dorsal fields, whereas the neuronal somata in the ventral fields are larger and the cell density is lower. Layer IV is heavily myelinated in all fields except in the sparsely myelinated AVF.

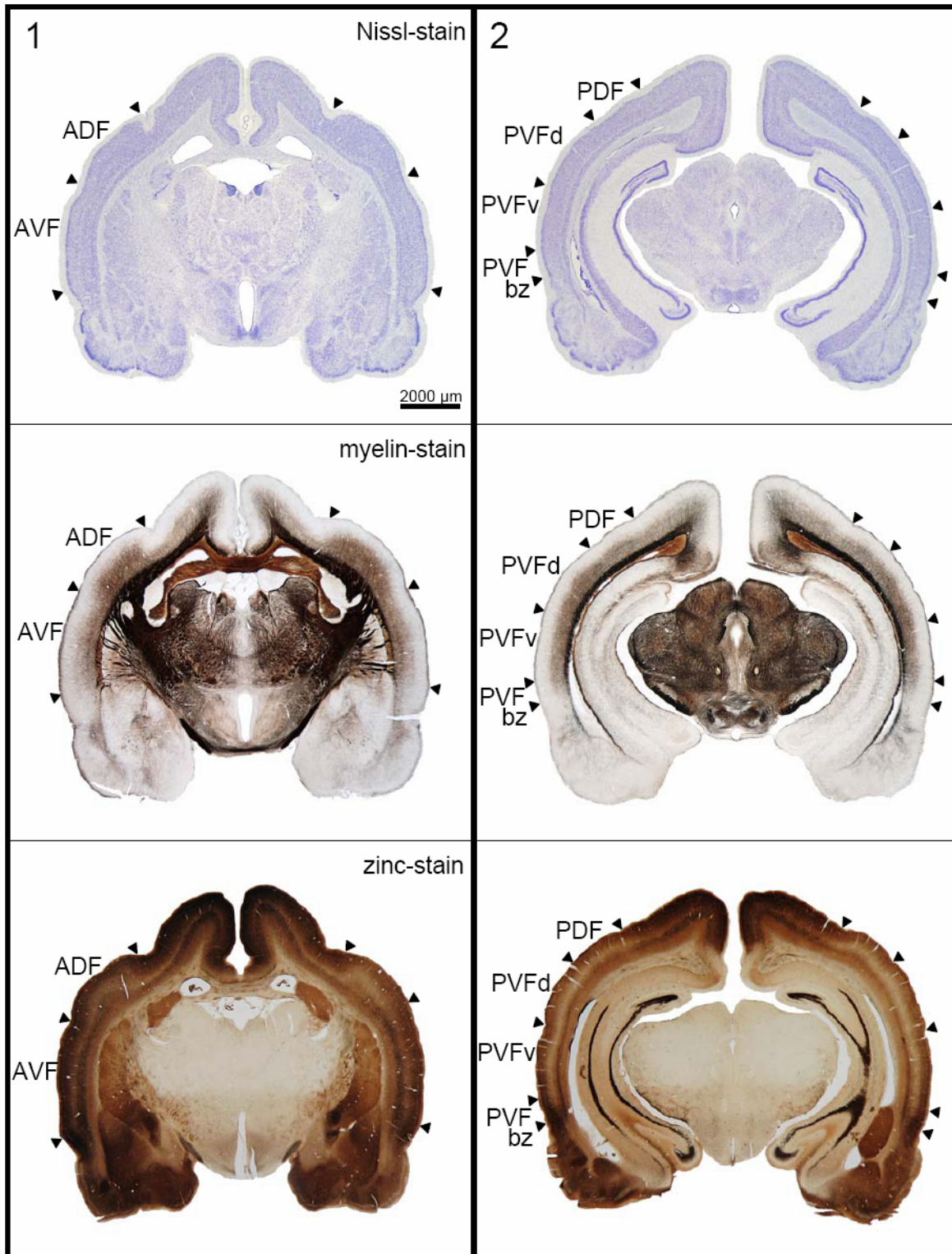


Fig. 2.2 Frontal sections at two rostro-caudal levels. The frontal sections are shown for positions indicated by the vertical lines in Fig. 2.1A. Top row: sections (40 µm thick) stained for cells (Nissl); middle row: neighboring sections stained for myelin; bottom row: sections stained for zinc at comparable rostro-caudal level from another series. Scale bar: 2000 µm. Abbreviations as in Fig. 2.1C.

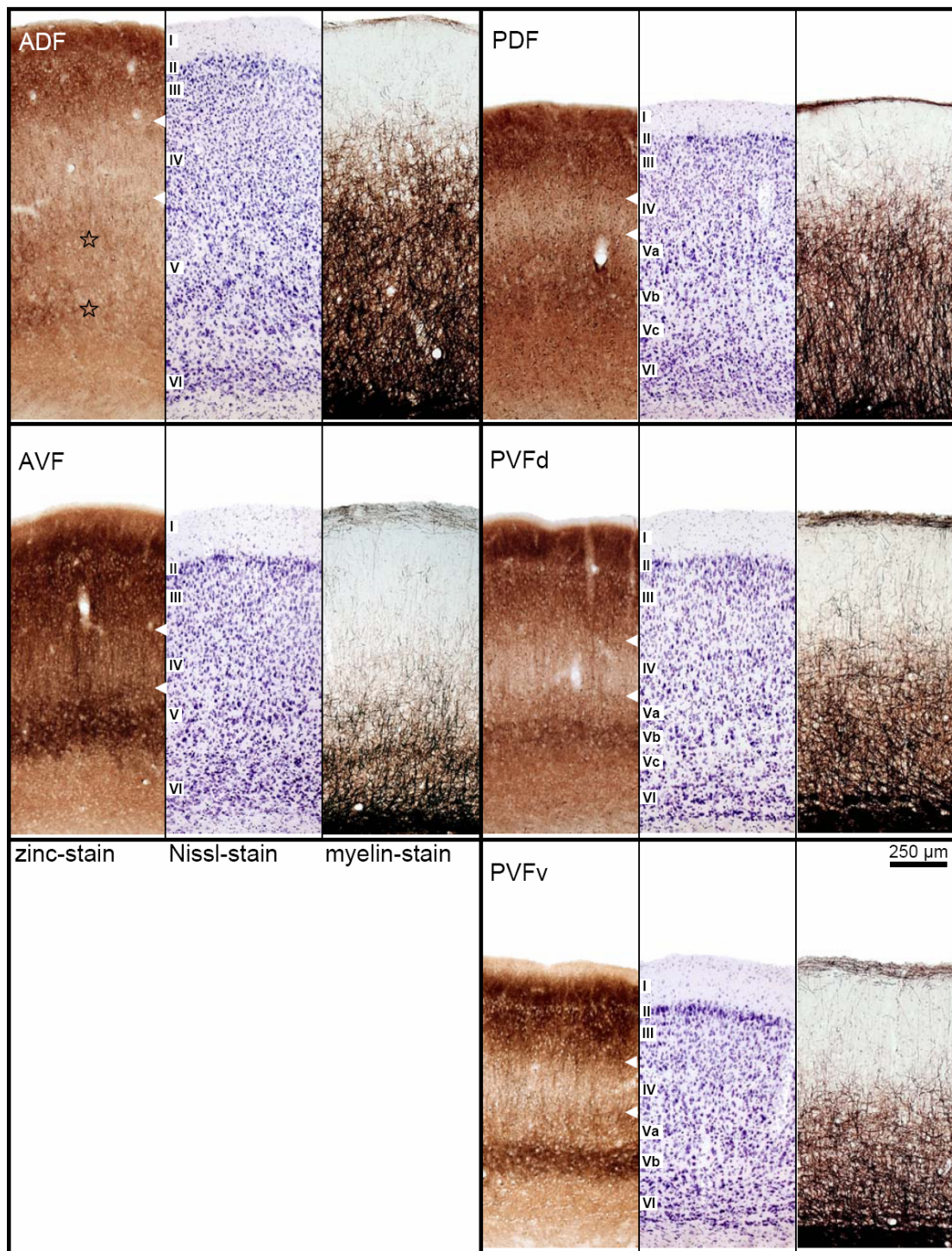


Fig. 2.3 Cut-outs of frontal sections from the centers of the different cortical fields. Field names are given in the zinc-stained sections and apply to the two neighboring photographs to the right. Indications of layers in the Nissl-stained sections apply to the neighboring left (zinc-stained) and right (myelin-stained) sections, respectively. White arrowheads in the zinc-stained sections indicate the borders of layer IV. Stars in the cut-out of the zinc-stained section of ADF highlight the two components of layer V. The scale bar of 250 μm applies to all cut-outs. Abbreviations as in Fig. 2.1C.

2.3.3 Basic neuronal response properties

Because it was not always possible to discriminate the activity of a single neuron, the term ‘unit’ will be used in the following to describe the activity of one neuron to clusters of three neurons recorded at a distinct recording site. Extracellular recordings were derived from a total of 849 units from both hemispheres of ten bats. The number of units recorded in one bat ranged from 18 (16 penetrations) to 201 (92 penetrations) with an average of 85 units (46 penetrations) per bat (Table 2.1). Thus, on average two units were recorded per penetration. Recording depths of units derived from roughly orthogonal electrode penetrations (bat #6 and #7) were in the range of 320 to 1700 μm from the cortical surface ($n = 183$; mean: $962 \pm 278 \mu\text{m}$).

	Bat 1	Bat 2	Bat 3	Bat 4	Bat 5	Bat 6	Bat 7	Bat 8	Bat 9	Bat 10
# of pen.	16	24	24	27	75	92	56	47	47	47
# of units	18	45	36	63	112	201	88	91	106	89

Table 2.1 Number of electrode penetrations and recorded units per bat. The first row shows the number of electrode penetrations in the AC of each bat, the total number of recorded units in each of the ten experimental animals is shown in the second row.

Best frequency and threshold: As shown in Fig. 2.4A, BFs of units ranged from five to 107 kHz ($n = 849$; median: 60 kHz; interquartile range: 44 to 67 kHz). Seventy nine percent (674 of 849) of the units had BFs above 40 kHz, i.e. in the range of the dominant harmonics of the echolocation pulse of *P. discolor*.

The response threshold at BF was determined in 764 units and varied between zero and 82 dB SPL. The frequency distribution of thresholds reaches its maximum around 45 dB SPL with roughly symmetric flanks to lower and higher thresholds (mean: 45 ± 16 dB SPL Fig. 2.4B).

Latency and response duration: The first spike latency was measured in 681 cortical units and ranged between five and 127 ms with a bias toward short latencies (Fig. 2.4D). Median latency of all units was 9 ms (interquartile range: 7 to 20 ms).

Units often exhibited onset responses to pure tones frequently followed by a sustained response component that generally exhibited a considerable amount of variability. Other response types e.g. on-off responses were not observed in the AC of *P. discolor*. The response duration to a 20 ms pure tone was determined in 730 units and ranged from three to 385 ms (median: 25 ms; interquartile range: 14 to 76 ms, Fig. 2.4E). Short phasic responses with durations below 20 ms (Fig. 2.4C) were found in 40 % (292 of 730) of units, medium

response durations between 20 and 100 ms (Fig. 2.4F) were found in 44 % (322 of 730) of units and 16 % (116 of 730) of units had response durations longer than 100 ms (Fig. 2.4I). Thus, in 60 % of units the response duration exceeded the duration of the pure tone stimulus (20 ms).

Frequency response areas: Q_{10dB} values covered a range between 0.5 and 76 (n = 590; median: 5.4; interquartile range: 3.9 to 7.5). The distribution showed a peak around five (Fig. 2.4G), indicating that sharp frequency tuning is rare in cortical units of *P. discolor*. The regression line in Fig. 2.4H shows that Q_{10dB} values roughly increased with increasing BFs. Q_{30dB} values covered the range between 0.3 and 66 (n = 414; median: 3.1; interquartile range: 2.2 to 4.4). The difference between the medians of the Q_{10dB} and Q_{30dB} values suggests that in many units the sharpness of frequency tuning was only slightly decreasing with increasing stimulus level.

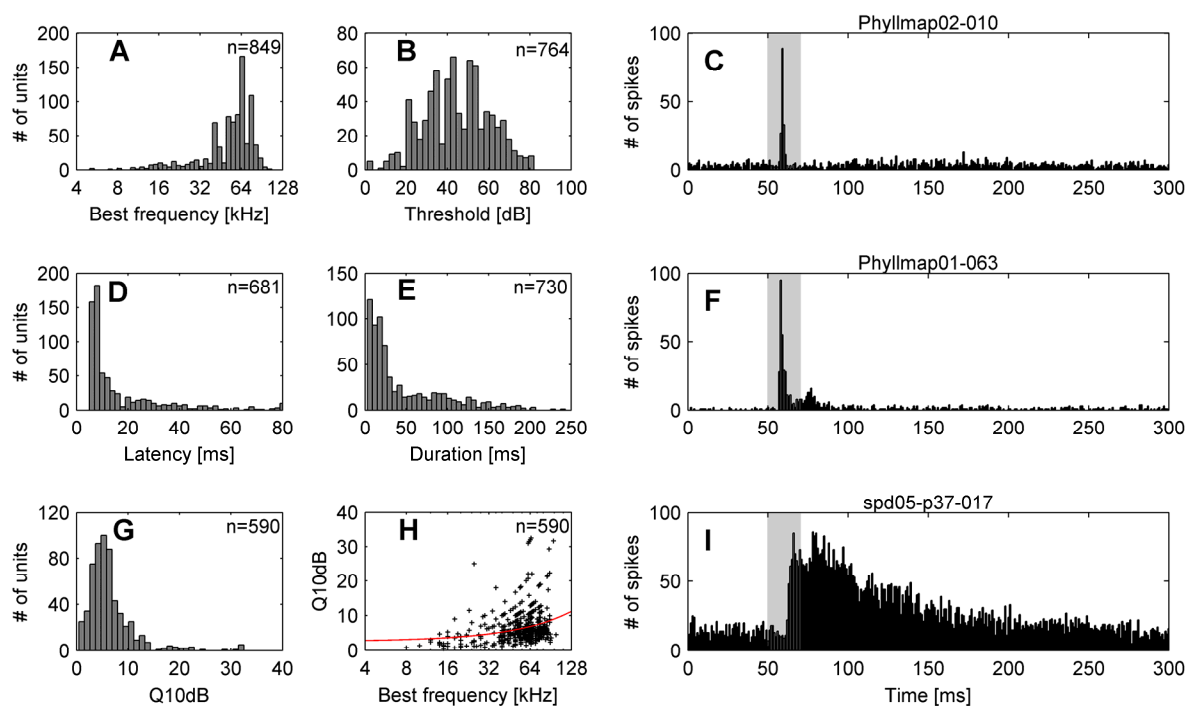


Fig. 2.4 *Distribution of response properties of cortical units and examples of PSTHs for different response types. The frequency distribution of neuronal response properties evoked by pure tone stimulation is shown for: A) Best frequency, B) Response threshold, D) First spike latency, E) Response duration and G) Q_{10dB} values. Peri-stimulus time histograms (PSTHs) show examples of cortical units with different response types: C) phasic response, F) phasic response with a sustained component and I) tonic response. The binwidth of the histograms is 1 ms. The grey bar represents the acoustic stimulus (20 ms pure tone). Panel H) shows the Q_{10dB} values as a function of best frequency. The regression line is shown in red.*

In 745 units, the FRAs could be classified into six different types (Fig. 2.5). Most units (65 %, 489 of 745) showed a V-shaped FRA with equal share of monotonically (Fig. 2.5A) and non-monotonically (Fig. 2.5B) responses. Sixteen percent (120 of 745) of cortical units showed double- or multi-tuned FRAs two thirds (80 of 120) of which displayed monotonic (Fig. 2.5C) and one third (40 of 120) non-monotonic response behavior (Fig. 2.5D). In 48 % (58 of 120) of multiple tuned units, threshold minima were roughly harmonically related. In six percent (43 of 745) of units, the FRAs constituted closed areas in the frequency-intensity field with spike rates dropping to zero at all frequencies with increasing stimulus level (Fig. 2.5E). The remaining units (13 %, 93 of 745) featured complex-shaped FRAs (Fig. 2.5F).

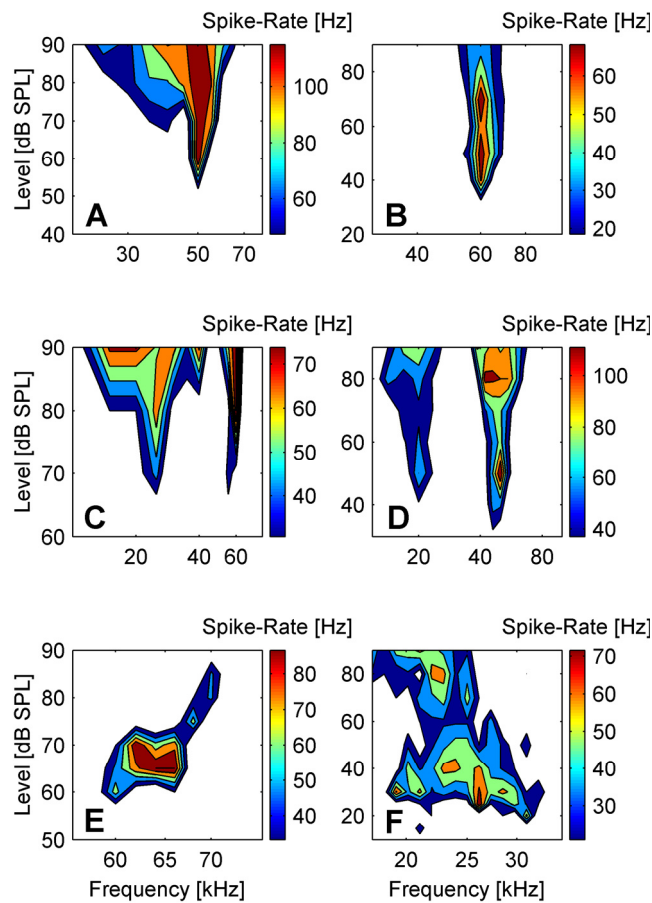


Fig. 2.5 *Examples of the six different FRA types of cortical units. Examples of the different classes of FRA types are shown for A) monotonically V-shaped, B) non-monotonically V-shaped, C) monotonically double tuned, D) non-monotonically double tuned, E) circumscribed and F) complex FRAs.*

Binaural response properties: In 394 units the binaural response properties were measured and units were classified following their contra versus ipsilateral response characteristics (see Methods). EE responses were measured in 39 % (154 of 394) of units, 32 % (126 of 394) of units were inhibited by the ipsilateral ear (EI) and 25 % (100 of 394) of units showed no reaction to ipsilateral stimulation (E0). Four percent (14 of 394) of units could not be classified in one of the above classes and were thus named as “other”.

2.3.4 Representation of neuronal response properties in cortical fields

The local representation of selected response properties on the cortical surface was visualized using the Voronoi tessellation method (see Methods). The tessellation field around the recording site has its limits at halfway distance to the next surrounding recording sites and its color displays the respective response strength of the unit at the center. This forcibly entails large tessellation fields in areas in which recording density is lower or in border regions. As a consequence, there is no proper meaning in the area of single tessellation fields, but rather the clustering or systematic trends of tessellation fields within the AC are important information. Response properties of cortical units were analyzed for the four major subfields. Possible anatomical subdivisions of PVF were not corroborated by the neurophysiological data, and thus, PVF was analyzed as a whole.

Representation of best frequency and Q_{10dB} : The organization of BFs within the AC of *P. discolor* is shown in Fig. 2.6A. Units in the dorsal fields had a relatively restricted range of mainly high BFs, which covered frequencies in the range of the dominant harmonics of the echolocation pulse of this species. Most units in the ADF had BFs above 45 kHz, whereas units in the PDF had mainly BFs above 60 kHz. Only at the most rostral positions of the ADF units with low BFs were found. No tonotopic arrangement of BFs was found in the dorsal fields. In contrast, fields in the ventral part of the AC showed a tonotopic organization of BFs. The frequency gradient in AVF developed along the rostro-lateral to caudo-medial axis with low BFs at rostro-lateral positions, whereas in PVF the BFs decreased from rostral to caudal cortical positions. Thus, PVF and AVF shared a common high-frequency border. The rough direction of BF gradients in the ventral fields is schematically shown in Fig. 2.6B. As shown in Fig. 2.6D, the median BF (65 kHz) in PDF was significantly higher than the median BFs of the other cortical fields (Kruskal-Wallis test, $p < 0.05$). The lowest median BF (50 kHz) was found in PVF.

Q_{10dB} values of units were also not uniformly distributed on the cortical surface but showed a tendency to increase from anterior to posterior locations (Fig. 2.6C). In both anterior fields, units showed broader frequency tuning with significantly lower Q_{10dB} values (Kruskal-Wallis test, $p < 0.05$) than found in units in the posterior fields (Fig. 2.6E).

Representation of threshold, latency and response duration: Figure 2.6F shows the cortical representation of response thresholds at BF within the different fields. Thresholds of units in the dorsal fields were significantly higher than thresholds of units in PVF (Kruskal-Wallis test, $p < 0.05$) but only slightly higher than those of units in AVF (Fig. 2.6I). Units in the ADF

had the highest median response threshold (50 dB SPL), whereas the lowest median response threshold was found in units in the PVF (40 dB SPL).

The distribution of first spike latencies in the AC of *P. discolor* is shown in Fig. 2.6G. As a general trend, short first spike latencies were preferentially represented in units in the two anterior fields, whereas in units in the posterior fields also long latencies were found. The median latency of PVF (13 ms; interquartile range: 8 to 28 ms) was significantly longer (Kruskal-Wallis test, $p < 0.05$) than the median latencies of ADF (median: 8 ms; interquartile range: 7 to 11 ms), AVF (median: 8 ms; interquartile range: 7 to 24 ms) and PDF (median: 9 ms; interquartile range: 7 to 20 ms, Fig. 2.6J).

The representation of response durations within the AC (Fig. 2.6H) showed the same trend as the representation of first spike latencies: short durations were characteristic for units in the anterior fields, whereas in the posterior fields units with long response durations were found, too. The median response duration of units in ADF (21 ms; interquartile range: 11 to 38 ms) and AVF (14 ms; interquartile range: 7 to 84 ms) were significantly shorter (Kruskal-Wallis test, $p < 0.05$) than the median response duration of units in PVF (43 ms; interquartile range: 19 to 97 ms) but only slightly shorter than the median response duration of units in PDF (26 ms; interquartile range: 15 to 72 ms). In addition, the median response duration in PDF was significantly shorter (median: 24 ms; interquartile range: 15 to 65 ms, Fig. 2.6K) compared to PVF.

Representation of FRA type and binaural response properties: The representation of the different FRA-types showed slight differences between anterior and posterior cortical fields (Fig. 2.7A). Most units of anterior fields had monotonic V-shaped or monotonic double tuned FRAs (ADF: 54 %; AVF: 52 %), whereas non-monotonic V-shaped and non-monotonic double tuned FRAs were mainly found in posterior fields (PDF: 45 %; PVF: 40 %, Fig. 2.7C). The cortical representation of double tuned FRAs with harmonically related components did not show a specific clustering within certain subfields.

Figure 2.7B shows the representation of the different binaural response types in the AC of *P. discolor*. The distribution of binaural response types in the dorsal cortical fields was significantly different (Chi-Square test, $p < 0.05$) compared to the ventral cortical fields (Fig. 2.7D). Units of the dorsal fields were mainly driven by input from both ears and were classified as EE (ADF: 62 %; PDF: 38 %). In contrast, units of the ventral fields were predominantly characterized by EI input type. In detail, 53 % of units in AVF and 47 % of units in PVF were excited only through the contralateral ear and were inhibited by ipsilateral stimulation.

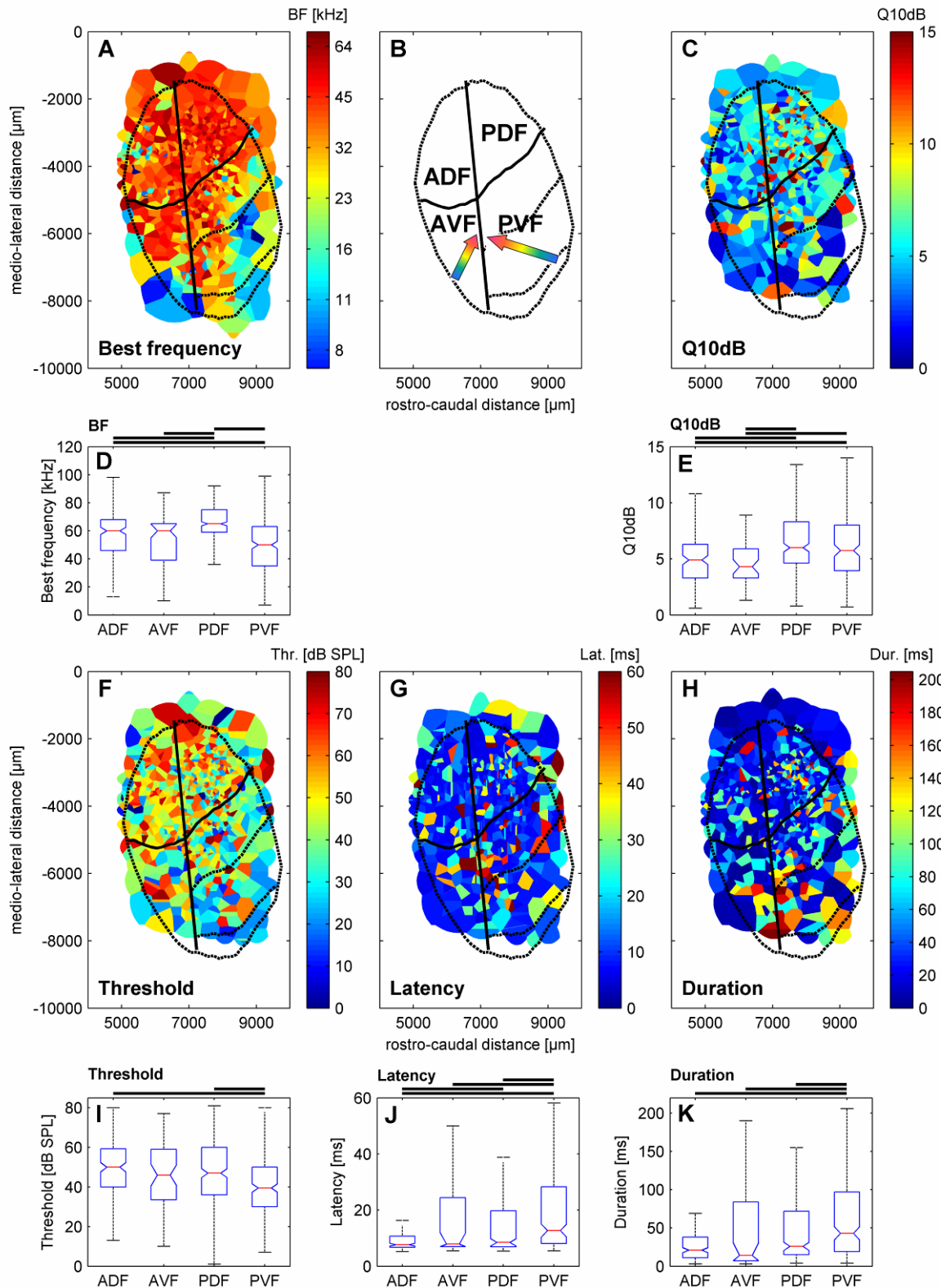


Fig. 2.6 *Spatial representation of response properties on the flattened cortical surface and statistical comparison between the four cortical fields. Tessellation maps of the spatial representation are shown for: A) Best frequency, C) Q_{10dB} value, F) Response threshold, G) First spike latency and H) Response duration. The outlines of AC and AC subfields are*

superimposed (black lines as in Fig 2.1). Panel **B**) shows the topographic position of the AC subfields of *P. discolor* derived from neuroarchitectural characteristics. The arrows indicate BF gradients in the tonotopically organized ventral fields. Statistical analysis of different cortical subfields are shown for: **D**) Best frequency, **E**) Q_{10dB} value, **I**) Response threshold, **J**) First spike latency and **K**) Response duration. Box plots show the median (red line) and the 25th and 75th percentiles. The 'whiskers' indicate the limits of the remaining percentiles. Outliers (Values >1.5 times the interquartile range) are not shown in the figure. The thick black lines above the plots indicate significant differences (Kruskal-Wallis test, $p < 0.05$). Abbreviations as in Fig. 2.1C.

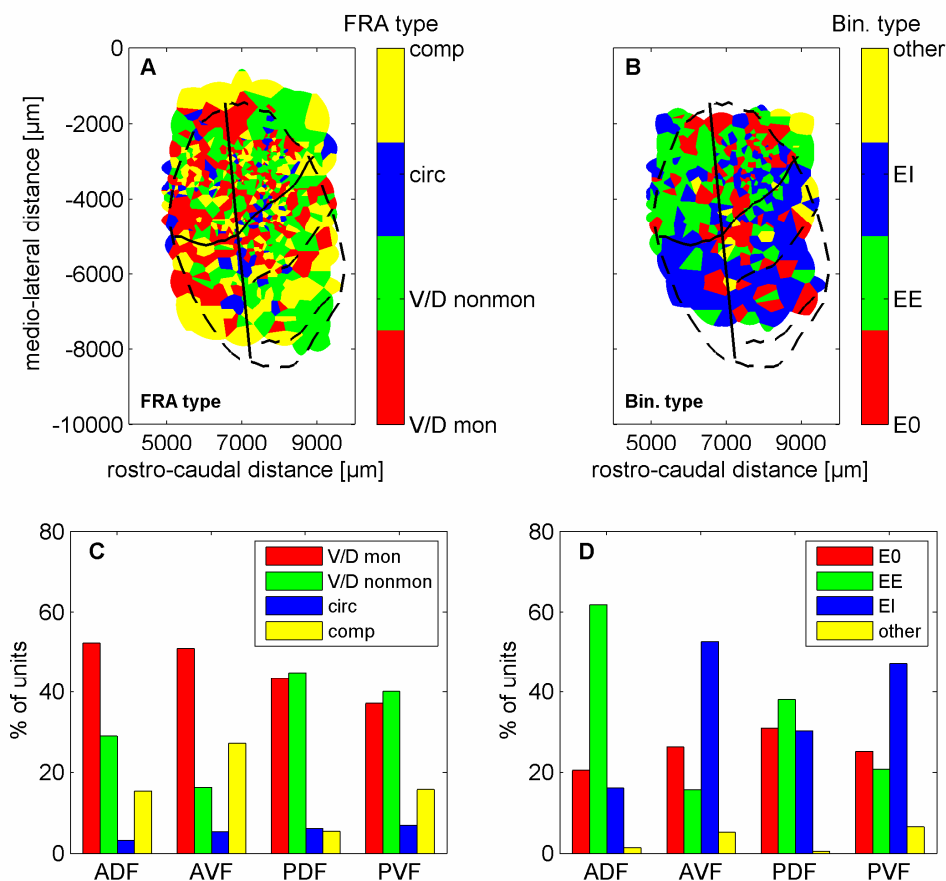


Fig. 2.7 Spatial representation of FRA types and binaural response types and distribution in different cortical subfields. Spatial representation **A**) and distribution in cortical subfields **C**) of the different FRA types. V/D mon: monotonically V-shaped/double-tuned; V/D nonmon: non-monotonically V-shaped/double-tuned; circ: circumscribed; comp: complex. Spatial representation **B**) and distribution in cortical subfields **D**) of the different binaural response types. EI: Excitatory/inhibitory; EE: Excitatory/ excitatory; E0: Excitatory/non-responsive. Abbreviation of field names as in Fig. 2.1C.

2.4 Discussion

This study investigated the localization, neuroarchitecture and basic physiological response properties of the AC of the bat *P. discolor*. The large area of neocortex responsive to acoustic stimulation comprises four anatomically distinguishable fields: a ventral part of the AC with an anterior and a posterior subdivision (AVF and PVF) and a dorsal part of the AC further divided into anterior and posterior subfields, ADF and PDF. The anatomical parcellation of the AC was consistent with the differentiated distribution of basic acoustical response properties of units in the cortical subfields. Location and extension of the AC of *P. discolor* as defined by neurophysiological and neuroarchitectural methods in this study roughly corroborated the findings from an earlier 2-DG study in the same species by Esser (1995).

2.4.1 Comparison with the auditory cortex of other bats

The distribution of BFs in the AC of *P. discolor* (see Fig. 2.4A) showed an overrepresentation of frequencies in the spectral range of the bat's echolocation pulse (40 to 90 kHz). This overrepresentation might be due to the fact that the dorsal fields are mainly containing units with BFs in the high-frequency range. Thus, a larger amount of cortical surface is devoted to units with high BFs as compared to units with low BFs. In addition, more units were recorded from the dorsal fields and this bias might also be reflected in the distribution of BFs. A similar overrepresentation of BFs in the spectral range of the echolocation pulses has been found in the AC of other microchiropteran bats e.g. *E. fuscus* (Jen et al. 1989), *Myotis lucifugus* (O'Neill 1995) and *C. perspicillata* (Esser and Eiermann 1999). In the CF/FM-bats *P. parnellii* (Suga and Jen 1976), *R. rouxi* (Radtke-Schuller and Schuller 1995) and *R. ferrumequinum* (Ostwald 1984) the overrepresentation of a narrow call-specific spectral range of the CF-part is reflected throughout the ascending auditory pathway (Schuller and Pollak 1979; Zook et al. 1985; Metzner and Radtke-Schuller 1987; Ross et al. 1988; RübSamen et al. 1988; Reimer 1991) and is based on specializations already implemented on the cochlear level (Kössl and Vater 1985; Vater et al. 1985; Kössl 1994).

In CF/FM-bats, a large part of the AC is involved in processing of specific combinations of the different harmonics in the echolocation pulse and echo. In *P. parnellii* and slightly less distinctive in *R. rouxi*, several fields can be segregated by virtue of selective responses of neurons to different combinations of FM-parts or CF components of call and echo. Neurons are tuned to delays between the components and are topographically ordered (O'Neill and Suga 1982; Suga and Horikawa 1986; O'Neill 1995). Such a complex representation of pulse and echo delay has generally not been found in FM-bats so far, although pulse-echo delay sensitive neurons exist in the AC of e.g. *M. lucifugus* (Paschal and Wong 1994) and in the dorsal parts of the AC of the phyllostomid bat *C. perspicillata* (Hackel and Esser 1998), which is closely related to *P. discolor*. In the present study, only pure tones but no echolocation related stimuli (e.g. FM/FM pairs) were used for acoustic stimulation (see Methods). Consequently, no statements concerning the functional involvement of cortical

subfields other than pure tone processing (e.g. delay sensitivity) can be made, so far. Besides that, the organization and parcellation of the AC of *P. discolor* is generally in accordance with that of *C. perspicillata*. The dorsal fields in the AC of *Carollia* were similarly characterized by neurons with BFs in the high-frequency range, and the ventral part of the AC was also composed of two tonotopically organized subfields, which shared a common high-frequency border (Esser and Eiermann 1999). In contrast, the AC of other non-phylostomid FM-bats like *M. lucifugus* and *E. fuscus* showed differentiation into subfields to a lesser degree (Wong and Shannon 1988; Dear et al. 1993). In both species tonotopically organized fields with frequency gradients running in opposite directions were found, but no fields with characteristics similar to the dorsal cortical fields in *P. discolor* were described.

A high percentage (55 %) of units in the AC of *P. discolor* had first spike latencies below 10 ms. As other studies in FM-bats reported mean latencies measured at 10 to 20 dB above threshold around 8 to 10 ms already on the level of the IC (Haplea et al. 1994; Klug et al. 2000), this seems to be unusually short. However, short latencies in the AC of FM-bats were also reported (Sullivan 1982). In addition, Haplea et al. (1994) showed that on the level of the IC latencies in *E. fuscus* still could be as short as about three milliseconds. Although most cortical neurons in *R. rouxi* had latencies in the range between 10 to 15 ms, short latencies below 10 ms were found in a substantial 18 % of neurons (Radtke-Schuller and Schuller 1995). The bias toward short latencies below 10 ms in *P. discolor* might be explained by the fact that a large number of recordings in our study were derived from dorsal regions of the AC where short latencies are predominately represented.

In contrast to findings in other mammals where the AI has been described to have the shortest latencies (Mendelson et al. 1997), the lowest median first spike latency in *P. discolor* was found in the ADF, whereas in the PVF, which might be equivalent to the AI, the longest first spike latencies were found. Our findings in *P. discolor* are supported by the fact that in the AC of *R. rouxi* shortest latencies were also found in the dorsal fields (Radtke-Schuller and Schuller 1995). In *R. rouxi*, ventral and dorsal cortical fields are not sequentially connected but rather receive connections from different parts of the auditory thalamus via different projection pathways (Fitzpatrick et al. 1998a; Radtke-Schuller 2004; Radtke-Schuller et al. 2004). In *P. discolor*, a similar connection pattern could explain the shorter latencies in the dorsal fields compared to the ventral fields. However, this hypothesis needs to be proved by future tracer studies in this species.

2.4.2 Influence of anesthesia and multi unit recordings on response patterns

A large proportion of units in the *P. discolor* AC showed onset-type responses. It is known that the response pattern of cortical neurons is influenced by anesthetics. For example, the use of barbiturates like pentobarbital that enhances GABA_A-mediated inhibition biased the distribution of response types toward short onset responses in the rat auditory cortex (Gaese and Ostwald 2001). The drug Midazolam used in our study, like other benzodiazepines, also

enhances action of GABA on GABA_A receptors. Thus, the high abundance of phasic onset-type responses in our study could be a consequence of the use of Midazolam. However, a high percentage of onset-type response patterns (68 %) were also found in neurons in the AC of awake *R. rouxi* (Radtke-Schuller and Schuller 1995) and awake mustached bats (Horikawa et al. 1994), indicating that even in the un-anesthetized bat phasic responses are common. This minimizes the potential effect of anesthetics on response types of cortical units in the present study. Another point that could have influenced the response pattern is that recordings in our study were not always derived from single units (see Methods). Seshagiri and Delgutte (2007) showed that adjacent neurons recorded simultaneously with tetrodes in the inferior colliculus of cats could differ significantly in their temporal discharge pattern although BFs and threshold were highly correlated. Therefore, blurring of response pattern is possible in some cases in multi unit recordings, but markedly dependent on the number of contributing neurons with dissimilar response types. As multi unit recordings in this study were generally derived from only up to three neurons (see Methods), and most units showed phasic responses the pooling of spikes in multi units should not have severely effected the response pattern in most cases.

2.4.3 Parcellation of the auditory cortex in *P. discolor*

One way of defining different fields of AC is by comparing the afferent connections with the auditory thalamus. Common to all mammals is a strong tonotopically organized projection from the ventral division of the medial geniculate body (MGBv) to AI (Winer et al. 2005). In contrast to this, non-tonotopically organized non-primary cortical areas receive major projections from the dorsal division of the MGB (MGBd) (Winer et al. 2005). CF/FM-bats like horseshoe bats (e.g. *R. rouxi*, (Radtke-Schuller 2004; Radtke-Schuller et al. 2004) and *P. parnellii* (Pearson et al. 2007)) follow this connectivity pattern. In both animals, AI contains a tonotopic map where frequencies of the CF-components of the calls are overrepresented while frequencies of the FM-components are largely absent (Suga and Jen 1976). In *R. rouxi*, neurons specialized for the processing of acoustic parameters relevant for echolocation (e.g. echo delay) are mainly represented in dorsally located cortical areas that are targeted by projections from the MGBd (Radtke-Schuller et al. 2004). The view of a congeneric projection from MGBv to AI covering the entire frequency range has been challenged by recent findings in the gleaning bat *Antrozous pallidus*. In this bat, the low frequency portion of a coherent frequency representation in the AC is innervated by the MGBv, whereas the high-frequency part received major projections from the supra-geniculate nucleus, a part of MGBd (Razak et al. 2007). Neurons in the high-frequency range were moreover of a distinct binaural input type (EO) and preferred FM-sweeps, whereas neurons in the low frequency part were classified as EI and responded preferentially to noise. Two functionally distinct pathways evidently exist in this bat species: first, a low frequency pathway serving for passive prey location and second, a high-frequency pathway serving for obstacle avoidance during active echolocation (Razak and Fuzessery 2002; Razak et al. 2007).

The approach that part of AI may not receive input from the MGBv challenges one of the traditional definitions for AI via connectivity that, however, does not constitute the only valid criterion.

The distribution of binaural response types in *P. discolor* resembles that in *A. pallidus*, whereas neuroarchitectonic and neurophysiological features argue for a cortical fields pattern of the AC in *P. discolor* similar to the arrangement in *R. rouxi* and other mammals. Tracer experiments were not included in the present study in *P. discolor*, and consequently data on thalamo-cortical connections are not available. However, neuroarchitectonic features provide valuable tools for the definition of subdivisions in AC when combined with neurophysiological outcomes. Undoubtedly, the combination of all three approaches would yield optimal possibilities to classify cortical subdivisions. The specific usefulness of different neurohistological stains to determine cortical fields will be discussed in the following: The staining for zinc proved to be specifically helpful, complementing staining for cells and myelinated fibers. The zinc stain reveals horizontal bands in the neocortex that show characteristic variation in width and staining intensity among cortical regions, sharply defining the borders between cortical areas and their subdivisions, and are generally coincident with the limits defined in the Nissl stained sections. The banding patterns are stable among the species studied so far, allowing for an interspecies comparison (e.g. rats: (Haug 1973; Zilles et al. 1990; Perez-Clausell 1996); mice: (Garrett et al. 1991); cats: (Dyck et al. 1993); wallabies: (Garrett et al. 1994) and humans (Franco-Pons et al. 2000)).

The PVF shows several features in the zinc stain characterizing primary sensory regions in the mammalian neocortex: conspicuous pale zinc staining of the outer portion of layer I, the differentiation of layer V in sublayers and, most characteristic, a wide, light band corresponding to layer IV encompassing the lower portion of layer III. In PDF, most distinctive to the PVF is the zinc staining of layer IV, which is narrower and more heavily stained, whereas layer V is thicker and of higher staining intensity. Zinc staining in AVF is generally intense. These features of PDF and ADF have been described to be characteristic for secondary sensory regions (rats: (Haug 1973; Perez-Clausell 1996; Zilles et al. 1990); mice: (Garrett et al. 1991); cats: (Dyck et al. 1993); wallabies: (Garrett et al. 1994) and humans (Franco-Pons et al. 2000)). Furthermore, the structure of ADF seems unique in that it could be an amalgam of auditory and neighboring non-auditory, probably somatosensory areas. Mixed auditory-somatosensory fields neighboring the AC rostrally have been reported for several mammalian species (flying fox and gray squirrel: (Krubitzer et al. 1986; Krubitzer et al. 1993); mouse: (Carvell and Simons 1987); cat: (Clemo and Stein 1983); rat: (Brett-Green et al. 2003)).

The accordance of response properties of cortical units in AVF and PVF with the anatomical partitioning of ventral auditory fields in the cortex is a further strong support, that the PVF might correspond to AI in *P. discolor*. PVF is tonotopically organized with BFs increasing from caudal to rostral. The AVF shows also a tonotopic organization but in contrast to the PVF, BFs increase from rostro-ventral to caudo-dorsal locations. This organization is in accordance to findings in other mammals where tonotopic gradients with roughly opposite

directions have also been identified in the AI and the AAF (e.g. cat: (Reale and Imig 1980); ferret: (Bizley et al. 2005); gerbil: (Thomas et al. 1993); bat: *C. perspicillata* (Esser and Eiermann 1999)). Because of the common high-frequency border of the AVF and PVF, high frequencies are represented all the way along the medial border of the PVF down to the most ventral border of this field (see Fig. 2.6A). In addition, no clear tonotopic gradient can be seen in the PDF that could be a tonotopic continuation of the frequency representation in the ventrally located PVF. Thus, it is unlikely that the PDF just represents the high-frequency portion of a contiguous frequency representation starting with low frequencies in the PVF as assumed for the AC of *A. pallidus* (Razak et al. 2007). It is more likely that the PDF represents a non-tonotopically organized field like the dorsal fields found in other bats before (e.g. *R. rouxi* (Radtke-Schuller and Schuller 1995) and *C. perspicillata* (Esser and Eiermann 1999), see above). However, also in *C. perspicillata* information about the thalamo-cortical connections is lacking.

In addition to BF, the distribution of several response properties like duration and first spike latency showed significant differences between the PDF and the PVF. To further test the possibility that high-frequency units in the PDF and PVF belong to a contiguous frequency representation like in *A. pallidus* (Razak et al. 2007), we additionally tested the differences of latency and response duration only for the high-frequency units (BF >50 kHz) of both cortical fields. Latency and response duration for high-frequency units alone was still significantly different (Mann-Whitney U test, $p < 0.05$) between PDF and PVF. These findings further strengthen our parcellation of the AC based on the anatomical findings.

2.5 Conclusions

In this study, four subfields were identified in the AC of the bat *P. discolor*. These differed in their neuroanatomical attributes and in the response properties of their units to pure tone stimulation. The neuroanatomical and neurophysiological properties of the tonotopically organized PVF reflected common characteristics of AI in the mammalian AC (e.g. very wide and pale zinc staining band in layer III/IV, BF gradient ascending from caudal to rostral). The AVF located rostrally to the PVF showed a tonotopic BF gradient running roughly in opposite direction to the gradient of the PVF. Thus, the AVF of *P. discolor* might represent the AAF described in other mammals. The dorsal part of the AC of *P. discolor* was non-tonotopically organized with BFs mainly in the high-frequency range. As most energy of the echolocation pulse of this bat species is contained in the frequency range between 60 to 80 kHz, the dorsal region of the AC of *P. discolor* seems to be particularly important for echolocation. With regard to the relative position of cortical fields and their basic properties of BF representation, the AC of *P. discolor* seems to follow the organizational pattern seen in other phyllostomid bats.

To further compare the parcellation of the AC of *P. discolor* with those of other bats and mammals, the specific connectivity between subdivisions of the AC and different divisions of the auditory thalamus of *P. discolor* must be investigated in future studies.

2.6 Methods

2.6.1 Experimental animals

All experiments were performed in agreement with the principles of laboratory animal care and under the regulations of the current version of German Law on Animal Protection (approval 209.1/211-2531-68/03 Reg. Oberbayern).

Five male and five female adult spear-nosed bats (*Phyllostomus discolor*, body weight: 30 to 45 g) were used in this study. The animals originated from a breeding colony in the Department Biology II of the Ludwig-Maximilians-University in Munich. For experiments, animals were kept separated from other bats under semi-natural conditions (12 h day/ 12 h night cycle, 65 to 70 % relative humidity, 28°C) with free access to food and water.

2.6.2 Anesthesia and surgical preparation

In a pre-recording surgical session, the bat was prepared under anesthesia to provide for stable stereotaxic fixation in well defined coordinates and proper access to the target area. For anesthesia, a combination of Medetomidin (Domitor®, Novartis, Mississauga, Canada), Midazolam (Dormicum®, Hoffmann-La Roche, Mississauga, Canada) and Fentanyl (Fentanyl-Janssen®, Janssen-Cilag, Neuss, Germany) was injected subcutaneously (MMF, 0.4, 4.0 and 0.04 µg/g body weight). Skin and muscles covering the upper part of the cranium were cut rostro-caudally along the midline and shifted aside laterally. The cranial bone was completely cleaned of all remaining tissue and a small metal rod was fixed onto the caudal part of the bat's skull using light-curing dental cement (Charisma®, Heraeus Kulzer, Wehrheim Germany). After surgery, the anesthesia of the animal was antagonized by injecting a weight-dependent dose of a mixture of atipamezole hydrochloride (Antisedan®, Novartis), Flumazenil (Anexate®, Hoffmann-La Roche) and Naloxon (DeltaSelect®, DeltaSelect, Dreieich, Germany) subcutaneously (AFN: 8.1, 0.034 and 0.32 µg/g bodyweight). To alleviate postoperative pain, the analgesic Meloxicam (Metacam®, Boehringer-Ingelheim, Ingelheim, Germany, 0.2 mg/kg bodyweight) was administered after full recovery of the bat.

2.6.3 Stereotaxic procedure and verification of recording sites and correlation with neuroarchitectural features

A detailed description of the stereotaxic procedure, determination of brain orientation and reconstruction of recording sites has been already published elsewhere (Schuller et al., 1986). In brief, the animal's head was fastened with the surgically mounted rod to a stereotaxic frame in a well defined orientation. The alignment of the animal's skull and consequently the

brain within the stereotaxic coordinate system was measured by scanning characteristic profile lines of the skull. The profile lines were measured in parasagittal and frontal planes (500 μm steps) relative to a fixed reference point and compared to a profile defining a standardized orientation of the skull and brain of *P. discolor* (Fenzl and Nixdorf, unpublished data), that also determines the normal axes of the available brain atlas of the animal. Thus, deviations of the actual alignment of the bat's head from the standardized position could be corrected by appropriate tilt and pitch of the animal within the experimental setup. Any reorientation of the skull is thus under accurate stereotaxic control. This procedure allowed the pooling and comparison of all electrophysiologically measured data, brain lesions and tracer deposits within one and among different experimental animals. Locations of lesions or marker (HRP, WGA-HRP) deposits were determined after transcatheter perfusion and subsequent histological processing of the brain based on the brain atlas. These atlas-oriented coordinates were compared with those of the physiologically determined reconstruction of the specific location. This allowed a verification of the validity of recording coordinates, or eventually indicated errors that could typically be corrected after retracing the mistake in localization.

For the analysis of the neuroarchitectural features of the auditory cortex, series of frontal sections stained for cresyl violet, myelin (Gallyas 1979) and zinc were available. For the detection of zinc, brains were processed according to a modification of the Timm method (Danscher 1981). Zinc plays an important role in cell physiology (Vallee and Falchuk 1993) and has synaptic signaling functions in the mammalian brain (Frederickson 1989; Frederickson and Moncrieff 1994). In the neocortex, the stain for zinc reveals horizontal bands that show marked variation in width and staining intensity among functionally different cortical regions. These characteristic banding patterns are generally coincident with the limits defined in the Nissl stained sections, but have the advantage that they are readily noticeable at low magnification.

Additional series of frontal sections stained for the calcium-binding proteins, acetylcholinesterase (ACHE), cytochrome-oxidase were not included in the analysis presented here, as they did not allow the differentiation between core and belt regions as clearly as described for other mammals with a more highly evolved neocortex (e.g., ACHE: (Wallace et al. 1991; Hackett et al. 2001); Cytochromoxidase: (Clarke and Rivier 1997); calcium-binding proteins: (Hackett et al. 1998; Cruikshank et al. 2001)). Therefore, although involving a complicated perfusion procedure, the stain for zinc was chosen as histochemical marker to delineate cortical areas.

2.6.4 Acoustic stimuli and recording of neuronal responses

All experiments were conducted in a heated (36°C), electrically shielded and anechoic chamber. They normally lasted 4 hours per session and were performed at four days a week for up to six weeks. For each session, the bat was anaesthetized using MMF (see above). Throughout the whole experiment the animals were supplied with oxygen. To lower

electrodes into the brain areas for recording of neural responses, small holes of about 500 microns in diameter were drilled into the animal's skull above the AC and the dura was perforated. Electrode penetrations were generally carried out in tangential direction, roughly parallel to the surface of the brain (bat #1 to 5, #8 and #9) or in a roughly perpendicular direction to the brain surface (bat #10). Two mapping experiments were done with orthogonal electrode penetrations (bat #6 and 7) to cover the entire AC in single individual bats and to neurophysiologically outline the borders and reveal possible tonotopic trends of the AC as a whole. Only basic properties like tuning and threshold were recorded in these two experiments.

Search stimuli for neuronal activity were pure tones with 20 ms duration produced with a frequency generator (Wavetek model 136, 186, FG-5000) and a custom-made pulse former. The attenuation of these stimuli could be modified manually (external attenuator AP401, adret électronique, France). The stimuli were presented via custom-made ultrasonic earphones (Schuller 1997) with a flat frequency response (± 3 dB SPL between 10 to 100 kHz). As it was not always possible to discriminate the activity of a single neuron, the term 'unit' is used in the text to describe the activity of one neuron to clusters of up to three neurons recorded at a distinct recording site. Once a unit was detected, its BF was determined audio-visually. For most units, the frequency response area (FRA) was determined in more detail. Therefore, pure tone stimuli (20 ms duration, 2 ms rise and fall time), in various frequency and sound pressure level combinations were presented contralaterally. Although *P. discolor* emits FM-pulses for echolocation, pure tone stimuli were used to allow comparison of the data to a previous study in a closely related phyllostomid bat, *C. perspicillata*, (Esser and Eiermann 1999). The stimulus duration of 20 ms is roughly intermediate between the short echolocation pulses (<3 ms) and longer social calls (about 50 ms, (Esser and Daucher 1996)) of *P. discolor*.

The binaural response properties were determined at the unit's BF by using ABI (averaged binaural intensity, (Irvine et al. 1996)). 20 ms long pure tones were presented binaurally with increasing intensity at contralateral and decreasing intensity at ipsilateral side and vice versa. The interaural intensity difference (IID) was changed from -20 dB SPL to +20 dB SPL in steps of 5 dB SPL. The level of the signals was chosen so, that both ears were stimulated at 20 dB SPL above the unit's auditory threshold. Thereafter, the same stimuli were presented monaurally to the contralateral and ipsilateral ear.

All stimuli for neuronal recordings were computer-generated (Matlab® 6.1; Mathworks, Natick, USA), digital-analog converted (RX6; sampling rate 260 kHz, Tucker Davis Technologies, Gainesville, USA) and attenuated (PA5, Tucker Davis Technologies, Gainesville, USA). The acoustical stimulus parameters (frequency/sound pressure level combinations) were presented pseudo-randomly with a repetition rate of 1.3 Hz, a silent interval of 10 to 50 ms leading stimulus onset and with 10 repetitions of the entire parameter set.

Responses from units in the AC were recorded extracellularly by using either borosilicate glass electrodes (#1B100F-3, WPI, Sarasota, USA) filled with 2 M NaCl and 4 % pontamine sky blue (3 to 8 M Ω impedance), carbon fiber microelectrodes (Carbostar-1, Kation Scientific, Minneapolis, USA; 0.4 to 0.8 M Ω impedance) or glass insulated tungsten

microelectrodes (Alpha Omega GmbH, Ubstadt-Weiher, Germany, 1 to 2 M Ω impedance). Responses were amplified (Electro 705, WPI; ExAmp-20 FB, Kation Scientific or RA16PA, Tucker Davis Technologies, Gainesville, USA for glass microelectrodes, carbon fiber electrodes or tungsten microelectrodes, respectively), band-pass filtered and fed into an A/D-converter (RP2.1 or RX5, Tucker Davis Technologies, Gainesville, USA, sampling rate: 25 kHz). Using the stimulation and analysis software “Brainware” (J. Schnupp, distributed by Tucker Davis Technologies, Gainesville, USA) action potentials were threshold discriminated and saved for offline analysis on a personal computer.

2.6.5 Data analysis

All non-commercial computer programs used for data analysis were written in Matlab[®]. Data analysis was done based on peri-stimulus time histograms (PSTH, 1 ms bin width) constructed from the spike responses to different parameter sets. The time window for analysis was adjusted to the total response duration of the unit. It started when the first bin exceeded the level of spontaneous activity and ended when the response reached steady spontaneous level again. The level of spontaneous activity was derived from the silent period preceding each stimulus onset. First spike latency was determined for stimuli presented at the unit’s BF at a level of 20 dB SPL above threshold (see below for details on BF and threshold). The latency of the first spike to each presentation was used to calculate the median value of first spike latency. Only spikes occurring within the time window for analysis were included in the calculation.

The response characteristics of units that were tested at different combinations of frequency and sound pressure level, were visualized as FRA constructed from the summed activity within the given time window. Responses at different frequency level combinations were considered to be significant if the spike rate exceeded 20 % of the absolute maximum response of the unit. Basic characteristic values of the units like best frequency and tuning quality (Q_{10dB} and Q_{30dB}) were directly derived from the FRA. The data basis for best frequency thresholds is the same as used for a previous publication (Hoffmann et al. 2008a). However, data was re-analyzed in the present paper regarding the topographical distribution of thresholds within the AC of *P. discolor*. FRAs of units were classified as V-shaped, circumscribed, double-tuned or complex following roughly the categories used by Heil and Irvine (1998) and Sutter (2000). The spike rate of units with circumscribed FRAs decreased at all frequencies to zero with increasing stimulus level. Double tuned units had FRAs that showed two clearly separable response regions, whereas complex FRAs consisted of multiple activity patches separated by regions of low activity. Cortical units classified as V-shaped responded over a contiguous range of frequency level combinations. V-shaped and double tuned FRAs were further distinguished according to their spike rate level function as monotonic or non-monotonic. The unit was labeled as non-monotonic if the spike-rate decreased again to below 75 % of the maximum at BF at higher levels. Thus, units with circumscribed FRAs always featured non-monotonic spike-rate-level functions by definition.

$Q_{10\text{dB}}$ values as a measure of sharpness of frequency tuning were calculated using the following equation: $Q_{10\text{dB}} = \text{BF}/\text{bandwidth}$ measured 10 dB SPL above threshold. Double tuned and complex units did not generally allow determining a $Q_{10\text{dB}}$ value. If the shape of FRAs allowed, $Q_{30\text{dB}}$ values were also measured.

To determine a unit's binaural properties, the mean number of spikes was plotted as a function of IID for binaural, monaural contralateral and monaural ipsilateral stimulation. Comparison of these curves allowed the grouping of the binaural properties into four categories. Units that were excited by monaural stimulation of each ear were named EE (excitatory-excitatory). Units that only received excitatory input from the contralateral ear are named E0 (excitatory input only from the contralateral ear). In case the unit was excited by monaural contralateral stimulation, did not respond to monaural ipsilateral stimulation and showed inhibition in binaural stimulation, it was classified as EI (excitatory-inhibitory). The last group ("other") contained units that could not be ranked into one of the previous groups.

The locations of recording sites were projected to the flattened surface of the auditory cortex. For a detailed description of the surface projection method, see (Schuller et al. 1991). Briefly, each recording site was projected to the location at the cortical surface that had the shortest distance to the recording site. For the flattening process, the distance of the projected recording site to the origin fixed at 2000 μm lateral from the midline of the brain (upper blue line in Fig. 2.1B) was calculated. Thus, distortions due to irregularity of the cortical surface (e.g. pseudocentral sulcus) were avoided.

Distribution and trends of parameters on the cortical surface are represented with the help of the Voronoi tessellation procedure in two dimensions implemented with Matlab[®]. In detail, recording sites of the chosen parameter are connected with all neighboring recording sites. Cells characterizing the value of a special parameter around recording sites are constructed as polygons whose sides pass equidistantly between recording sites and cross the connection lines perpendicularly.

2.7 Acknowledgements

We thank Claudia Schulte and Horst König for their technical help. Special thanks go to Tom Fenzl and Andreas Nixdorf for providing additional anatomical material and for help with the preparation of the *Phyllostomus* brain atlas. We also thank three anonymous reviewers whose comments helped to improve the manuscript. This work was supported by the Volkswagen Foundation (I/79782) and the Deutsche Forschungsgemeinschaft GRK 1091 "Orientation and Motion in Space".

3.A neural correlate of stochastic echo imaging

This study was published in 2006 by Uwe Firzlaff, Sven Schörnich, Susanne Hoffmann, Gerd Schuller and Lutz Wiegrebe, in the Journal of Neuroscience (Vol. 26(3), pp. 785-791).

The neurophysiological experiment was designed and implemented by Uwe Firzlaff. The acquisition of neurophysiological data was done by Uwe Firzlaff and me. The neurophysiological data was analyzed by Uwe Firzlaff, Lutz Wiegrebe and me. Gerd Schuller provided the equipment for the neurophysiological setup. The psychophysical experiment was designed by Lutz Wiegrebe and Sven Schörnich, and implemented by the latter. The psychophysical data was analyzed by Sven Schörnich. The parts of the paper concerning the psychophysical experiment were written by Sven Schörnich and Lutz Wiegrebe, and the parts concerning the neurophysiological experiment were written by Uwe Firzlaff and Gerd Schuller.

3.1 Abstract

Bats quickly navigate through a highly structured environment relying on echolocation. Large natural objects in the environment, like bushes or trees, produce complex stochastic echoes, which can be characterized by the echo roughness. Previous work has shown that bats can use echo roughness to classify the stochastic properties of natural objects. This study provides both psychophysical and electrophysiological data to identify a neural correlate of statistical echo analysis in the bat *Phyllostomus discolor*. Psychophysical results show that the bats require a fixed minimum roughness of 2.5 (in units of base 10 logarithm of the stimulus fourth moment) for roughness discrimination. Electrophysiological results reveal a subpopulation of 15 of 94 recorded cortical units, located in an anterior region of auditory cortex, whose rate responses changed significantly with echo roughness. It is shown that the behavioral ability to discriminate differences in the statistics of complex echoes can be quantitatively predicted by the neural responses of this subpopulation of auditory cortical neurons.

3.2 Introduction

Through echolocation, a bat can determine not only the position of an object in the dark, but also its structural features, which are encoded in the acoustic image of the object within the echo. The acoustic image of an object is defined as the sum of the reflections in response to

an acoustic impulse of theoretically infinite shortness and infinite amplitude (Dirac impulse), and is referred to as the impulse response (IR) of the object. Technically, the echo a bat will perceive is the convolution of the bat's sonar emission and the IR. Larger natural objects like trees have a very complex structure with thousands of reflective surfaces which are provided by the leaves and branches. Moreover, this structure (and thus, its IR) will be highly unstable over time because movements of the leaves caused by wind will occur and a bat will rarely encounter a tree twice from exactly the same angle. Echoes reflected from these surfaces will have no systematic spectral interference pattern. However, a bat should be able to identify natural objects to navigate within complex surroundings or, in the case of frugivorous bats, for the classification of trees that provide food. A comparative analysis of the IRs of two different trees has indicated that the degree of envelope fluctuation of the IRs (i.e., the IR roughness) is a good predictor for the correct association of the IRs to the corresponding tree (Muller and Kuc 2000). A broad-leafed tree with relatively fewer but larger reflective surfaces will produce a rough IR, whereas the small leaves of a conifer will produce many reflections with low amplitude, resulting in a smooth IR. A free-field study confirmed the high predictive power of the IR roughness for the classification of natural objects (Stilz 2004).

In a psychophysical playback experiment with phantom objects, Grunwald et al. (2004) showed that the fruit-eating bat *Phyllostomus discolor* can learn to discriminate echoes generated with a smooth IR from echoes generated with a rough IR, and that once they had learned this discrimination task, *P. discolor* spontaneously classified unknown IRs according to IR roughness. A functional auditory simulation of these results suggested that modulation-sensitive neurons in the midbrain with best modulation frequencies above ~80 Hz could provide a neural basis for this performance.

Neural processing of echo roughness has not been studied so far. It is especially interesting to directly relate neural processing to behavioral performance, an attempt that has only been made a few times in bats (Riquimaroux et al. 1991; Riquimaroux et al. 1992). Thus, two questions are pursued here: (1) what are the behavioral thresholds for auditory-object discrimination based on IR roughness in *P. discolor* and (2) is there an auditory cortical correlate of the behavioral performance? The first question is addressed with a psychophysical phantom-object experiment. The second question is addressed with electrophysiological recordings from neurons in the auditory cortex of *P. discolor* with a stimulation paradigm that closely matches the psychophysical paradigm.

3.3 Materials and methods

3.3.1 Animals

The experimental animal, the lesser spear-nosed bat *P. discolor*, forages for fruit, nectar, pollen, and insects in a neotropical forest habitat and navigates through highly structured surroundings. *P. discolor* emits brief (<3 ms), broad-band multiharmonic echolocation calls covering the frequency range between 40 and 90 kHz.

3.3.2 Psychophysics

The psychophysical experiments were implemented as virtual-object playback experiments. The bats were required to evaluate the echoes of their echolocation calls. These echoes were generated by convolving in real time the calls with the acoustic impulse response of a virtual object. Thus, unlike in classical psychoacoustic experiments, the bats did not hear sounds unless they emitted echolocation calls.

Four female bats were used for the psychophysics. All four animals were housed together with access to water *ad libitum*, except during individual training sessions. Training sessions were usually conducted 5 d per week, followed by a 2 d break. On training days, the bats received food only as a reward (consisting of banana pulp) in the training setup. On the days without training they had access to mealworms (larvae of *Tenebrio molitor*) *ad libitum*.

Impulse responses. We created complex IRs with different degrees of roughness, similar to a previous experiment (Grunwald et al. 2004). Each IR consisted of sparse noise, which is generated by inserting random-width temporal gaps between the amplitude values of Gaussian noise (Hübner and Wiegrebe 2003). All IRs generated this way had chaotic waveforms (see Fig. 3.3, first column) and frequency-independent (white) magnitude spectra (data not shown). Thus, the magnitude spectra do not vary systematically with IR roughness. When such an IR is convolved with an echolocation call, the resulting echo has the magnitude spectrum of the echolocation call (see Fig. 3.3, third column) because a convolution in the time domain corresponds to a multiplication in the frequency domain.

IR roughness was quantified in terms of the fourth moment (M_4 ; the IR wave form raised to the power of four divided by the squared wave form raised to the power of two (Hartmann and Pumplin 1988)). Roughness values are given as the base 10 logarithm of the M_4 ($\log_{10}M_4$). The IRs were sorted into 31 groups ranging from a roughness of 0.5 to $3.5 \log_{10}M_4$. Each group contained 25 different IRs of the same roughness, giving a total of 775 IRs, thereby ensuring that each IR was rarely presented twice. All IRs had the same root-mean-square amplitude. At a sampling rate of 250 kHz, the IRs had a duration of 14.4 ms, equivalent to an object depth of ~ 2.5 m.

Experimental setup. The bats were trained in a two-alternative, forced choice playback setup. It consisted of a Y-shaped maze, inversely mounted on the wall of an echo-attenuated chamber at an angle of 45 degrees. The starting perch was located at the top end. In each branch, a reward feeder, a 0.25 inch microphone (model 4135; B&K Instruments, Naerum, Denmark), and a speaker (model EAS10 TH800D; Matsushita, Osaka, Japan) were mounted facing toward the starting perch. During the experiment, the emitted echolocation calls were recorded by both microphones. Each microphone output was amplified (model 2610; B&K Instruments), bandpass filtered (30–100 kHz; model 3550; Krohn Hite, Brockton, MA), and digitized by a data-acquisition board [data acquisition processor (DAP) 5200a; Microstar, Bellevue, WA] at a sampling rate of 250 kHz. The boards convolved the input with two different IRs (a smooth IR on one side and a rougher IR on the other) on the DAP-boards by zero-padding both the recorded call and the IRs to 4096 samples, and multiplying the

complex spectra of the recorded call and IR. This procedure corresponds to the formation of an echo of a phantom object, that is to say, every change in the bat's echolocation call results in an immediate change in the artificial echo. The artificial echo was amplified (model 6110; Harman/Kardon, Château du Loir, France) and played back to the bat after a total delay of 18 ms, corresponding to a target distance of ~3 m.

Procedure. All four bats were trained to discriminate IR roughness in a two-alternative, forced-choice paradigm. To obtain a food reward the bats had to crawl toward the end of that branch of the Y maze where the echo generated with the IR of reference roughness originated. The test IR roughness was always higher than the reference roughness. When the bats' performance exceeded 85 % correct in this discrimination task, psychometric functions were obtained. Whereas the reference roughness was kept constant, the test roughness was changed randomly. The stochastic IRs were refreshed for every presentation. Each point of the psychometric function is based on 30 trials. The discrimination threshold was set to 75 % correct, which, on the basis of 30 trials, corresponds to a significance level of $p < 0.05$. The experiment was repeated four times with four different reference roughnesses, namely 0.5, 1.8, 2.5, and 2.8 log₁₀M4.

3.3.3 Neurophysiology

Surgery. All experiments complied with the principles of laboratory animal care and were conducted under the regulations of the current version of the German Law on Animal Protection (approval 209.1/211-2531-68/ 03, Reg. Oberbayern). The principle surgical procedure has been described in detail previously (Schuller et al. 1991). In brief, bats were anesthetized using a combination of medetomidin, midazolam, and fentanyl (0.4, 4, and 0.04 µg/g body weight, respectively). The skin overlying the skull was opened along the midline and the skull surface was freed from tissue. A small metal tube was fixed to the skull using a microglass composite to secure the animal to a stereotaxic device, and the accurate skull position in stereotaxic coordinates was determined as described in detail previously (Schuller et al. 1986).

Stimulus production and recording of neural responses. Experiments were conducted in an anechoic chamber. Acoustic stimuli were computer generated (Matlab; Mathworks, Natick, MA), digital-analog converted (RV8; sampling rate, 400 kHz; Tucker Davis Technologies, Gainesville, FL), filtered and attenuated (TDT FT-6; TDT PA5; Tucker Davis Technologies), and binaurally presented via custom-made ultrasonic earphones with a flat frequency response (± 3 dB) between 10 and 100 kHz (Schuller 1997). Stimuli consisted of a typical echolocation call of *P. discolor* (frequency range, 40-90 kHz) convolved with a stochastic IR. After the convolution, the stimuli had a duration of 18 ms. Fifty IRs in five groups of roughness were used (1.8, 2.0, 2.3, 2.5, and 2.8 log₁₀M4) (i.e., in the range of the behavioral experiments). Stimuli were randomly presented at 20-30 dB above the pure-tone threshold of a neuron, with 10-20 repetitions of the entire set and a silent interval of 10 ms before stimulus onset. The repetition rate was 1.3 Hz. Action potentials from neurons in the auditory cortex of three

lightly anesthetized bats were recorded extracellularly using glass microelectrodes filled with 2 M NaCl and 4 % pontamine sky blue (3-8 M Ω impedance). Because it was not always possible to clearly discriminate the activity of a single neuron, the term “unit” will be used in the following to describe the collective activity of one to three neurons recorded at a recording site. Neural activity was monitored audiovisually, and threshold and best frequency of a unit were roughly determined. Action potentials were amplified using conventional methods and recorded using an analog-to-digital converter (RP2.1; Tucker Davis Technologies; sampling rate, 25 kHz) and Brainware (Tucker Davis Technologies). Electrode penetrations were tangential to the brain surface. After the completion of an experiment, lesions were made to the brain to reconstruct the position of recording sites from subsequent histological processing in standardized coordinates of a brain atlas of *P. discolor* (A. Nixdorf, T. Fenzl, B. Schweltnus, unpublished data).

Data analysis. Spike responses from all 50 stimuli were displayed as peristimulus time histograms (PSTH; 1 ms bin width) and raster plots. Units typically responded with an onset response followed by a clearly distinguishable sustained response component. As will be seen below, the onset response occurred with each of the 50 stimuli independent of roughness. Therefore, it was excluded from additional analysis by setting a time window containing only the sustained response. Size and position of the window were derived from the PSTH. The analysis window started immediately after the end of the onset response and ended when the sustained response level reached the level of spontaneous activity. Spontaneous activity was derived from the 10 ms time window preceding stimulus onset. Responses to stimuli from each of the five roughness groups were tested for statistically significant differences using a Kruskal–Wallis Test with a correction for multiple testing (Matlab statistics toolbox; Mathworks). Significance was set at $p < 0.05$.

3.4 Results

3.4.1 Psychophysics

A psychometric function for IR roughness discrimination with a reference roughness of 1.8 (in units of $\log_{10}M4$) is shown in the inset of Figure 3.1. Data are averaged across the four animals. The Stochastic Echo Processing function shows that for a reference roughness of 1.8, the bats need a test roughness of at least 2.5 to reliably discriminate IR roughness.

The four horizontal bars present the summary results for the four values of reference roughness. Each bar shows the minimal roughness difference needed to significantly discriminate IRs with the test roughness from IRs with the reference roughness. These results show that there is a fixed behavioral threshold for IR roughness discrimination; a roughness of ~ 2.5 is required by the bats to reliably discriminate an IR with this roughness from a smoother one. Above this threshold, discrimination performance improves substantially.

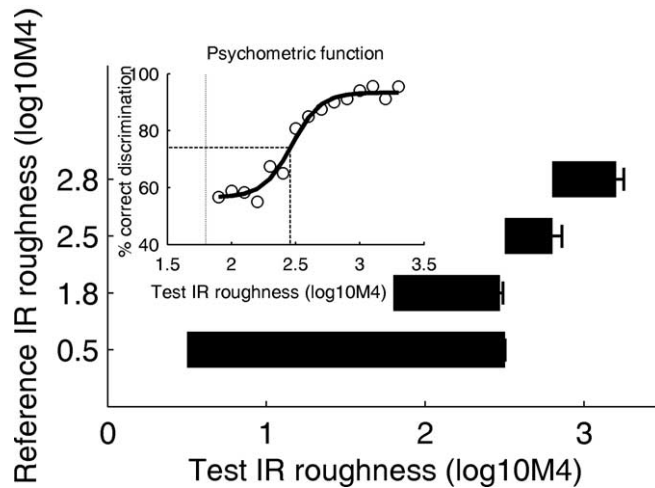


Fig. 3.1 Results of the psychophysical experiments. The inset shows a psychometric function for IR-roughness discrimination (open circles). The reference IR roughness was 1.8 (vertical dotted line). The discrimination threshold was determined by fitting a sigmoid function (strong solid line) and extracting the 75 % correct value (dashed lines). The horizontal bars show the average results for the four values of reference roughness. The left end of each bar shows the reference roughness, and the right end shows the discrimination threshold. Error bars represent across-animal SE.

3.4.2 Neurophysiology

Results are based on 94 cortical units. All units responded well to frequencies in the range of the echolocation calls of *P. discolor* (40-90 kHz). A total of 15 of 94 units responded with significant difference to stimuli with different degrees of roughness ($p < 0.05$; Kruskal-Wallis nonparametric one-way ANOVA). The raster plot and the summary PSTH in Figure 3.2 reveal a strong onset response followed by a variable degree of sustained activity. For the response-strength analysis, only the sustained activity was used. The analysis window was terminated when the level of spontaneous activity was reached. The range of analysis-window durations of all roughness-sensitive units was from 19-126 ms (median, 34 ms). The stimulus duration was 18 ms. Thus, the analysis window was often considerably longer than the stimulus duration.

Examples of responses of four units whose firing increased significantly with increasing stimulus roughness are shown in the right panels of Figure 3.2. Note that the stimuli with different roughnesses share the same sound-pressure level and the same power spectrum (compare Fig. 3.3). Except for one unit, all units with significant roughness coding responded stronger to stimuli with higher roughness. This is shown in a summary plot of all units in Figure 3.4. The regression line for roughness-sensitive units has a significantly steeper slope

compared with the regression line for non-sensitive units [ANCOVA linear regression; Matlab signal processing toolbox (Mathworks); $p < 0.001$].

The relative strengths of onset and sustained responses do not correlate to the ability of the units to encode echo roughness. In 70 of the 94 units, the onset-response magnitude was weaker than the sustained response; in 24 units the opposite was true. Of the 14 roughness-sensitive units in which responses increased significantly with increasing roughness, eight had a stronger onset response than sustained response, and the other six had a stronger sustained response.

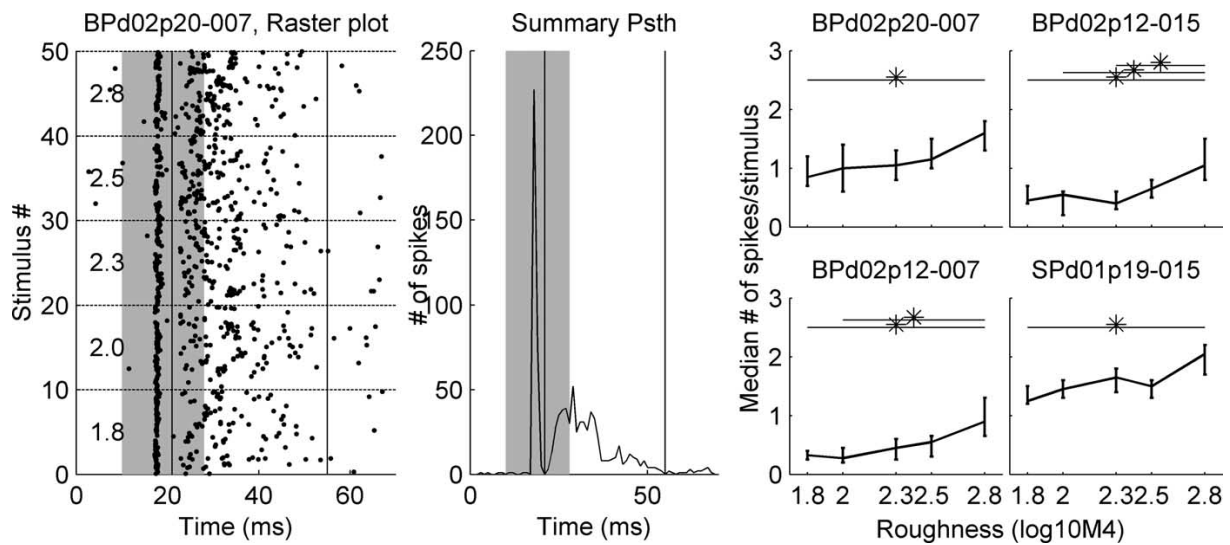


Fig. 3.2 *Electrophysiological results. The left plot shows a raster plot of a roughness-sensitive unit to 10 repetitions of all 50 stimuli; the middle plot shows the PSTH summed over all stimuli and repetitions. The summary PSTH was used to exclude the onset responses from additional analysis by setting a time window (vertical solid lines in the PSTH and raster plot), which started immediately after the end of the onset response and ended when the sustained response level reached the level of spontaneous activity. The time of stimulus presentation is indicated by the gray area in the PSTH and raster plot. Response strength as a function of IR roughness is shown for four roughness-sensitive units in the auditory cortex of *P. discolor* in the four panels on the right. Response strength is shown as the median number of spikes per stimulus across 10 different echoes sharing the IR roughness given on the abscissa. Vertical bars represent the range of the 25 and 75% percentile. Significant response differences (Kruskal–Wallis test, $p < 0.05$) are indicated by the horizontal lines and asterisks.*

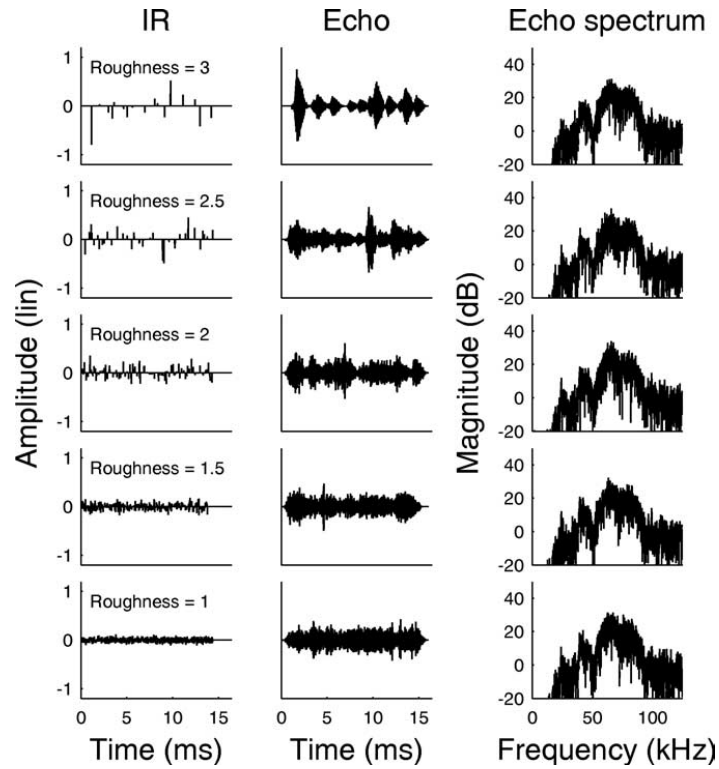


Fig. 3.3 Examples from the stimulus set for the psychophysical and neurophysiological experiments in *P. discolor*. The first column shows the IRs used to generate the echoes in the psychophysical playback experiment. The roughness of the IRs, quantified as the base 10 logarithm of the waveform fourth moment is shown in each panel. The second column shows echoes generated from the IRs in the first column with a standard *P. discolor* echolocation call. These echoes were used as stimuli for the neurophysiological experiments. The magnitude spectra of the echoes are shown in the third column. Note that the magnitude spectra and the overall sound-pressure level are independent of roughness.

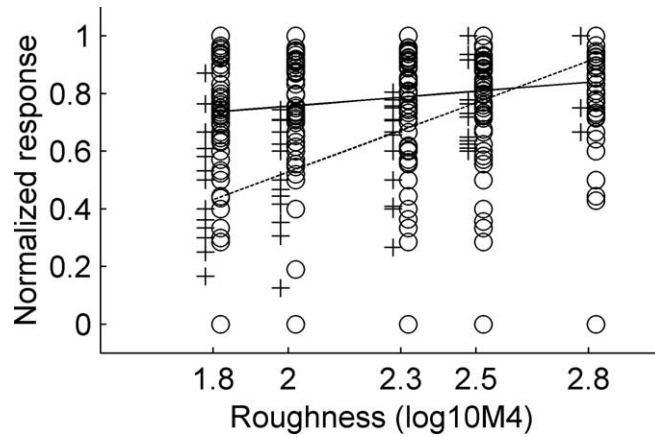


Fig. 3.4 Comparison of the regression lines of response strength calculated for all 14 roughness-sensitive units for which responses increased with increasing roughness (dashed line) and all nonsensitive units (solid line). IR roughness is shown on the abscissa, and normalized response strength is shown on the ordinate. The crosses show normalized response strength for roughness-sensitive units, and the circles show response strength for nonsensitive units. The slope of the regression line is significantly steeper for the roughness-sensitive units, indicating that the response of sensitive units increases with IR roughness ($p < 0.001$; ANCOVA). The slope of the regression line of the roughness-insensitive units is very shallow, showing that, for these units, the response strength is not correlated with IR roughness.

The recordings were derived from locations covering a distance of $\sim 3500 \mu\text{m}$ along the rostrocaudal axis and $\sim 3000 \mu\text{m}$ along the dorsoventral axis (compare Fig. 3.5), which corresponds to the neuroanatomically evaluated dimension of the auditory cortex of *P. discolor* (S. Radtke-Schuller, personal communication). Units with significant responses to roughness were not uniformly distributed on the auditory cortical surface but were almost exclusively located in anterior regions of auditory cortex (Fig. 3.5). The only unit that responded more strongly to smooth stimuli was located in the posterior part of the auditory cortex.

The clustering of sensitive units in the anterior parts of the auditory cortex also means that the relative percentage of sensitive units is underestimated when calculated for the total cortical area scanned in our experiments. The relative density of roughness-sensitive units would increase if only calculated for the anterior parts; however, because we do not yet have the accurate anatomical limits of different cortical fields, such an analysis was not possible.

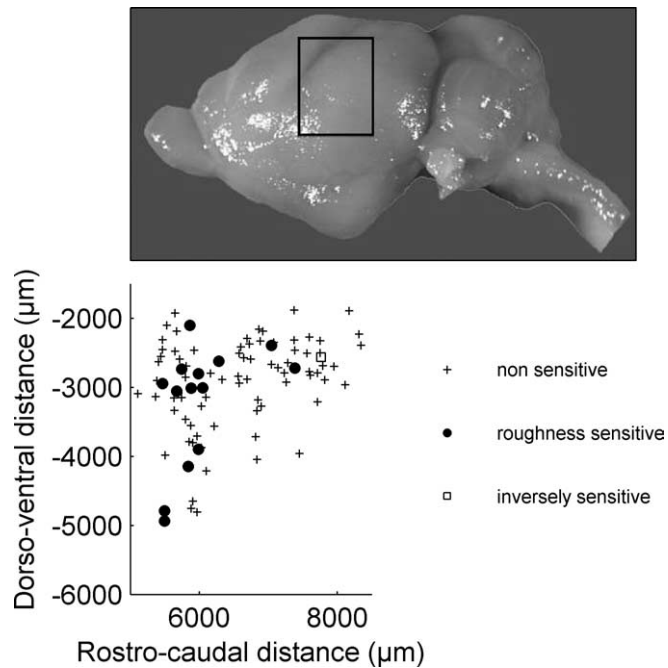


Fig. 3.5 Location of recording sites in the auditory cortex of *P. discolor*. The limits of the scatter plot are superimposed on a photograph of the *P. discolor* brain. Units that were not significantly sensitive to IR roughness are shown as crosses, and roughness-sensitive units are shown as filled circles. The one open square represents a single unit that showed inverse roughness sensitivity (i.e., the rate response decreased with increasing IR roughness).

3.4.3 Comparison of psychophysics and neurophysiology

To compare the psychophysical discrimination performance and the roughness sensitivity of cortical units, a receiver operating characteristics (ROC) analysis was used (Green and Swets 1966; Britten et al. 1992) to generate a neurometric function along the same axes as the psychometric function. The neurometric function reflects the probability that an ideal observer could accurately discriminate IR roughness basing his judgments on responses like those recorded from the units under study.

The ROC analysis was performed by generating a so-called ROC curve for the comparison of each signal condition (roughness >1.8) and the standard condition (roughness, 1.8). The ROC curve shows the probability that both the rate response in a signal condition and the response in the standard condition exceed a certain threshold (e.g., one spike per stimulus). This probability was plotted as a function of the height of the threshold. From there, the (neural) percentage of correct discrimination for each signal condition was generated by calculating the area under the ROC curve.

For the current comparison, we pooled the responses of all 14 units whose response increased significantly with IR roughness. The resulting neurometric function is shown together with a

replot of the psychometric function with a reference roughness of 1.8 in Figure 3.6. The analysis shows that there is a good agreement between the psychophysical performance and the ideal-observer performance based on the subgroup of roughness-sensitive units.

Note that the psychometric function for a reference roughness of 0.5 was very similar to that for a reference of 1.8, indicating that the animals could not discriminate roughness <1.8 . The neurophysiological data set was therefore limited to the roughness region between 1.8 and 2.8.

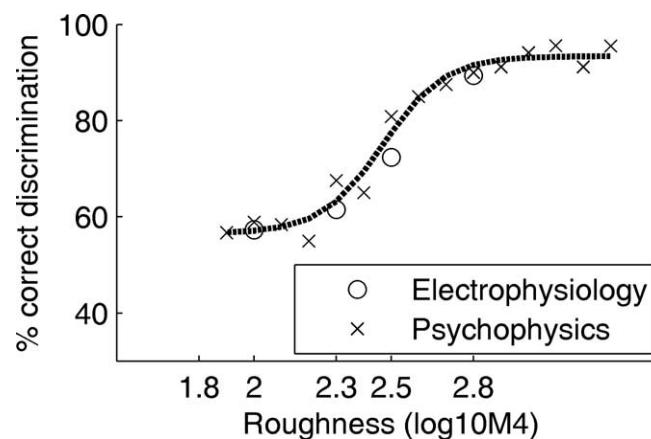


Fig. 3.6 Comparison of the psychophysical and neurophysiological roughness discrimination performance. The crosses show the psychophysical performance with a reference roughness of 1.8; the dotted line is a sigmoidal fit to the psychophysical data. The open circles show the performance of an ideal observer (using a receiver-operating-characteristics analysis) basing its decisions on the pooled responses of the 14 roughness-sensitive cortical units found in this study.

3.5 Discussion

In the present study, neurons were found in anterior regions of the auditory cortex of the bat *P. discolor* that encoded echo roughness in their response strength. The performance of these neurons closely matched the bats' behavioral sensitivity to echo roughness as a physiological correlate to statistical echo analysis in the auditory cortex.

Because the exact partitioning of the auditory cortex and the location of different cortical fields is not yet known for *P. discolor*, the location of roughness-sensitive units in the auditory cortex cannot be precisely attributed to defined cortical areas. However, Esser and Eiermann (1999) have investigated the organization of the auditory cortex in a closely related phyllostomid bat species *Carollia perspicillata*. They described six different auditory fields including the primary auditory cortex (AI), a rostrally adjoining anterior auditory field (AAF),

and two dorsally located auditory fields. It can be assumed that the general organization of the auditory cortex is not very different in *P. discolor*. Roughness-sensitive units were found mainly in anterior regions over the whole dorsoventral distance. Thus, roughness-sensitive units seem to be mainly located in two cortical fields, probably representing the AAF and an anterior dorsal field. Only a few recordings were derived from units in posterior ventral regions where the AI might be located, so no clear assertion about encoding of echo roughness can be made for neurons in the AI.

Complex response patterns consisting of a phasic onset response followed by a sustained excitatory response have been described for neurons in the inferior colliculus (IC) and the auditory cortex of various mammals (Geisler et al. 1969; Heil 1998; Brosch and Scheich 2003). Several studies showed that different stimulus features can be differentially encoded by onset and sustained-response components. Heil (1998) showed that binaural envelope transients are encoded by the onset response of neurons in the inferior colliculus of rats, whereas the binaural combination of steady state intensities is encoded by the sustained response. For the auditory cortex, it was also shown that the onset-response strength is related to the rising-envelope slope rather than to the steady-state intensities (Heil 1997; Heil and Irvine 1998). Ahissar et al. (1992) showed that the majority of motion-sensitive neurons in the auditory cortex of awake monkeys showed motion sensitivity in their sustained components. These findings support our results: whereas the stimulus onset evoked a strong onset response independent of roughness, the sustained response was highly dependent on stimulus roughness.

Grunwald et al. (2004) argued that modulation-sensitive units possibly located in the inferior colliculus may play a role in the processing of echo roughness. Physiological modulation sensitivity has mainly been tested with sinusoidally amplitude-modulated (SAM) stimuli. The envelope spectra of these stimuli (the magnitude spectra of their Hilbert envelopes) are narrow band and they show a pronounced peak at the modulation frequency. The envelope spectra of the stimuli used in this study differ substantially. Because of the aperiodic and transient nature of the IRs, the envelope spectra of the echoes are broad band and with increasing roughness, the envelope magnitude increases for all modulation frequencies. The systematic effect of echo roughness on the envelope spectra is shown in Figure 3.7. The roughness-dependent changes are most prominent in the envelope-frequency region ~ 500 Hz. The IR roughness sensitivity investigated in this study is, thus, most closely related to modulation-depth sensitivity rather than to modulation-frequency sensitivity, per se.

Human psychophysical sensitivity to the modulation depth of SAM noise has been measured first by Wakefield and Viemeister (1990). Later studies (Ewert and Dau 2004) confirmed for a broad stimulus set that, above the SAM detection threshold, modulation-depth discrimination is constant at ~ 1 dB. Although there are no data on modulation-depth discrimination in bats, the envelope spectra of the current stimuli (Fig. 3.7) indicate changes in the envelope spectra clearly exceeding the human 1 dB threshold.

Krishna and Semple (2000) investigated responses of inferior-colliculus neurons in the Mongolian gerbil to SAM tones varying in both modulation frequency and modulation depth.

They showed that the rate modulation transfer function depended significantly on modulation depth. Dependent on modulation frequency, changes in modulation depth could result in either suppression or enhancement of the rate responses. Thus, Krishna and Semple (2000) demonstrated that at the level of the inferior colliculus, some units can encode modulation depth. However, as outlined above, the envelope spectra differ substantially from those of our stimuli.

Stimuli that are more similar to ours have been used by Kvale and Schreiner (2004) in the inferior colliculus of cats. They used pure-tone carriers modulated with an 800 Hz rectangular modulator and stochastic modulation-depth variations. Like our current stimuli, these stimuli have a broad-band envelope spectrum. Also similar to a roughness increase in our current stimuli, an increase in the variance of modulation depth results in an increase of the envelope magnitude for this broad range of envelope frequencies. Kvale and Schreiner showed that neurons in the inferior colliculus can detect dynamic changes in variance of their modulation depth distribution in their firing rate. These studies suggest that roughness-related response changes may exist at the level of the inferior colliculus in the bat *P. discolor*.

To our knowledge, modulation-depth coding has not been studied at the level of the auditory cortex. Figure 3.7 shows that sensitivity to relatively high-modulation frequencies ~500 Hz is a prerequisite for the encoding of IR roughness. Therefore, tuning to modulation frequency cannot be ignored in this context. Schreiner and Urbas (1988) found that neurons in the AAF of cats had highest best modulation frequencies for both phase-locked and rate responses, whereas best modulation frequencies in AI and the posterior auditory field were markedly lower. Thus, the localization of roughness-sensitive units in anterior parts of the auditory cortex of *P. discolor* resembles the representation of high-frequency amplitude modulations in the auditory cortex of the cat.

Phase locking in auditory-cortex neurons to SAM is limited to low-modulation frequencies (Langner 1992). Previous reports suggest that various cellular and network properties such as adaptation and synaptic depression may underlie this low-pass response behavior (Joris et al. 2004; Wehr and Zador 2005). However, Lu et al. (2001) showed that a distinct population of neurons exists in the auditory cortex of marmosets that encodes high-modulation frequencies as a rate code. A rate code for high-modulation frequencies in the auditory cortex was also reported in other studies (Bieser and Müller-Preuss 1996; Liang et al. 2002; Lu and Wang 2004). Our current results suggest that neurons in the auditory cortex of *P. discolor* represent IR roughness as a rate code.

In addition to intracortical mechanisms underlying the generation of a rate code for high-modulation frequencies, a transformation of the temporal code into a rate code at the level of the IC is also discussed (Langner 1992). Hewitt and Meddis (1994) simulated the transformation of a temporal code for amplitude modulation in cochlear-nucleus sustained-chopper cells into a rate code of amplitude modulation through inferior-colliculus coincidence-detector cells. Ongoing experiments in our lab try to localize the neural substrate for the transformation of roughness into a rate code.

Although the auditory cortex may simply reflect properties of periodicity coding generated in the midbrain, the auditory cortex is crucial for relating an auditory representation to behavior (Heffner and Heffner 1990; Riquimaroux et al. 1991; Smith et al. 2004). It has been suggested that the role of the auditory cortex might be to organize sound features already extracted by lower levels into auditory objects (Nelken 2004). Previous work indicates that for *P. discolor*, the IR roughness contributes to auditory object formation (Grunwald et al. 2004). Thus, the neural correlate of psychophysical performance for auditory object identification is most likely to be found in the auditory cortex.

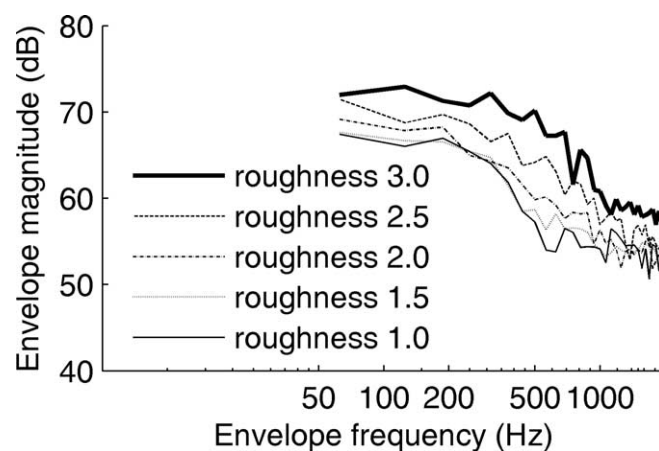


Fig. 3.7 Envelope magnitude spectra of echo stimuli presented in the neurophysiological experiments. Unlike the magnitude spectra of the waveform (compare Fig. 3.1, right column), the envelope spectra vary systematically with roughness. With increasing roughness, the envelope magnitude increases for all envelope frequencies; however, the increase is most pronounced in the envelope-frequency range, ~500 Hz.

The current comparison of the psychophysical and neuronal performance was based on the pooled responses of all 14 roughness-sensitive units. The response of no single unit on its own matched the psychophysical performance. To investigate the least number of units required to match the psychophysical performance, we repeated the ROC analysis for subsets of the roughness-sensitive units. The ideal-observer results are shown together with the psychophysical performance in Figure 3.8. With a lower number of units included for the ROC analysis, the ideal-observer performance drops remarkably. Note that the repeated random drawings of a subset of the 14 roughness-sensitive units resulted in quite stable predictions of ideal-observer performance. This finding confirms that this small population of 14 units is in itself homogeneous.

It is highly likely that there are many more roughness-sensitive units in the auditory cortex of *P. discolor*. Thus, it must be assumed that the animal's ability to combine the neural information across units is suboptimal.

Although the current data show a high correlation between the psychophysical performance and the performance of a subpopulation of cortical neurons, this correlation does not prove a causal connection between the two. To this end, additional experiments should be performed in which the regions containing this subpopulation of roughness-sensitive neurons should be reversibly inactivated while the animals perform the psychophysical task. Nevertheless, the current results show that psychophysical sensitivity to IR roughness as an ecologically meaningful parameter is quantitatively encoded in the auditory cortex of the echolocating bat *P. discolor*.

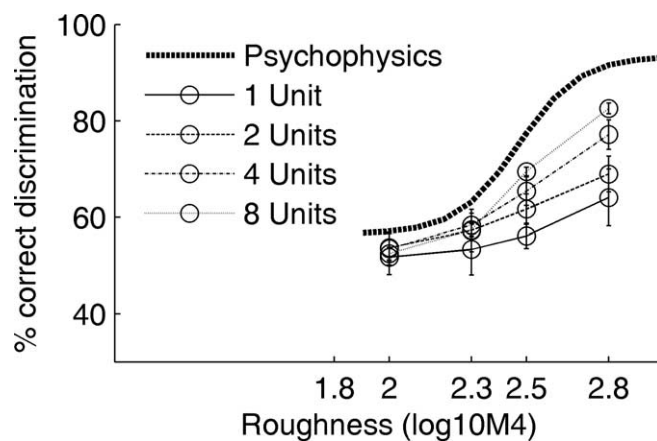


Fig. 3.8 Ideal-observer performance for roughness discrimination as a function of the number of pooled unit responses. The strong dotted line shows the psychophysical performance replotted from Figure 3.6. The ideal-observer responses were obtained by 10 random draws of the specified numbers of units from the set of the 14 roughness-sensitive units. The error bars show SE across these 10 draws. With increasing number of pooled unit responses, the performance improves.

3.6 Acknowledgements

This work was supported by the Deutsche Forschungsgemeinschaft Grants WI 1518/6 (L.W.) and SCH 390/6 (G.S.), and by the VW-Stiftung (I/79782). We thank Benedikt Grothe, George Pollak, Gerhard Neuweiler, Michael Burger, and two reviewers for helpful and constructive comments on previous versions of this paper. Many thanks also to Susanne Radtke-Schuller

for her help with the reconstruction of recording sites. We also thank Claudia Schulte and Britta Schwellnus for their help.

4. An area sensitive to apparent acoustic motion in the auditory cortex of the bat *Phyllostomus discolor*

Manuscript

4.1 Abstract

The acoustical environment of an actively orienting and hunting bat is in continuous move, and stationary sound sources belong to the rarest episodes in the life of echolocating bats. The exciting question arises whether the neuronal system has developed features matching this ever-moving situation. To answer this question, neuronal responses to apparent sound movement in acoustic space have been recorded in the auditory cortex (AC) of anaesthetized bats, *Phyllostomus discolor*. Apparent motion in the horizontal plane was generated by binaural presentation of pairs of tones with different interaural intensity differences (IIDs) and varying inter-pulse intervals (IPIs). Thus the specific parameters of apparent motion, spatial extent and motion direction, changed for each stimulus pair. A complete stimulus ensemble consisted of 81 IID-combinations in the range between -40 to +40 dB IID. Stimulus pairs were randomly presented via earphones at up to six different IPIs (6.25 to 150 ms).

Fifteen percent (36 of 236) of the extracellularly recorded cortical units were motion sensitive in terms of strongly facilitated responses to acoustic motion compared to static stimulation. All motion sensitive neurons changed the center and/or size of their dynamic azimuthal response area when the IPI decreased. Most interestingly, the motion sensitive neurons were almost exclusively (86 %, 31 of 36) clustered in the caudal part of the dorsal AC indicating that this cortical area is specifically involved in the processing of acoustic motion. Twenty eight percent (10 of 36) of motion sensitive neurons focused their azimuthal response area on small movements in forward direction at very short IPIs. These units may presumably be relevant for the detection of moving targets during the phase of final approach towards a target.

4.2 Introduction

Motion of objects in space can be perceived by different sensory systems. At various levels of the visual system in animals and humans, moving visual signals have been recognized as significant stimuli for certain neurons. These motion sensitive neurons have distinct preferences for the direction or velocity of movements (for review see Borst and Egelhaaf 1989). The movement of a visual target is related to a temporal change in location and is directly represented on the receptive level, whereas the location of an auditory signal in space and its temporal changes are deduced from binaural differences and their dynamic changes. Thus, microchiropteran bats which use pulsed echolocation for orientation perceive the spatial position of an ensounded target via the IIDs and direction-dependent spectral cues of the returning echo (Fuzessery and Pollak 1984; Wotton et al. 1995). Each change of spatial position of the echo source relative to the bats head provokes spectral differences and IID changes between two successive echoes. Depending on the rate of emitted ultrasonic vocalizations and their ensuing echoes, the bat receives a more or less sharply resolved stroboscopic representation of its dynamic environment. By analyzing echo delay (O'Neill and Suga 1982) and Doppler induced frequency shift (Suga 1989; Olsen and Suga 1991a), bats can determine range and velocity of the radial component of a moving echo source. But how do these animals process and analyze echoes reflected from objects moving in azimuthal or tangential directions through their auditory receptive field?

In previous studies on bats, neurons sensitive to horizontal acoustic motion have been found in the AC of *Rhinolophus rouxi* (Firzlaff and Schuller 2001b), in the inferior colliculus of *Rhinolophus rouxi* (Kleiser and Schuller 1995), *Pteronotus parnellii* (Wilson and O'Neill 1998) and *Rhinolophus ferrumequinum* (Schlegel 2002) and in the lateral lemniscus and superior olivary complex of *R. ferrumequinum* (Schlegel 2002). Classification of a neuron as motion sensitive was mostly linked either to a shift of the best orientation of its azimuthal response area when dynamically stimulated or to a clear preference for a distinct direction of the movement. In most studies, azimuthal acoustic motion was simulated by sequentially changing the spatial position of a sound source over a large range of both hemifields, whereas movements restricted to small angular ranges (e.g. within forward direction) were rarely investigated. The present study was designed to test cortical auditory neurons with a high variability of virtual acoustical movements using a randomized stimulus paradigm that covered a large range of step width and starting positions of azimuthal movements. Furthermore, short IPIs below 25 ms were used that more realistically simulated echo repetition rates perceived by bats while approaching a target (Griffin et al. 1960; Moss and Surlykke 2001).

The aim of the present study was to find out whether AC neurons of *P. discolor* specifically respond to virtual azimuthal motion of sound, to quantify the dynamical response features as compared to the static situation, and to determine whether motion specificity is restricted to distinct sub-regions of the AC.

4.3 Methods

4.3.1 Experimental animals and surgical preparation

All experiments were performed in agreement with the principles of laboratory animal care and under the regulations of the current version of German Law on Animal Protection (approval 209.1/211-2531-68/03 Reg. Oberbayern). One male and two female adult spear-nosed bats (*Phyllostomus discolor*, body weight: 30 to 40 g) were used in this study. The animals originated from a breeding colony in the Department Biology II of the Ludwig-Maximilian-University in Munich. During the experimental period animals were kept separated from the bat colony under semi natural conditions (12 h day / 12 h night cycle, 65 to 70 % relative humidity, 28 °C) with free access to food and water.

For surgical preparation, the bats were deeply anaesthetized with a combination of Medetomidin, Midazolam and Fentanyl (MMF, 0.4, 4.0 and 0.04 µg/g body weight, respectively). For later immobilization of the skull in the stereotaxic recording setup, a metal rod was fixed onto the bat's skull using light-curing dental cement. The details of all surgical procedures can be found in Hoffmann et al. 2008b. After surgery and experiments, the anesthesia was antagonized by injecting a compound of Atipamezole hydrochloride, Flumazenil and Naloxon (AFN: 8.1, 0.034 and 0.32 µg/g body weight, respectively). In order to alleviate postoperative pain, an analgesic (2 µl/g body weight Meloxicam) was administered after full recovery of the bat.

4.3.2 Stereotaxic procedure and verification of recording sites

A detailed description of the stereotaxic procedure, determination of brain orientation and reconstruction of recording sites has been already published elsewhere (Schuller et al. 1986). Briefly, the surgically mounted rod on the bat's skull was fastened to the stereotaxic device in an unequivocal way, so that the skull, and consequently the brain, had a distinct orientation within the stereotaxic coordinate system even after repeated repositioning of the bat throughout the recording series. The actual orientation of the skull relative to a reference orientation was determined by measuring the parasagittal and frontal profile lines of the exposed skull. The parasagittal profile was compared to the standard parasagittal skull profile that represented the skull-to-brain correlation in the stereotaxic atlas of *P. discolor* (T. Fenzl, A. Nixdorf and B. Schweltnus, unpublished data). The frontal profile showed how much the actual skull position eventually deviated from the upright orientation. Deviations from the standardized orientation (used in the brain atlas series) could be corrected by appropriate tilt and pitch of the animal within the experimental setup. This coordinate frame allowed to refer all recording locations on a standard brain atlas system and to pool data within one and among different experimental animals. For verification of the stereotaxic procedure, electrolytic lesions and tracer injections were routinely made. The locations were reconstructed in standardized brain atlas coordinates and compared to the histological findings after

transcardial perfusion of the bat and histological processing of the brain. Stereotactic precision was typically 150 μm .

4.3.3 Acoustic stimulation used for determination of basic neuronal response properties

Stimuli for detecting neurons during electrode advance were hardware generated pure tones of 20 ms in duration and a trapezoidal envelope (frequency generator: Wavetek model 136, 186, FG-5000, pulse shaper: custom-made). The sound pressure level (SPL) of the stimulus was controlled by manually operated attenuators (AP401, adret electronique, France). Stimuli were amplified and presented monaurally or binaurally via custom-made ultrasonic capacitive earphones (Schuller 1997) with a flat frequency response (± 3 dB) between 10 and 100 kHz. Once a neuron was detected, stimulus command was transferred to software controlled presentation. The excitatory frequency response area (FRA) and binaural response properties were determined as basic response properties for each unit before proceeding to the measurement of responses to dynamic stimuli. The stimulation procedure for recording of FRAs and binaural response properties has exactly been described in Hoffmann et al. 2008b. In short, FRAs were determined by recording neural responses to contralateral presentation of 20 ms pure tone stimuli in various frequency and SPL combinations. The binaural response properties were determined at the unit's BF using ABI (averaged binaural intensity (Irvine et al. 1996)). With this method, pure tones were presented binaurally with increasing intensity at the contralateral and decreasing intensity at the ipsilateral ear and vice versa. Thereafter, the same stimuli were presented monaurally to the contralateral and ipsilateral ear, respectively.

4.3.4 Two-tone stimuli (apparent horizontal acoustic motion)

The two-tone paradigm to test a neuron for motion sensitivity is schematically exemplified in Fig. 4.1 for three random pairs of two-tone stimuli binaurally presented to the animal. As in an almost realistic echolocation situation of the bat, the two successive tone-stimuli that differ in their azimuthal position mimic the start- (signal 1) and end-position (signal 2) of a horizontal acoustic movement. Different positions in azimuth are implemented by different IIDs of the two tones with IIDs covering a range of -40 to +40 dB in 10 dB steps. In the present paradigm, negative IID values represent azimuthal positions within the ipsilateral hemifield, positive IID values represent azimuthal positions within the contralateral hemifield and 0 dB IID represents the frontal azimuthal position. An estimate of perceived azimuthal angles caused by an IID can be deduced from the head-related transfer function of *P. discolor* (Firzlaff and Schuller 2003). An IID of ± 40 dB at a frequency of 60 kHz would yield a perceived deviation from the forward direction of approximately ± 30 degrees. As signal 1 and signal 2 could each assume one of nine different IID values (azimuthal positions), a total of 81 possible tone combinations, i.e. 81 different movements could be simulated. Depending on

the azimuthal position of signal 1 and signal 2, movements could vary either in motion direction or in the size of azimuthal angle change (stimulus A vs. stimulus B in Fig. 4.1) or in the azimuthal sector in which the movement occurred (stimulus A vs. stimulus C in Fig. 4.1). For presentation of stationary two-tone stimuli (0 dB Δ IID), signal 1 and signal 2 had identical azimuthal positions. Furthermore, time delays between the onset of signal 1 and the onset of signal 2 (IPIs) of 6.25, 12.5, 25, 50, 100 and 150 ms were used. The inter-stimulus interval (ISI, time between the onset of signal 2 of the first two-tone stimulus and the onset of signal 1 of the successive two-tone stimulus) was kept constant at 500 ms to avoid interactions between signal 2 and signal 1 of the following two-tone stimulus.

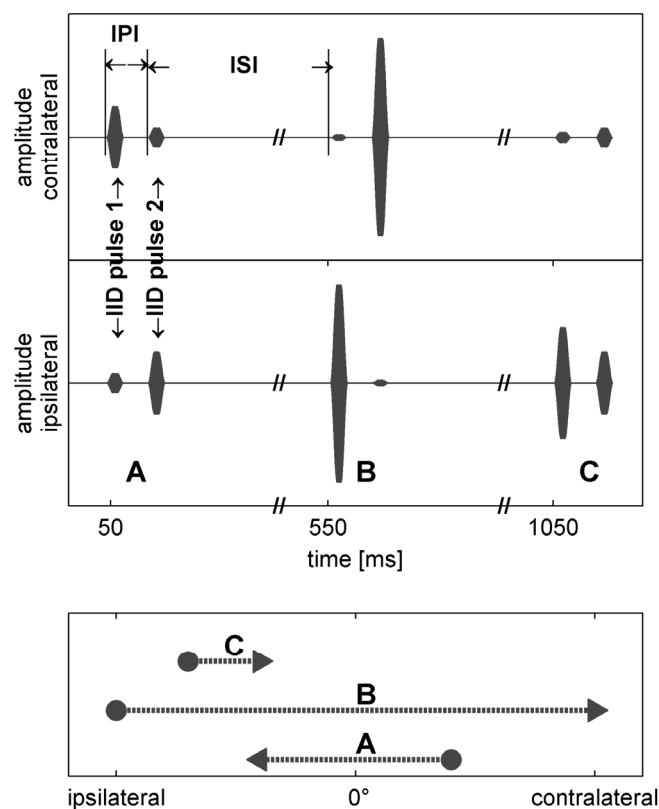


Fig. 4.1 Schematic of a sequence of three two-tone stimuli representing three different azimuthal movements. The upper panel shows three (A to C) different azimuthal movements (as indicated by length and direction of the arrows in the lower panel). The amplitude at the ipsi- and contralateral ear is plotted against the time and thus indicates the IID of the particular signal. The IPI (variable) between the two pulses of a stimulus and the ISI (always 500 ms) between two successive two-tone stimuli is indicated by the thin vertical lines. (A) represents a small movement from a contralateral to an ipsilateral azimuthal position. A large movement starting at a lateral position on the ipsilateral azimuth and ending at lateral position on the contralateral azimuth is represented by (B) and (C) represents a small contralaterally directed movement starting and ending in the ipsilateral azimuthal field.

Figure 4.2 depicts a schematic drawing of the 81 different two-tone stimuli within one IPI step arranged as a 9x9 matrix. The stimulus matrix is divided into quadrants. Positions in the upper left quadrant represent movements from the contralateral azimuth to the ipsilateral azimuth and positions in the upper right quadrant represent movements within the contralateral azimuth. Positions in the lower right quadrant represent movements from the ipsilateral azimuth to the contralateral azimuth and positions in the lower left quadrant represent movements within the ipsilateral azimuth. The diagonal line marks the positions of stationary two-tone stimuli that were separated only in time but not in azimuthal position. Each position above this line indicates a movement in ipsilateral direction, whereas positions below indicate contralaterally directed movements. In addition, the three examples of two-tone stimuli shown in Fig. 4.1 are indicated (stimulus A to C).

Pure tones of five milliseconds in duration (rise and fall time of three milliseconds) were used that mimicked approximately the duration of naturally occurring echoes. Neurons in the AC of *P. discolor* respond consistently to pure tone stimulation as has been shown in Hoffmann et al. 2008b. Frequency modulated or natural echolocation stimuli would have added uncontrollable complications for an attempt to interpret the results on the basis of stationary responses to azimuthal parameters at the distinct frequencies the units are tuned to. The two-tone stimuli were computer-generated (Matlab® 6.1; Mathworks, Natick, USA), D/A-converted (RX6; sampling rate 260 kHz, Tucker Davis Technologies, Gainesville, USA) and attenuated (PA5, Tucker Davis Technologies, Gainesville, USA). They were presented binaurally via ear-phones at the neuron's BF (visually determined from the FRA) and were at zero dB IID 20 dB SPL above threshold. Each stimulus pair was presented 20 times in random order.

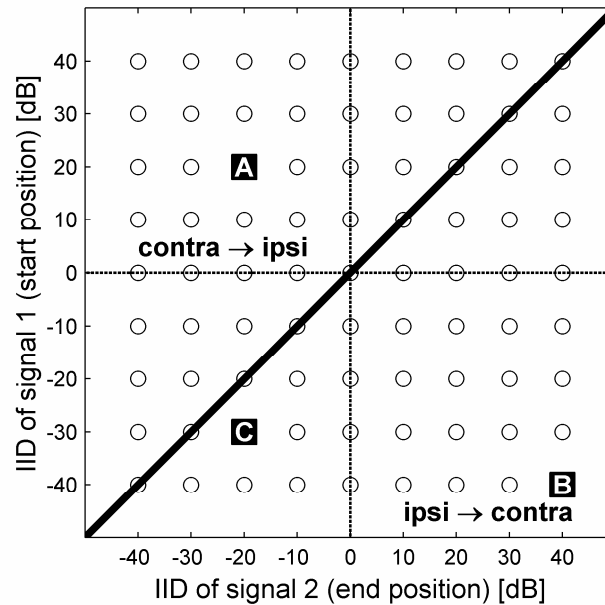


Fig. 4.2 Schematic of the 9x9 stimulus matrix. The open circles represent the 81 two-tone stimuli. The spatial positions of signal 1 (start) and signal 2 (end) of the 81 different dynamic stimuli are plotted on the ordinate and abscissa, respectively. Contralateral and ipsilateral azimuthal positions are indicated by positive and negative IID values, respectively. The dashed lines sub-divide the stimulus matrix in contralateral and ipsilateral quadrants. The diagonal line indicates two-tone stimuli without concurrent IID changes, which represent a repetitive presentation of a stationary sound source. Circles above the diagonal line indicate movements towards the ipsilateral side and circles below the diagonal line indicate contralaterally directed movements. The corresponding positions in the stimulus matrix of the three two-tone stimuli (A to C) shown in Fig. 4.1 are indicated.

4.3.5 Recording of neural responses

All experiments were conducted in a heated (36°C), electrically shielded and anechoic chamber. Recording sessions of normally four hours were repeated at four days a week for up to six weeks. Bats were lightly anesthetized with MMF and supplied with oxygen throughout the whole experiment. Recording electrodes were introduced through small trepanation holes (200 to 500 μm in diameter) in the animal's skull and meninges overlaying the AC. Electrode penetrations were guided either roughly perpendicular to the cortical surface (bat #3) or approximately parallel to the surface of the cortex (bat #1 and #2).

Extracellular recordings were obtained with fiber microelectrodes (Carbostar-1, Kation Scientific, Minneapolis, USA; 0.4 to 0.8 M Ω impedance) or glass-insulated tungsten microelectrodes (Alpha Omega GmbH, Ubstadt-Weiher, Germany; 1 to 2 M Ω impedance).

Neural responses were amplified (RA16PA, Tucker Davis Technologies, Gainesville, USA), band-pass filtered (0.3 to 3 kHz, RX5, Tucker Davis Technologies, Gainesville, USA) and fed into an A/D-converter (RX5, Tucker Davis Technologies, Gainesville, USA, sampling rate: 25 kHz). Using “Brainware” (J. Schnupp, distributed by Tucker Davis Technologies, Gainesville, USA) action potentials were threshold discriminated and saved for offline analysis on a personal computer. The term ‘unit’ is adopted for responses of clusters of up to maximally three simultaneously discriminated neurons.

4.3.6 Data analysis

4.3.6.1 Basic response properties

Programs for data analysis were written in Matlab® (Matlab 6.1; Mathworks, Natick, USA). Spike responses of a unit were pooled over all repetitions of stimuli of the FRA and binaural paradigm, respectively, and displayed as peristimulus time histogram (PSTH, 1 ms bin width). Spontaneous activity was derived from the silent period of 50 ms before the onset of each stimulus. The analysis window started when the first bin of the response exceeded the level of spontaneous activity and ended when the response reached spontaneous level again. The response duration of a unit was directly measured from the analysis window. The best frequency (BF: frequency at which auditory threshold is lowest) and auditory response threshold of a unit were determined from the FRA. The binaural response type was determined from the binaural stimulus paradigm and grouped into four categories. Units which were excited by monaural stimulation of each ear were named EE (excitatory-excitatory). Units that only received excitatory input from the contralateral ear are named E0 and 0E for ipsilateral excitatory input. In case the unit was excited by monaural contralateral stimulation, did not respond to monaural ipsilateral stimulation and showed inhibition in binaural stimulation, it was classified as EI (excitatory-inhibitory). A detailed description of the analysis of the basic neuronal response properties is found in Hoffmann et al. 2008b.

4.3.6.2 Response properties to dynamic two-tone stimulation

Figure 4.3 illustrates how the neuronal data obtained from stimulation with the two-tone paradigm was analyzed. For each IPI step, neural responses were pooled over all repetitions of each of the 81 two-tone stimuli (9x9 stimulus matrix) and displayed as a single PSTH. The static azimuthal response area was determined from the response to signal 1 of the stimulus set presented with the longest IPI. The responses to signal 1 and signal 2 were always clearly separable in these recordings. A temporal analysis window was determined the same way as for the FRA and set to the response period of signal 1 (Fig. 4.3A). The mean spike count elicited by signal 1 within this analysis window was calculated for each azimuthal position and normalized to the spontaneous spike count determined from a 50 ms time window

preceding the onset of the first stimulus. The 50 % cut-off of the resulting IID-curve determined the extend of the static azimuthal receptive field of the individual unit (Fig. 4.3B). For analyzing the neural responses to apparent acoustic motion stimuli, the spike numbers elicited by signal 2 of each of the 81 two-tone-stimuli were calculated within a time window analog to that applied to signal 1 but shifted by the time period of the particular IPI (Fig. 4.3A). The spike count was also normalized to the spontaneous spike count (see above) and displayed as contour plot (Fig. 4.3C). The dynamic response area is indicated by the green area (bordered by the thick black line) with the 50 % value of the maximum response elicited by signal 2 of the particular IPI step.

For short IPIs, the analysis window of signal 2 could partially overlap the response period of signal 1. In this case, the response to signal 2 had to be corrected by subtracting the appropriate number of spikes elicited by signal 1 alone in the window of overlap. This spike number was determined at the largest IPI step where responses were clearly separable.

To quantify the relation between the response to dynamic stimulation and the sum of the responses elicited by static stimulation with the single components of the corresponding dynamic stimulus, an interaction index (InI, e.g. (Dear and Suga 1995)) was calculated for each position in the stimulus matrix. Thus, an interaction matrix was derived for each unit and each IPI step (Fig. 4.3D). The InI was calculated using the following equation:

$$\text{InI} = (\text{DR} - \text{SR}) / (\text{DR} + \text{SR})$$

where DR is the response to dynamic stimulation displayed in each position of the response matrix of signal 2 and SR is the summed number of spikes elicited by static stimulation. If the InI in any position exceeded zero, the unit showed facilitation to signal 2, if the InI assumed a negative value, the response to signal 2 was inhibited by the response to signal 1, and if the InI was zero, no interaction occurred between signal 1 and signal 2.

The dynamic stimulus that elicited the maximum response within the response matrices of signal 2 of all IPI steps was determined for each unit. This so called best stimulus indicated the best signal combination and the best IPI. To determine whether a unit was motion sensitive, the InI for the best stimulus was calculated for each unit and the mean and standard deviation was calculated from the InIs of the best stimulus of all units. If the InI of the best stimulus of a unit exceeded a threshold of 0.47 (mean of InIs of best stimulus for all units plus standard deviation), this unit showed strong facilitation and was classified as motion sensitive. Otherwise, the unit was classified as motion insensitive.

A preference in motion direction was assumed when a significant difference between the responses to acoustic motion in contralateral direction (positions below the diagonal line in the response matrix of signal 2) and that in ipsilateral direction (positions above the diagonal line in the response matrix of signal 2) was established through a Mann-Whitney U test ($p < 0.05$) for each unit and each IPI step.

Distribution and trends of the InI of the best stimulus on the cortical surface are represented with the help of the Voronoi tessellation procedure in two dimensions implemented with

Matlab®. In detail, recording sites of the chosen parameter are connected with all neighboring recording sites. Cells characterizing the value of a special parameter around recording sites are constructed as polygons whose sides pass equidistantly between recording sites and cross the connection lines perpendicularly.

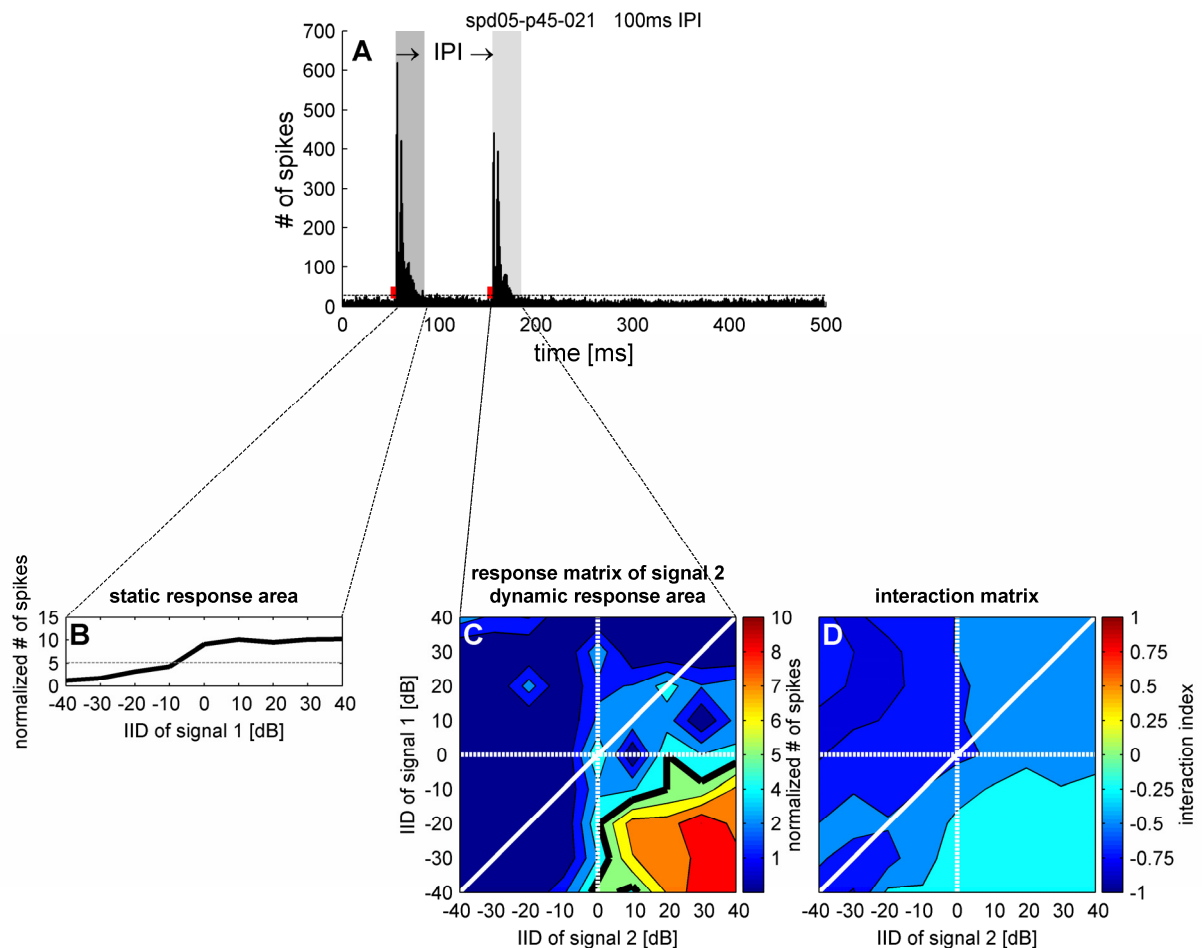


Fig. 4.3 Schematic representation of the analysis procedure of the responses to two-tone stimulation. **A)** PSTH (bin width of 1 ms) of a unit pooled over 20 repetitions of 81 two-tone stimuli at an IPI of 100 ms. The small red squares represent the two acoustic signals, the dashed line indicates the spontaneous level, the gray and light gray bar represents the response window for signal 1 and signal 2, respectively. **B)** Static response area of this unit obtained from the response to signal 1. The gray dashed line indicates the 50 % cut-off that limits the static response area. **C)** Contour plot of the response matrix obtained from the response to signal 2. The dynamic receptive field is indicated by the green area (bordered by the thick black line). Meaning of solid and dashed white lines as in Fig. 4.2. **D)** Contour plot of the interaction matrix obtained by calculating the interaction index (InI) for each position

in the response matrix of signal 2. A positive InI indicated facilitation and a negative InI indicated inhibition. Meaning of solid and dashed white lines as in Fig. 4.2.

4.4 Results

Neural responses to apparent horizontal acoustic motion stimuli were recorded extracellularly from 236 cortical units of both hemispheres of three adult *P. discolor*. All 236 units responded well to pure tone stimulation, and thus basic response properties like BF and response duration could be determined. Binaural response properties could be determined in 233 units.

During dynamic stimulation, all units showed inhibition of the response to signal 2 by signal 1 in at least one position of the interaction matrix of each IPI step. However, in 74 % (175 of 236) of units the response to signal 2 was facilitated by a certain degree at least at the position of the best stimulus at the best IPI step. As shown in Fig. 4.4, InIs of the best stimulus of all units ranged from -0.55 to 0.93 (mean: 0.2 ± 0.27). In 15 % (36 of 236) of units the response to signal 2 of the best stimulus was strongly facilitated and had an InI above 0.47 (i.e. $\text{InI} > \text{mean InI} + \text{standard deviation}$). These units were classified as motion sensitive.

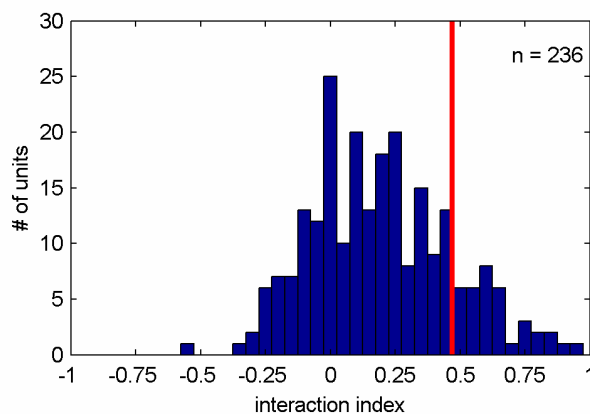


Fig. 4.4 Distribution of interaction indices. Binwidth of the histogram: 0.05. Number of units: 236. The vertical red line indicates the threshold for motion sensitivity of 0.47.

4.4.1 Motion insensitive units

Eighty five percent (200 of 236) of recorded units did not show strong facilitation to dynamic stimulation and were classified as motion insensitive. The size of the dynamic response area of these units often decreased with decreasing IPI. Furthermore, the spatial position of the dynamic response area shifted with decreasing IPI in the way that only movements from most ipsilateral positions to most contralateral positions could elicit a response at short IPIs. Dynamic stimuli eliciting maximal responses were in most cases located in the lower right quadrant of the stimulus matrix representing contralaterally directed movements.

Figure 4.5 shows the raster plots and PSTHs for four different IPI steps of a typical motion insensitive unit. Each raster plot compiles the spike responses to 20 repetitions of the 81 two-tone stimuli for one distinct IPI. At all IPI steps, the unit responded consistently to each signal 1 for IIDs between -40 to +40 dB. Responses evoked from far ipsilateral positions of -30 and -40 dB IID were slightly weaker (Fig. 4.5A-D). At an IPI of 100 ms, signal 2 could also elicit a consistent response at IIDs between -40 to +40 dB (Fig. 4.5A). With decreasing IPI, however, the response to signal 2 was progressively inhibited by signal 1 (Fig. 4.5B-D). At an IPI of 6.25 ms, responses to signal 2 could only be elicited when the dynamic stimulus started at an azimuthal position at which signal 1 could elicit only a weak response (Fig. 4.5D).

In Fig. 4.6 the static response area (Fig. 4.6A), the response matrices of signal 2 with the IPI dependent dynamic response areas (Fig. 4.6B-E) and the corresponding interaction matrices (Fig. 4.6F-I) are shown for the four different IPI steps of the motion insensitive unit. The static azimuthal response area of this unit covered azimuthal positions between -40 and +40 dB IID, however, at far ipsilateral positions (-40 to -30 dB IID) the units' response was slightly weaker (Fig. 4.6A). At a long IPI of 100 ms, the dynamic response area (green area bordered by the thick black line) of this unit was similar in size and azimuthal position to the static azimuthal response area (Fig. 4.6B). With decreasing IPI, the size of the dynamic response area decreased and only large movements could elicit a response (Fig. 4.6C, D). At a short IPI of 6.25 ms, responses to signal 2 could only be elicited when the dynamic stimulus started at an azimuthal position at which signal 1 elicited a weaker response (Fig. 4.6E). As shown by the interaction matrices in Fig. 4.6F-I, InIs of this unit were always below zero, indicating inhibition of the response to signal 2 by signal 1 for all dynamic stimuli and all IPIs. The amount of inhibition and the extend of inhibited positions within the interaction matrix increased with decreasing IPIs, but was always strongest for dynamic stimuli with signal 1 at contralateral positions and signal 2 at ipsilateral positions.

The maximal dynamic response (indicated by the black asterisk in Fig. 4.6C) was elicited by a dynamic stimulus with signal 1 at the most ipsilateral position (-40 dB IID) and signal 2 at the most contralateral position (40 dB IID) and with an IPI of 25 ms. This maximal response equaled the maximum of the static response area.

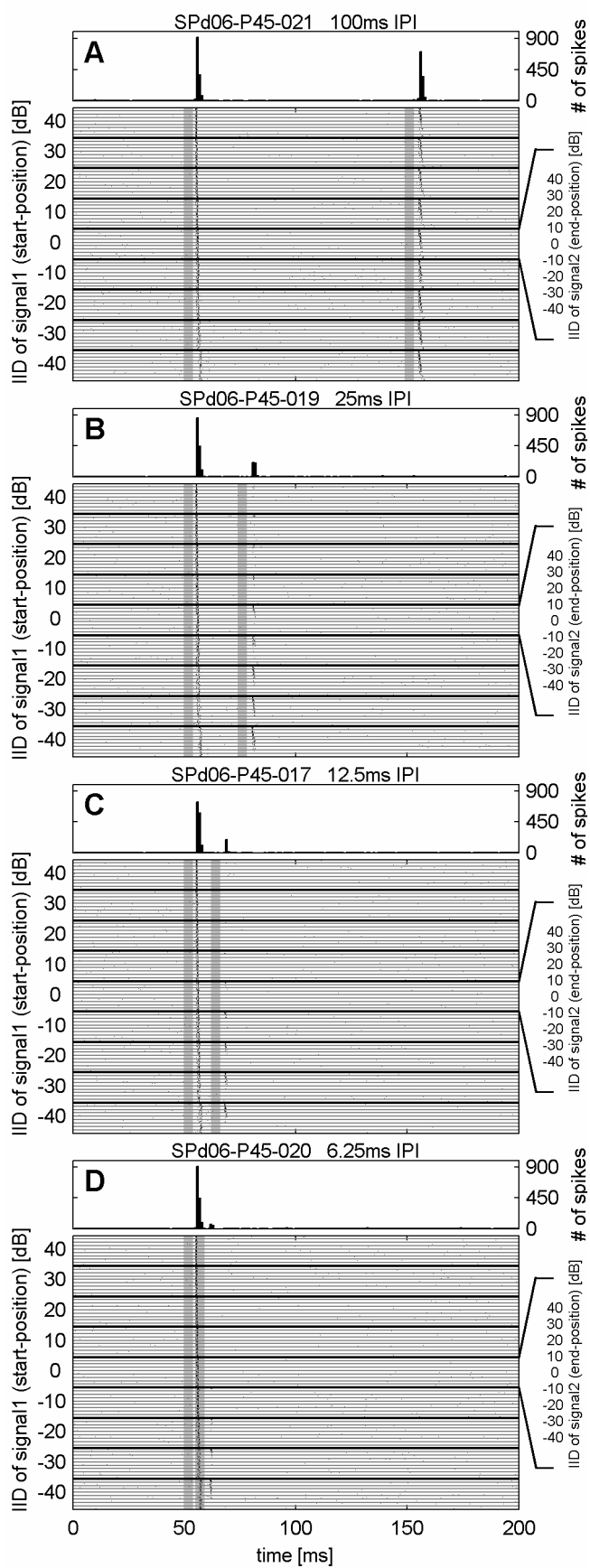


Fig. 4.5 *PSTHs and dot raster plots of a motion insensitive unit for four different IPI steps. The y-axis of the dot raster plots is double scaled.*

The thick horizontal black lines mark the nine azimuthal positions of signal 1 and the thin horizontal black lines between two thick lines mark the nine azimuthal position of signal 2. The gray bars represent the temporal position of the two successive acoustic signals of the 81 two-tone stimuli.

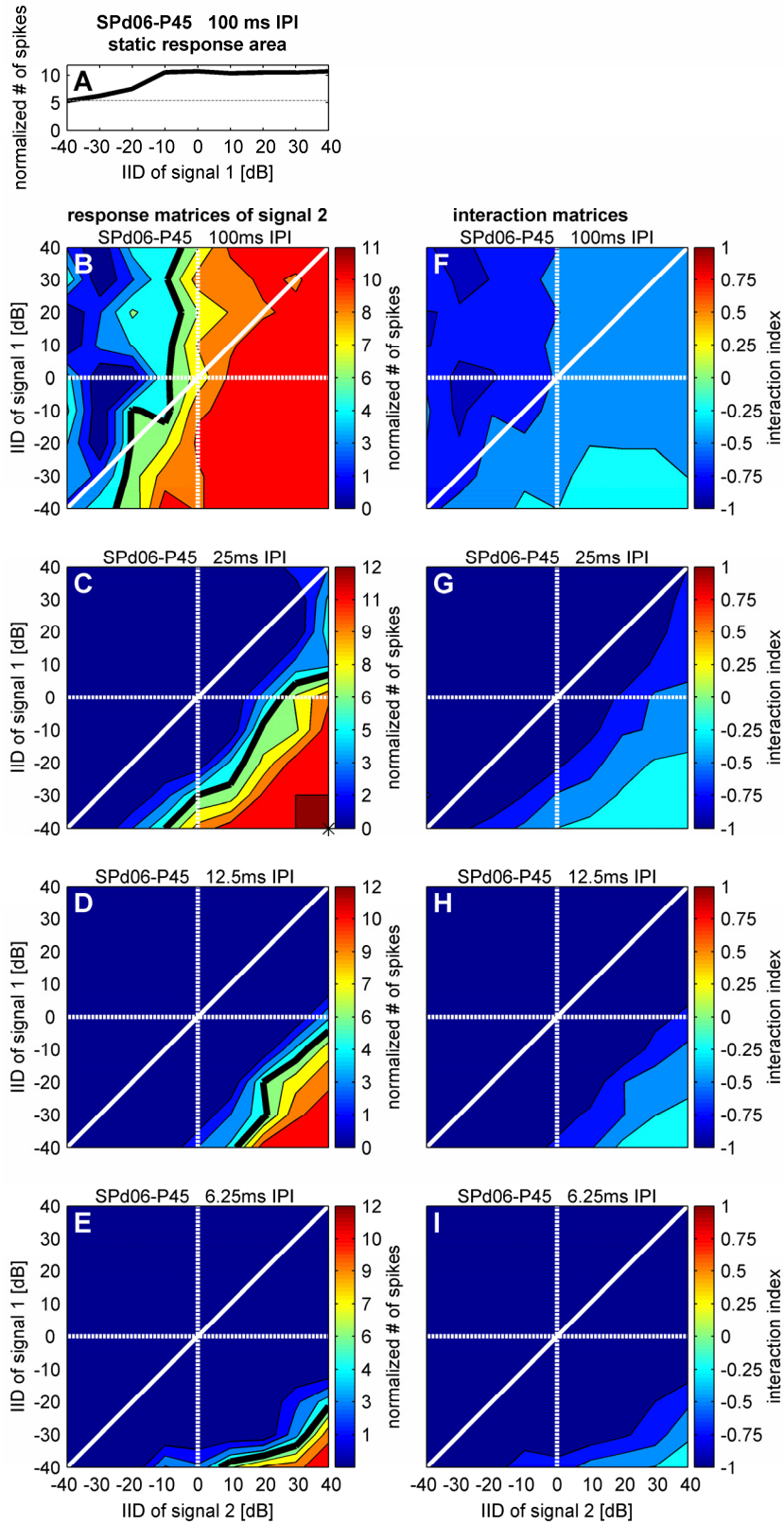


Fig. 4.6 *A)* Static response area, *B-E)* response matrices of signal 2 and *F-I)* interaction matrices of the motion insensitive unit in Fig. 4.5 for four IPI steps. The black asterisk indicates the best stimulus at the best IPI. Meaning of solid and dashed lines as in Fig. 4.3C.

4.4.2 Motion sensitive units

Fifteen percent of the units (36 of 236) showed strong response facilitation to apparent acoustic motion and were classified as motion sensitive.

Figure 4.7 depicts raster plots and PSTHs for four different IPI steps of a typical motion sensitive unit. At all IPI steps, the unit responded well to each signal 1 for IIDs between -20 to +40 dB (Fig. 4.7A-D). At a large IPI of 100 ms, the unit showed a weaker response to signal 2 compared to signal 1 (Fig. 4.7A). With decreasing IPI, however, the response strength to signal 2 increased in this unit. At an IPI of 25 ms, the unit showed strongest responses to signal 2 when signal 1 was presented at far ipsi- and far contralateral positions (Fig. 4.7B). At an IPI of 12.5 ms, the unit responded consistently to signal 2 independent on the azimuthal position of signal 1. Furthermore, signal 2 elicited a stronger response than signal 1 in this IPI step (Fig. 4.7C). At a short IPI of 6.25 ms, the response strength for signal 2 decreased again. Spikes were only elicited by signal 2 when signal 1 was presented from ipsilateral and central azimuthal positions (-40 to +10 dB IID, Fig. 4.7D).

In Fig. 4.8 the static response area (Fig. 4.8A), the response matrices of signal 2 with the IPI dependent dynamic response areas (Fig. 4.8B-E), and the corresponding interaction matrices (Fig. 4.8F-I) are shown for the four different IPI steps of the motion sensitive unit. The static azimuthal response area of this unit covered azimuthal positions between -25 and +40 dB IID with strongest responses to static stimuli presented at -20 dB IID (Fig. 4.8A). At a long IPI of 100 ms, the dynamic response area (green area bordered by the thick black line) of this unit was mainly located below the diagonal line (i.e. representing movements starting in the ipsilateral hemifield and moving to the contralateral hemifield, Fig. 4.8B). As shown in the interaction matrix for this IPI step, strong inhibition is displayed for dynamic stimuli moving within the contralateral hemifield (upper right quadrant in Fig. 4.8C). With decreasing IPI, the size of the dynamic response area increased in this unit. At an IPI of 25 and 12.5 ms, the dynamic response area was extended towards positions in the response matrix representing two-tone stimuli that did not elicit a dynamic response at an IPI of 100 ms (Fig. 4.8C, D). Furthermore, the corresponding positions of the dynamic response area showed strong facilitation in the interaction matrix (Fig. 4.8G, H). At the short IPI of 6.25 ms, the dynamic response area of this unit was focused on a restricted range corresponding to movements starting and ending at frontal positions in azimuth (IID of start-position: -10 to +15 dB; IID of end-position: +5 to +25 dB). Maximum responses at this IPI step were elicited by movements starting at 0 and +10 dB IID and ending at +10 and +20 dB IID, respectively (Fig. 4.8E). In this unit, the amount of facilitation and the extend of facilitated positions within the interaction matrix changed with different IPIs. However, it is important to notice that facilitation still occurred for the shortest IPI step where the dynamic receptive field of the unit showed focusing to frontal azimuth positions (Fig. 4.8I).

In this unit, the maximal response to a dynamic stimulus of 60.1 spikes was elicited by an acoustic movement that started at -40 dB IID and ended at 20 dB IID and had an IPI of

12.5 ms (black asterisk in Fig. 4.8D). The response at this position was far above the maximum of the static response area.

A similar pattern of variation of the dynamic response area was found in 28 % (10 of 36) of motion sensitive units, which also exhibited comparable changes in size and position of the dynamic response area (i.e. focusing on a restricted range of azimuthal positions) at different IPI steps. Figure 4.9 shows the stationary and the variable dynamic response areas at different IPI steps of three additional motion sensitive units. The unit shown in Fig. 4.9A-D gives another example for the focusing of the dynamic response area on frontal azimuthal positions at short IPIs. The unit in Fig. 4.9E-I shows an enlarged dynamic response area at best IPI (Fig. 4.9H) in comparison to the static response area indicating that in the dynamic condition azimuthal positions could elicit a response that were unresponsive during static stimulation. A similar enlargement of the dynamic response area in comparison to the static response area is found in the unit shown in Fig. 4.9J-N. In contrast to the previously described units in which the motion direction eliciting strongest responses was the same for all IPIs (contralaterally directed motion), the present unit changed the direction of motion for which strongest responses occurs as the IPI decreased. In detail, for long IPIs (50 ms, Fig. 4.9K), ipsilaterally directed motion elicited strongest responses and the dynamic response area was restricted to positions above the diagonal white line in the response matrix. The dynamic response area was enlarged towards positions indicating contralaterally directed motion at an IPI of 25 ms and 12.5 ms (Fig. 4.9L, M). However, at the shortest IPI of 6.25 ms the unit showed strongest responses only to contralaterally directed motion and the dynamic response range was positioned below the diagonal white line in the response matrix (Fig. 4.9N). In motion sensitive units, two-tone stimuli without concurrent IID changes, representing a repetitive presentation of a stationary sound source (diagonal line in the response matrix), are not always well responded (see Fig. 4.8B-E, Fig. 4.9). Thus, acoustic motion rather than delay sensitivity appears to be the relevant stimulus parameter that provokes strong facilitation in motion sensitive units.

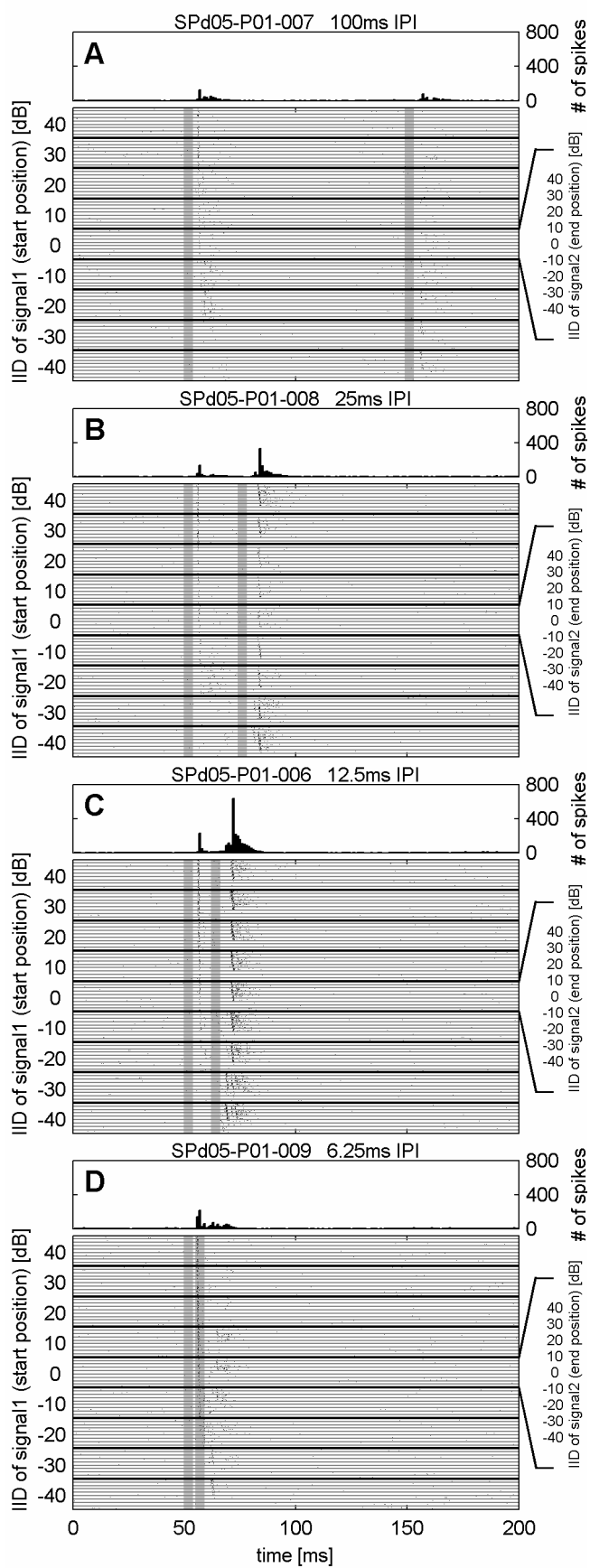


Fig. 4.7 *PSTHs and dot raster plots of a motion sensitive unit for four different IPI steps. The y-axis of the dot raster plots is double scaled.*

The thick horizontal black lines mark the nine azimuthal positions of signal 1 and the thin horizontal black lines between two thick lines mark the nine azimuthal position of signal 2. The gray bars represent the temporal position of the two successive acoustic signals of the 81 two-tone stimuli.

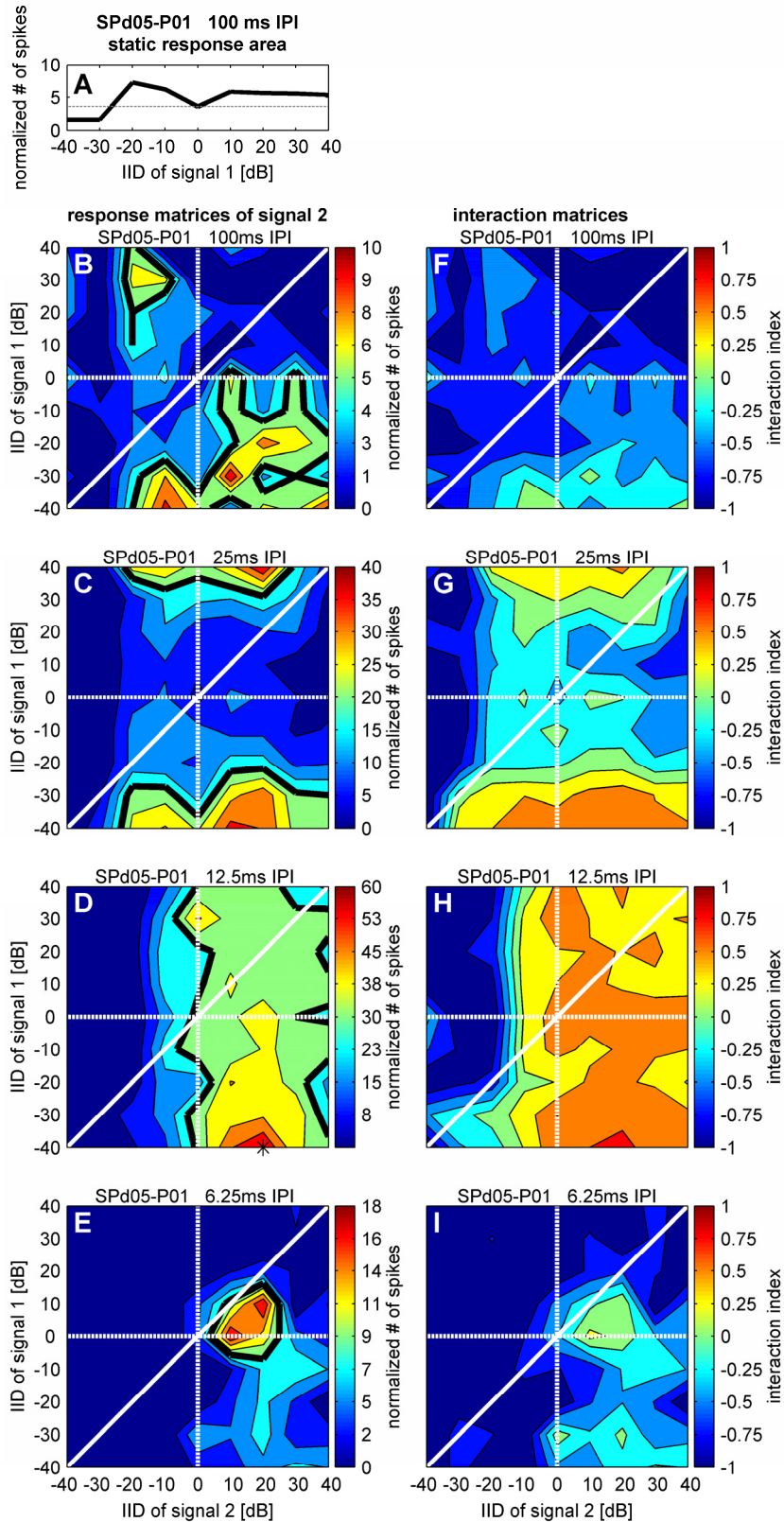


Fig. 4.8 A) Static response area, B-E) response matrices of signal 2 and F-I) interaction matrices of the motion sensitive unit in Fig. 4.7 for four IPI steps. The black asterisk indicates the best stimulus at the best IPI. Meaning of solid and dashed lines as in Fig. 4.3C.

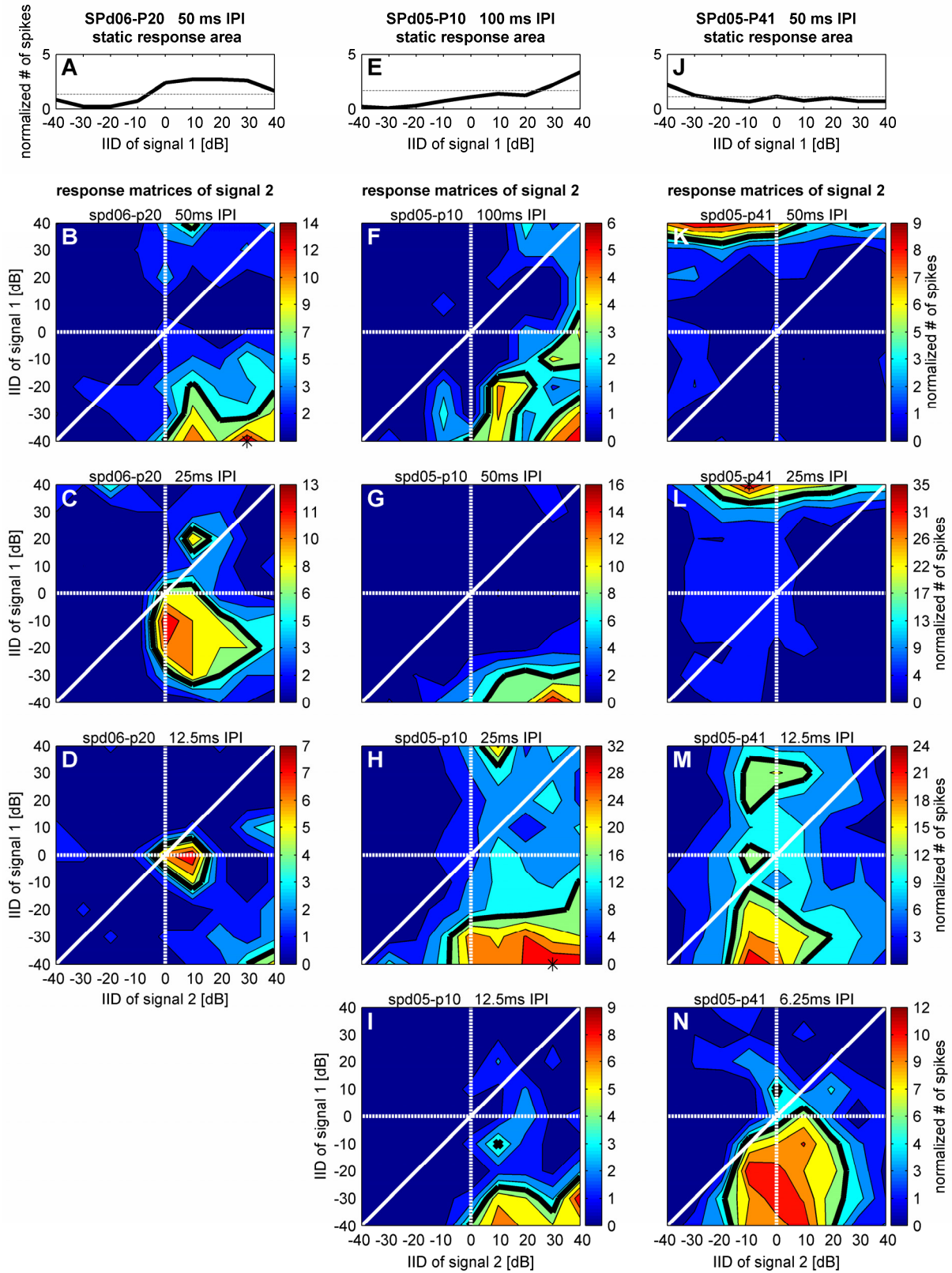


Fig. 4.9 *A, E, J) Static response areas, B-D, F-I, K-N) response matrices of signal 2 of three motion sensitive units for different IPI steps. The black asterisks indicate the best stimulus at the best IPI of the particular unit. Meaning of solid and dashed lines as in Fig. 4.3C.*

4.4.3 Representation of motion sensitivity at the cortical surface

Figure 4.10A shows the locations of the 236 recording sites on the cortical surface of the lateral view of the brain of *P. discolor*. Borders of the AC and auditory cortical subfields are indicated. A tessellation map (see Methods) of the spatial representation of the InIs of the best stimulus is projected on the flattened surface of the AC (Fig. 4.10B, for details on the projection procedure see Hoffmann et al. 2008b). Figure 4.10C depicts a projection of the motion sensitive recording sites (red squares) and the motion insensitive recording sites (black squares) on the flattened surface. Interestingly, recording sites of motion sensitive units cluster at the posterior dorsal field (PDF) of the AC (see Hoffmann et al. 2008b for partitioning of the AC of *P. discolor*), whereas recording sites of motion insensitive units are more uniformly scattered over different cortical fields. In the anterior dorsal field, anterior ventral field, and posterior ventral field motion sensitive units were rare with only 3 % (1 of 40), 9 % (1 of 11), and 7 % (3 of 44) units, respectively, whereas in the PDF 22 % (31 of 141) units showed strong response facilitation to dynamic stimulation and were classified as motion sensitive.

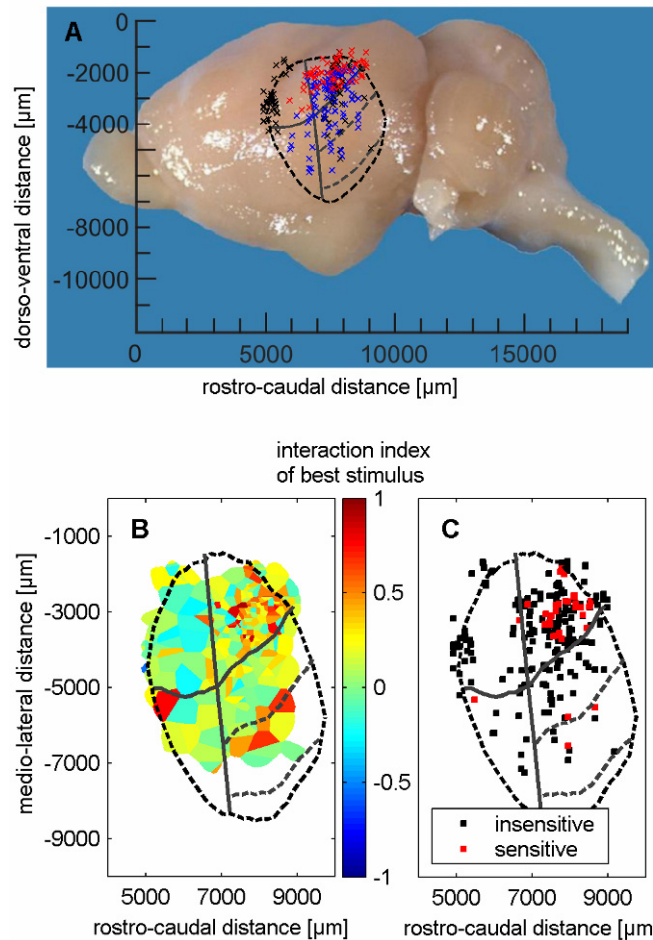


Fig. 4.10 Location of recording sites and cortical representation of motion sensitivity. *A)* Brain of *P. discolor* in a lateral view. Recording sites in bat 1 (black crosses), bat 2 (blue crosses) and bat 3 (red crosses) are projected onto the brain surface. The borders of the AC are marked by the dashed black lines and the borders of the auditory cortical subfields are marked by the gray solid lines (adapted from Hoffmann et al., 2008b). *B)* Tessellation map of the interaction indices of the best stimuli for 236 units projected onto the unrolled and flattened surface of the auditory cortex. *C)* Spatial distribution of motion sensitive and insensitive units at the auditory cortex of *P. discolor*. Recording sites of motion sensitive units are indicated by red squares and recording sites of motion insensitive units are marked by black squares.

4.4.4 Basic response properties of motion sensitive and insensitive units in the PDF

The following basic response properties were obtained by acoustic stimulation with pure tones of 20 ms in duration.

BFs and response thresholds were determined from the FRA and ranged for motion sensitive and motion insensitive units within the motion sensitive area, PDF, from 54 to 78 kHz (mean: 65.7 ± 6.4 kHz) and 22 to 70 dB SPL (mean: 41.4 ± 13.4 dB SPL), and 39 to 92 kHz (mean: 67.6 ± 11.2 kHz) and 0 to 73 dB SPL (mean: 43 ± 13.7 dB SPL), respectively. First spike latencies measured at BF and 20 dB above threshold of motion sensitive and motion insensitive units within the motion sensitive cortical area covered a range between 5 and 50 ms (mean: 11.1 ± 9 ms) and 5 and 45 ms (mean: 9.8 ± 7.2 ms), respectively. Response durations ranged from 6 to 205 ms (mean: 56.3 ± 47.4 ms) for motion sensitive units within the motion sensitive area, and from 3 to 182 ms (mean: 39.8 ± 41.1 ms) for motion insensitive units within the motion sensitive area. Units with the binaural response types E0 / 0E, EE and EI / IE were observed in both, motion sensitive and insensitive units.

The distributions of basic response properties like BFs, thresholds and latencies, response durations and binaural response types are shown in Fig. 4.11A-E. No significant difference (Mann-Whitney U test, $p < 0.05$) between motion sensitive and motion insensitive units within the motion sensitive area could be observed for BFs, thresholds and response latencies. However, response durations were significantly longer in motion sensitive units than in motion insensitive units (Mann-Whitney U test, $p < 0.05$). The distribution of binaural response types was also different for motion sensitive compared to insensitive units. In motion insensitive units, EE was the most frequently observed binaural response type, whereas it was rarely observed in motion sensitive units.

4.4.5 Motion specific response properties of motion sensitive and insensitive units in the PDF

Response properties described in the following paragraph were obtained by analyzing the response to signal 2 of the two-tone paradigm.

As shown in Fig. 4.11F, best IPIs measured at discrete IPI steps given by the experimental paradigm ranged between 6.25 and 50 ms for motion sensitive units and between 6.25 and 150 ms for motion insensitive units within the PDF. The distribution of best IPIs is significantly different (Kolmogorov-Smirnov test, $p < 0.05$) for both types of units. Most motion sensitive units (81 %, 25 of 31) responded best to two-tone stimuli with short IPIs (12.5 to 25 ms), whereas motion insensitive units also showed long best IPIs up to 150 ms. Figure 4.11G, H shows the azimuthal start- and end-positions of the best stimulus for motion sensitive and insensitive units within the PDF. The azimuthal start position (signal 1) of the

best stimulus was located at the most ipsilateral positions of -40 to -30 dB IID for most motion sensitive (71 %, 22 of 31) and motion insensitive (54 %, 59 of 110) units in the PDF (Fig. 4.11G). The distribution of azimuthal-end positions (signal 2) of the best stimulus showed slight differences between motion sensitive and insensitive units in the PDF, which, however, are not significant (Kolmogorov-Smirnov test, $p < 0.05$). Motion sensitive units often responded best when movements ended at frontal positions in azimuth, i.e. between -10 and +20 dB IID, whereas a large amount of motion insensitive units (45 %, 49 of 110) responded best to movements toward the most contralateral azimuthal positions of +30 and +40 dB IID (Fig. 4.11H). Consequently, motion sensitive units generally responded best to shorter motion distances in contralateral direction whereas motion insensitive units favored longer motion distances in contralateral direction.

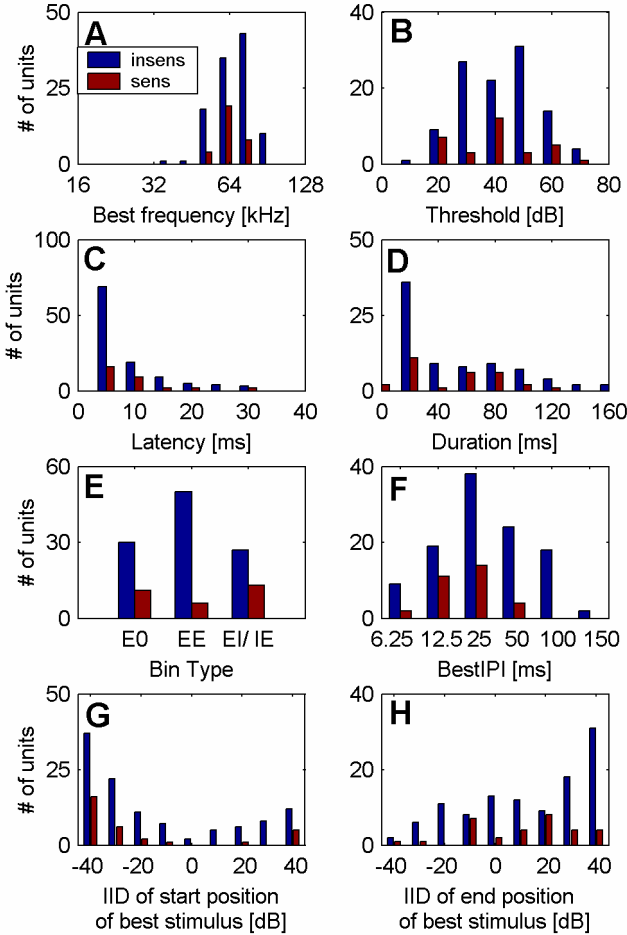


Fig. 4.11 Distribution of **A)** best frequency, **B)** threshold, **C)** latency, **D)** duration, **E)** binaural response type, **F)** best IPI, **G)** and **H)** azimuthal start and end position, respectively, of the best stimulus at best IPI for motion sensitive (red) and insensitive (blue) units.

The motion direction that elicited the strongest response in motion sensitive units was generally the direction toward azimuthal positions eliciting highest responses in the static azimuthal response area (in most cases towards contralateral positions). However, this preferred motion direction could change with IPI in some cases (see Fig. 4.9K-N for an example). In motion insensitive units strongest responses were also elicited by motion into the static response area but in contrast to sensitive units the preferred motion direction did normally not change (Fig. 4.6B-E).

4.5 Discussion

For the present study, neuronal responses to apparent sound movement in acoustic space have been recorded in the AC of anaesthetized bats, *P. discolor*. Apparent motion in the horizontal plane was generated by binaural presentation of tone pairs with different IIDs and varying IPIs. Thus the specific parameters of apparent motion, spatial extent and motion direction, changed for each stimulus pair. Motion sensitivity characterized by strongly facilitated responses to dynamic stimulation in contrast to static stimulation was observed in 15 % of units. Motion sensitive units had typically shorter best IPIs in comparison to motion insensitive units. The majority of 86 % of motion sensitive units clustered at the PDF of the AC of *P. discolor* indicating the involvement of this cortical subfield in motion processing. Most interestingly, 28 % of motion sensitive units focused their dynamic response area to narrow range movements in the frontal field with decreasing IPIs. Thus, the present study has demonstrated that units in the AC not merely respond to dynamic changes of IIDs simulating azimuthal movements, but can display a distinct preference to moving compared to stationary sound sources. In addition, these movement preferring units are concentrated on a distinct location in the dorso posterior part, indicating that certain specificity to azimuthal movements is limited to a distinct subset of auditory cortical units.

4.5.1 Comparison to other studies

In previous studies on motion processing in the auditory system of bats, the stimulus paradigms were rather inflexible considering the large variability of sound source movements typical for a bat's acoustic environment. Acoustic motion started in general at the extreme ipsilateral or contralateral location and moved to the most contralateral or ipsilateral position, respectively. This was done either by sequentially activating successive loud speakers which were positioned along the horizontal plane (Kleiser and Schuller 1995; Wilson and O'Neill 1998) or by changing the IID of successive sound stimuli which were binaurally presented via ear phones (Firzlaff and Schuller 2001b; Schlegel 2002). No small distance movements and no IPIs below 25 ms have been tested in previous studies. The most interesting range of IPIs below 20 ms as used by FM-bats while they are approaching a target (Griffin et al. 1960; Moss and Surlykke 2001) has therefore not been used. The stimulus paradigm of the present

study makes a difference in that a large repertoire of acoustic horizontal movements with different amplitudes and azimuthal positions were presented. The short IPIs below 25 ms more realistically mimicked echo repetition rates perceived by bats while approaching a target. This range of short IPIs proved to be appropriate, as most motion sensitive units preferred short IPIs (see Fig. 4.11F).

4.5.2 Motion sensitivity

Motion sensitivity of cortical units manifested as strong facilitation of responses to dynamic stimulation in contrast to static stimulation has not been described in bats before. Facilitated neuronal responses in bats have been recorded to combinations of time shifted spectral elements of the bat's echolocation call in the inferior colliculus of *P. parnellii* (Mittmann and Wenstrup 1995), in the medial geniculate body of *P. parnellii* (Olsen and Suga 1991b) and in the AC of *R. rouxi* and *P. parnellii* (Suga and Horikawa 1986; Schuller et al. 1991) and of *M. lucifugus* (Tanaka et al. 1992). Delay-tuned neurons activated by combinations of FM components of the echolocation call and echo encode target range (Feng et al. 1978; O'Neil and Suga 1979), whereas neurons with facilitatory responses to combinations of the CF part of the call and the echo may be involved in identifying the velocity of a sound source moving towards the animal in a radial direction (Suga 1989; Olsen and Suga 1991a). Facilitated responses in these studies were related to the temporal sequence of the different spectral components, and the spatial position of the stimulus source remained constant. In the present study, the spectral content of the stimulus components remains constant since pure tones at BF of the particular unit were used. Furthermore, the spatial positions with the maximum dynamical response of motion sensitive units (black asterisks in Fig. 4.8D and 4.9B, H and L) never coincided with positions on the diagonal line of the dynamic response area designating stationary two-tone stimuli. Thus, facilitation was strongest when two successive stimuli were separated in spatial position as well as in time, and therefore essentially resulted from acoustic motion in space. However, as shown for delay tuned combination sensitive neurons, in the AC of *P. parnellii* (Suga 1990), *R. rouxi* (Schuller et al. 1991) and *C. perspicillata* (Esser and Eiermann 2004), motion sensitive neurons with strongly facilitated responses in *P. discolor* were located in the dorsal region of the AC above the tonotopically organized primary auditory areas. But in contrast to delay tuned combination sensitive neurons in the AC of the closely related phyllostomid bat *C. perspicillata*, motion sensitive neurons with facilitatory responses in *Phyllostomus* were not equally distributed in dorsal cortical subfields but were confined to the caudal sub-region of the dorsal AC, the posterior dorsal field (PDF). This indicates that the PDF is especially involved in processing of acoustic motion and supports the finding of a previous study investigating the organization of basic response properties in the AC of *P. discolor* where PDF was supposed to be particularly important for processing of information derived from echolocation (Hoffmann et al. 2008b). Concluding, it is obvious that motion sensitivity in the AC of *Phyllostomus* is somehow related to combination sensitivity in the AC of other bats. But whereas combination sensitivity in the previous

studies is simply an effect of delay tuning, motion sensitivity in the present study is an effect of delay tuning with a compulsive spatial component.

Up to now, motion sensitivity was always characterized either by a shift of the azimuthal response area during stimulation with moving sounds or by a preference for a certain motion direction (Sovijärvi and Hyvärinen 1974; Wagner and Takahashi 1990; Ahissar et al. 1992; Kleiser and Schuller 1995; Wilson and O'Neill 1998; Firzlauff and Schuller 2001b; Schlegel 2002). However, these criteria did not serve for distinguishing motion sensitive from insensitive units in the present study, because units of both types showed response area shifts and preferences for a certain motion direction. The size and spatial position of the azimuthal response area of units in the present study was always influenced by the IPI. In motion sensitive units the azimuthal response area increased with decreasing IPI and thus was expanded towards previously unresponsive positions. With further decreasing IPI the azimuthal response area decreased again and at shortest IPIs often focused on small distant movements passing frontal azimuthal positions. Thus, these neurons seem to be presumably relevant for the detection of moving targets during the phase of final approach towards a target when the repetition rate of emitted calls and returning echoes, respectively, is highest. This point of view is supported by a study on the sonar beam pattern of *E. fuscus* (Ghose and Moss 2003). Ghose and Moss described that the bat first scans its environment with the sonar beam. After a target was selected, *Eptesicus* increases the repetition rate of its calls and centers the axis of its sonar beam at the target while approaching it. The angle between the beam axis and the target progressively decreases with decreasing time to contact, indicating that the bat first perceives the target at peripheral positions of its acoustic gaze and when it gets closer to the target, the bat actively focuses its sonar beam onto the target. At a time to contact of 300 ms, the bat locked its beam onto the target with an accuracy of $\pm 3^\circ$. At this point in time, the IPI between successively emitted calls and returning echoes, respectively, is below 50 ms and it further decreases with decreasing time to contact. Ghose and Moss hypothesize, that the motor action of focusing the sonar beam to the direction of a target is a naturally occurring behavior and is part of the target selection and tracking process. The motion sensitive cortical units in the present study, which focused their azimuthal response area on small movements in the frontal field at short IPIs could probably provide acoustic feedback information for the vocal motor action. For example, the unit depicted in Fig. 4.8F-I responded strongest to largely scaled movements starting at peripheral azimuthal positions (-40 to -30 and 30 to 40 dB IID) at an IPI of 25 ms (scanning phase) and focused its azimuthal response area to small movements in the frontal field at an IPI of 6.25 ms. The hypothesis is further supported by the distribution of best IPIs in motion sensitive units. In these units best IPIs were never above 50 ms, which is the IPI occurring between emitted vocalizations 300 ms before contact with the target, i.e. the point in time when the bat locked its beam axis onto the selected target (Ghose and Moss 2003).

4.5.3 Inhibition by dynamic stimulation

In contrast to previous studies, motion insensitive units in the AC of *P. discolor* did also show IPI dependent response area shifts. But other than in motion sensitive units, azimuthal response areas of insensitive units mostly decreased in size with decreasing IPI. In the inferior colliculus of *R. rouxi*, a narrowing of the azimuthal response range with decreasing IPI of motion stimuli was observed in 38 % of tested units and was suggested to be a result of a suppression of the lagging pulse by the leading pulse (Kleiser and Schuller 1995). In IC neurons of the guinea pig, a decrease of the size of azimuthal response areas with decreasing IPI was suggested to be due to adaptation of excitation by repeated stimulation (Ingham et al. 2001). This hypothesis has been supported by a study investigating the influence of inhibition on acoustic motion sensitivity in cortical units in *R. rouxi* (Firzlaff and Schuller 2001a). They found that adaptation of excitation, as well as cortex specific GABAergic inhibition, contribute to motion-direction sensitivity in the AC of *Rhinolophus*. Suppressive effects found in motion insensitive units of the present study, which resulted in a narrowing of the dynamic azimuthal response area might be mainly due to a combination of spatial and temporal inhibitory mechanisms. One can see that the temporal suppressive effect is limited to certain spatial positions of signal 2. At an IPI of 25 ms and at a spatial position of signal 1 of +40 dB IID, the response to signal 2 was suppressed at spatial positions between -40 and +20 dB IID, but at a spatial position of +30 to +40 dB IID signal 2 still elicited a neural response (Fig. 4.5B). If the suppression of the neural response to signal 2 would be due to adaptation of excitation by signal 1, signal 2 should not be able to elicit a response at an IID of +40 dB because the adaptive effect should be strongest when signal 1 and signal 2 are equal. Thus, the motion induced suppressive effect, which resulted in a narrowing of the dynamic azimuthal response area in motion insensitive units found in the present study is probably not a result of adaptation but might be better explained in the following way: Each unit demonstrated a certain spatial tuning, which was constituted as the units static azimuthal response area. During static stimulation with binaural stimuli, units showed excitation to stimuli from one side and inhibition to stimuli from the other side. During dynamic stimulation, this binaural inhibition was enhanced by a preceding stimulus. The degree of inhibition and thus the extent of the narrowing of the dynamic azimuthal response area strongly depended on the spatial position of signal 1 and the time interval between the two signals. A decrease of the time interval between the two signals further amplifies the binaural inhibitory effect (Fig. 4.5C-D). Similar findings are described for collicular neurons of the big brown bat, *E. fuscus*. Wu and Jen (1996) showed that repeated stimulation with different repetition rates narrows the azimuthal receptive range of about one half of tested neurons. In a subsequent study Zhou and Jen (2002) demonstrated, that GABA-mediated inhibition, which might be due to synaptic depression, contributes to pulse repetition rate-dependent shaping of the azimuthal response area. Consequently, the narrowing of the azimuthal response area with decreasing IPI in motion non-sensitive units of the present study might be rather an effect of repetition rate dependent binaural sensitivity than of motion sensitivity.

4.6 Acknowledgements

This work was supported by the Deutsche Forschungsgemeinschaft GRK 1091 “Orientation and Motion in Space”.

General discussion

The present work comprises four independent studies investigating the AC of the echolocating bat *P. discolor*. In the first study, the behavioral audiogram and neural audiograms of the IC and AC of *P. discolor* were obtained. The data on both behavioral and neuronal hearing thresholds indicated that hearing in this bat is quite sensitive with absolute thresholds down to 0 dB SPL and below. The neural audiograms obtained from the IC and the AC showed a high degree of similarity. In both cases, threshold minima were in the mid frequency range around 35 to 55 kHz. The detection and analysis of conspecific communication calls takes place in the low frequency range around 30 kHz, where *P. discolor* has very good hearing as both, the behavioral and neural audiograms showed. The behavioral data also indicated very low thresholds in the spectral range of *P. discolor* echolocation calls as an adaptation for faint echoes from the relatively low-intensity echolocation calls emitted by *P. discolor*. However, this high sensitivity around 80 kHz was not reflected in the neural data exhibiting roughly 20 dB higher thresholds. Psychophysically and neurophysiologically determined absolute hearing thresholds in *Phyllostomus* matched well those of other bat species (Grinnell 1970; Sterbing et al. 1994; Esser and Eiermann 1999; Heffner et al. 2003; Koay et al. 2002; Koay et al. 2003). The data suggested, however, that *P. discolor* has considerably better absolute auditory thresholds than estimated in a previous study (Esser and Daucher, 1996).

The second study focused on the delimitation of the AC within the neocortex of *P. discolor* and its parcellation. The auditory cortical area of *P. discolor* covered the parieto-temporal portion of the neocortex with approximately 4800 x 7000 μm^2 in rostro-caudal and medio-lateral extension, respectively. The location and extension of the AC in *P. discolor* as defined in this study roughly corroborated the findings from an earlier 2-DG study in the same species (Esser 1995). The large area of neocortex responsive to acoustic stimulation comprised four major anatomically distinguishable fields: a ventral part of the AC with an anterior and a posterior subdivision (AVF and PVF) and a dorsal part of the AC further divided into anterior and posterior subfields, ADF and PDF. The neuroarchitectural delimitation of the AC was in concert with the differentiation based on acoustical response properties of units in the cortical subfields. The two ventral fields were distinguished by their tonotopic organization with opposing frequency gradients. The neuroanatomical and neurophysiological properties of the tonotopically organized PVF reflected common characteristics of AI in the mammalian AC. The AVF, located rostrally to the PVF, showed a tonotopic BF gradient running roughly in opposite direction to the gradient of the PVF. Thus, the AVF of *P. discolor* might represent

the AAF described in other mammals. The dorsal cortical fields were not tonotopically organized and contained only neurons responsive to high frequencies. As most energy of the echolocation pulse of this bat species is contained in the frequency range between 60 to 80 kHz, the dorsal region of the AC of *P. discolor* seems to be particularly important for echolocation. With regard to the relative position of cortical fields and their basic properties, the AC of *P. discolor* seems to follow the organizational pattern seen in other phyllostomid bats (Esser and Eiermann 1999).

The third study investigated neural correlates of a behaviorally relevant echo parameter i.e. echo roughness in the AC of *P. discolor*. In a roughness discrimination task bats only performed successfully if a minimum roughness of 2.5 (in units of base 10 logarithm of the stimulus fourth moment) was presented. Sixteen percent of cortical units, located in an anterior region of AC encoded echo roughness in their response strength. The performance of these neurons closely matched the bats' behavioral sensitivity to echo roughness. The neural responses of this subpopulation of auditory cortical neurons allowed a quantitative prediction of the behavioral ability to discriminate differences in the statistics of complex echoes. Roughness-sensitive units were accumulated in anterior cortical areas throughout the entire dorsoventral extension, probably in AAF and the anterior dorsal field. Occurrence of units encoding echo roughness in posterior ventral regions, presumably AI, was rare. In summary, the results show that psychophysical sensitivity to echo roughness as an ecologically meaningful parameter is quantitatively encoded in the AC of the echolocating bat *P. discolor*.

The fourth and last study investigated the cortical response characteristics to acoustic motion in the different subfields of the AC in *P. discolor* using a two-tone paradigm. Apparent horizontal acoustic motion was simulated by two successive binaural tone stimuli that differed in IID. Strongly facilitated responses to dynamic stimulation in contrast to static stimulation were observed in 15 % (36 of 236) of extracellularly recorded cortical units, which were termed as motion-sensitive. Motion-sensitive units typically responded best to binaural two-tone combinations with short temporal gaps, i.e. short delays between the two tones, that represented the start and end position of a virtual horizontal acoustic movement. All motion-sensitive neurons changed the center and/or size of their dynamic azimuthal response area depending on the temporal gap between the two tones. Motion-sensitive neurons were almost exclusively (86 %, 31 of 36) clustered in the caudal part of the dorsal AC indicating that this cortical area is specifically involved in the processing of acoustic motion. Most interestingly, 28 % (10 of 36) of motion-sensitive units focused their dynamic azimuthal response area on small movements in forward direction at very short temporal gaps between the two tones, indicating that these units may be relevant for the detection of moving targets during the phase of final approach towards a target (Griffin et al. 1960; Simmons et al. 1979). The motion-sensitive cortical units, which focused their azimuthal response area on small movements in the forward direction at short IPIs, can probably provide information on the target's actual position, and feedback to the motor control of head movements necessary to

keep the ultrasonic beam locked to the target. Ghose and Moss (2003) have shown that the bat *E. fuscus* actually centers its ultrasonic beam axis on a selected target when tracking it in flight.

Based on all studies, four major subfields could be distinguished in the AC of *P. discolor*. The ventral two subfields seem to represent the primary auditory “core” region, whereas the two subfields that are located dorsally seem to constitute a secondary auditory “belt” region. Furthermore it has been shown, that different aspects of sound (e.g. temporal envelope fluctuations and acoustic motion) are processed specifically in different subfields of the *Phyllostomus* AC, predominantly in the “belt” region. The specialization of different subfields for the processing of different aspects of sound is in register with the view of parallel processing along the auditory pathway, also implemented in separate pathways (e.g. Casseday et al. 1989; Rauschecker et al. 1997). In addition, recent studies showed that specialized information analysis of a subset of sound parameters is often associated to distinct neuronal subpopulations (Selezneva et al. 2006; Firzlaff et al. 2007; Nelken and Bar-Yosef 2008).

The parcellation of the *Phyllostomus* AC in comparison to other bats

Subdividing the AC according to functional and/or neuroarchitectural characteristics has led to a variety of cortical fields in different species of echolocating bats. The AC of the insectivorous FM-bat *M. lucifugus* consists of three functionally determined subregions: a dorsally located tonotopically organized zone, a more ventrally located time delay-sensitive zone, and an intermediate zone of major overlap (Wong and Shannon 1988). The AC of the insectivorous FM-bat *E. fuscus* is similar in its organization to the AC of *Myotis* and consists of an anterior and a posterior tonotopically organized field and a medial division with highly variable BF organization (Dear et al. 1993). The AC of insectivorous CF/FM-bats seems to be more specialized by showing a higher number of subfields. In the mustached bat *P. parnellii*, the AC consists of six functionally different subfields: a tonotopic zone, three dorsal fields including the dorsal fringe, FM-FM and CF-CF areas that are involved in processing of temporal information, and two ventral fields including the ventral fringe and ventral anterior area (Suga 1990). In *R. rouxi* five auditory cortical subfields can be distinguished. Besides three tonotopically organized subfields, the AC of *Rhinolophus* contains a dorsally located FM-FM field and a rostro-dorsally located CF-CF field (Schuller et al. 1991; Radtke-Schuller and Schuller 1995). Frugivorous bats such as *P. discolor* and the closely related short-tailed fruit bat *C. perspicillata* may play an intermediate role regarding their auditory cortical organization. With four major subfields existing in the AC of *Phyllostomus* (see Hoffmann et al. 2008b) and six subfields existing in the AC of *Carollia* (Esser and Eiermann 1999), respectively, frugivorous FM-bats show a higher number of auditory cortical subfields compared to insectivorous FM-bats. The organization pattern of the AC in *Phyllostomus* and *Carollia* is rather consistent with that observed in CF/FM-bats. As in the AC of *P. parnellii*

and *R. rouxi* (Suga 1990; Radtke-Schuller and Schuller 1995), primary auditory regions (e.g. AI and AAF) are located in the ventral part of the AC in frugivorous FM-bats, whereas auditory “belt” regions are dorsally located (Hoffmann et al. 2008b; Esser and Eiermann 1999). However, subfields of the AC in *P. discolor* and *C. perspicillata* do not show such a high degree of specialization for processing of echo information as it has been found in the AC of CF/FM-bats (e.g. the Doppler-shifted CF (DSCF) region in the AC of *Pteronotus*, the FM-FM and CF-CF areas in *Pteronotus* and *Rhinolophus*, for review see O’Neill 1995).

Functional role of different auditory cortical subfields in bats

Many previous studies investigating the AC of bats focused on the encoding of frequency and timing of acoustical signals. The frequency of a sound is already analyzed in terms of a “place code” in the cochlear by activation of the corresponding location along the basilar membrane (Lippe 1986). This tonotopical frequency representation has been found throughout all levels of the ascending auditory pathway of bats (Pollak and Schuller 1981; Ostwald 1984; Vater et al. 1985; Covey and Casseday 1986; Zook and Leake 1989; Radtke-Schuller and Schuller 1995; O’Neill 1995; Wenstrup 1999). Special to the tonotopically organized AI in *P. parnellii* is the DSCF area, which stretches the tonotopic sequence and contains neurons with BF’s around the bat’s resting and reference frequency (Suga and Jen 1976). A similar overrepresentation of the reference frequency range has been found in *R. ferrumequinum* and *R. rouxi* (Ostwald 1984; Radtke-Schuller and Schuller 1995). Due to the extremely sharp frequency tuning of neurons within this area, it is called the “acoustic fovea”. Neurons in the foveal area are highly sensitive to minute frequency modulation caused for example by fluttering insect wings and were therefore suggested to be important for the detection of fluttering targets (Schuller and Radtke-Schuller 1995; O’Neill 1995).

Simple pure tone stimuli are rare in a natural environment and the auditory system must be able to analyze sounds with considerably more complex spectro-temporal structure. Firzlaff and Schuller (2007) demonstrated that neurons in the AC of *P. discolor* can encode the specific spectral shape of an auditory object independently of the stimulus amplitude. The nectar-feeding bat *Glossophaga soricina* shows a similar scale-independent performance when discriminating flower-like objects independent of their size by using the spectral pattern representing the auditory object (von Helversen 2004). Thus, cortical neurons as found in the electrophysiological study (Firzlaff and Schuller 2007) might be the neural correlate of the size- or amplitude-independent recognition of characteristics of auditory objects, like echoes from specific flowers.

The neuronal encoding of temporal properties of sound events e.g. sound onset, sound duration and rate of modulation of frequency or amplitude has also been intensively investigated in most parts of the auditory system in bats (Covey and Casseday 1991; Olsen and Suga 1991a; Fitzpatrick et al. 1993; Casseday et al. 1994; Fuzessery and Hall 1999;

Grothe et al. 2001). The most frequently investigated temporal sound feature in bats is the time interval (delay) occurring between successive sound events. This sound parameter is especially important for echolocating bats because they use the time delay between an emitted call and a returning echo to calculate the range of the target that reflected the echo (O'Neil and Suga 1979). "Delay sensitive" or "delay tuned" neurons have been found in the AC of all bats studied so far (*P. parnellii*: (Suga 1990), *R. rouxi*: (Schuller et al. 1991), *M. lucifugus*: (Wong and Shannon 1988), *E. fuscus*: (Dear et al. 1993), *C. perspicillata*: (Esser and Eiermann 2004), *P. discolor*: Chapter 4 of this thesis). In *Eptesicus* and *Myotis* delay tuning occur in neurons that are co-located with "unspecialized" neurons within the tonotopically organized primary auditory cortical areas, whereas in *Pteronotus* and *Rhinolophus* as well as in *Carollia* and *Phyllostomus* delay-tuned neurons are segregated into dorsally located non-tonotopically organized auditory cortical subfields. In CF/FM-bats delay tuning is most often linked to combination sensitivity. Only a combination of the first harmonic of the echolocation call and a higher harmonic of the echo with a certain time delay can elicit a strong response in delay-sensitive FM-FM neurons in the AC of *P. parnellii* and *R. rouxi* (Suga et al. 1978; Schuller et al. 1991). In contrast, delay tuning in FM bats is not limited to combinations of specific spectral components of the echolocation call and echo. In the AC of *Carollia*, delay-tuned neurons respond best if the acoustic stimulus consists of virtually identical FM-sweeps that differ by no more than 3 kHz (Esser and Eiermann 2004). Delay-sensitivity in neurons in the AC of *Myotis* is also not reliant on combinations of different harmonics (Berkowitz and Suga 1989). Delay-sensitive cortical neurons in *Phyllostomus* also respond well to temporally separated pure tones with identical frequency. Strongest responses in these units, however, are elicited by stimuli that are separated in time and azimuthal position (Chapter 4 of this thesis). Thus, delay-tuned neurons in the AC of bats may be involved in processing of other parameters besides target range as suggested by the results of the fourth series of experiments (Chapter 4 of this thesis). Neurons in the posterior dorsal field of the AC in *Phyllostomus* are not simply delay-sensitive but in addition respond best to stimulus combinations with specific spatial separation. Delay-dependent strong facilitation to dynamic stimuli with changing spatial positions indicates that these neurons encode preferentially acoustic motion, since a change of spatial position in successive echoes is perceived by the bat as movement of the echo source. The large spatial receptive fields with uniform response magnitudes found by Suga et al. (1990) in delay-tuned FM-FM neurons in *Pteronotus* led them to the conclusion that directional information is probably processed in parallel by a separate population of neurons other than delay-tuned FM-FM neurons. As the spatial receptive fields in *Pteronotus* were measured statically this is no contradiction to the findings in *Phyllostomus* showing clear motion specificity in delay-tuned cortical neurons.

The only further study on acoustic motion processing in the AC of bats has been performed in the CF/FM-bat *R. rouxi*. Motion sensitive neurons in this bat are characterized by either a preference for motion direction or by a shift of the azimuthal receptive field in the dynamic situation. Motion sensitive neurons were detected in the anterior- and posterior-dorsal fields as well as in the primary field in the AC of *R. rouxi* (Firzlaff and Schuller 2001b). Only few

neurons in the dorsal portion of the dorsal field, which is the area in the AC of *R. rouxi* that contains delay-tuned FM-FM neurons (Schuller et al. 1991), were tested with acoustic motion stimuli. It is therefore unclear whether delay-tuned FM-FM neurons in *R. rouxi* are able to encode directional information.

As mentioned before, motion sensitive units are uniformly distributed within the three tested subfields of the AC in *R. rouxi*, whereas in the AC of *P. discolor* neurons involved in acoustic motion processing accumulate in the posterior dorsal subfield. Thus, for the first time in auditory research in bats, the present work gives evidence for an auditory cortical subfield whose functional role seems to be the encoding of horizontal acoustic motion stimuli.

The localization of a subfield involved in processing of spatial information in the posterior dorsal belt area of the AC fits well in the general view on the existence of two separate processing streams for object and spatial sensory information. As first described in the visual cortex of non-human primates, the ventrally directed “what” pathway contains areas with neurons selective for color and size of visual objects (Zeki 1983; Desimone and Schein 1987), whereas the dorsally directed “where” pathway covers visual cortical areas with neurons selective for the direction of motion (Movshon and Newsome 1996). A study on the functional specialization and hierarchical organization of multiple areas in the rhesus monkey AC indicated that the cortical auditory system in primates also is divided into two different streams for the processing of “what” and “where” (Rauschecker and Tian 2000). The dorsal stream originates in the caudal part of the superior temporal gyrus and projects via the parietal cortex to caudal dorsolateral prefrontal cortex. The ventral pattern or object stream originates in the more anterior portions of the lateral belt and targets rostral and ventral prefrontal areas (Romanski et al. 1999).

Outlook

The results of the third and fourth study indicate that processing of complex auditory parameters takes place at the highest level of auditory processing, the auditory cortex. Other recent studies in bat AC showed that cortical responses to sound are highly dynamic and dependent upon stimulus context (Washington and Kanwal 2008; Medvedev and Kanwal 2008; Razak et al. 2008). However, the neural mechanisms underlying the perceptual consequences of acoustic stimulus context remains still unclear and connections with physiological correlates are speculative. Thus further neurophysiological studies investigating neural correlates of auditory perception in un-anaesthetized and behaving animals using complex sound stimuli are necessary to understand the neural basis of auditory perception.

All data presented within this work were obtained from anesthetized bats. It is known that anesthetics can influence neural processing of acoustic stimuli in the AC (Gaese and Ostwald 2001; Syka et al. 2005; Rennaker et al. 2007). For example, benzodiazepines like Midazolam, which was used in the present studies, enhances GABA_A-mediated inhibition. Furthermore, it has been recently shown that attention can modulate the activity of the auditory system (Fritz et al. 2007; Rinne et al. 2008). Thus, during the present studies, effects due to anesthesia may have influenced the response properties (e.g. response pattern) of cortical neurons. Motion sensitivity in chapter four of this thesis was characterized by strong facilitation of neuronal responses to dynamic stimulation. Response facilitation in combination sensitive and delay-tuned neurons is suggested to be created by coincidence of a postinhibitory rebound excitation elicited by a first stimulus with an excitation evoked by a second stimulus (Nataraj and Wenstrup 2005). Thus, one could suggest that an enhancement of GABA_A-mediated inhibition due to the anesthesia could have influenced the facilitatory responses of motion sensitive neurons. However, a recent study found that exclusively glycinergic inhibitory inputs are required to evoke facilitatory combination sensitive interactions (Sanchez et al. 2008).

Nevertheless, the investigation of motion sensitive neurons in an awake and behaving bat would be highly interesting especially to evaluate the influences of attention on the neural processing of behaviorally important sound parameters.

Although, the present work compiles basic and complex response properties of neurons in the different subfields of the AC in *P. discolor*, it is limited by the lack of data on neuronal connectivity between these partially specialized subfields and other brain structures. For example, a strong connection between the motion sensitive posterior dorsal field and vocally active brainstem areas that are involved in the functional control of echolocation calls may support the assumption that motion sensitive neurons in the PDF provide dynamic auditory feedback for the vocal-motor control during target tracking. Injections of neuronal tracers

should be made at neurophysiologically defined sites within the different subfields of the AC in *Phyllostomus* to investigate the neural connectivity, which could further contribute to the functional characterization of these subfields.

References

- Ahissar,M., Ahissar,E., Bergman,H. & Vaadia,E. (1992) Encoding of sound-source location and movement: Activity of single neurons and interactions between adjacent neurons in the monkey auditory cortex. *J Neurophysiol*, **67**, 203-215.
- Andersen,R.A., Knight,P.L. & Merzenich,M.M. (1980) The thalamocortical and corticothalamic connections of AI, AII and the anterior auditory field (AAF) in the cat: evidence for two largely segregated systems of connections. *J Comp Neurol*, **194**, 663-701.
- Berkowitz,A. & Suga,N. (1989) Neural mechanisms of ranging are different in two species of bats. *Hear Res*, **41**, 255-264.
- Bieser,A. & Müller-Preuss,P. (1996) Auditory responsive cortex in the squirrel monkey: Neural responses to amplitude-modulated sounds. *Exp Brain Res*, **108**, 273-284.
- Bizley,J.K., Nodal,F.R., Nelken,I. & King,A.J. (2005) Functional organization of ferret auditory cortex. *Cereb Cortex*, **15**, 1637-1653.
- Bohn,K.M., Boughman,J.W., Wilkinson,G.S. & Moss,C.F. (2004) Auditory sensitivity and frequency selectivity in greater spear-nosed bats suggest specializations for acoustic communication. *J Comp Physiol A Neuroethol Sens Neural Behav Physiol*, **190**, 185-192.
- Borst,A. & Egelhaaf,M. (1989) Principles of visual motion detection. *Trends Neurosci*, **12**, 297-306.
- Brett-Green,B., Fifkova,E., Larue,D.T., Winer,J.A. & Barth,D.S. (2003) A multisensory zone in rat parietotemporal cortex: intra- and extracellular physiology and thalamocortical connections. *J Comp Neurol*, **460**, 223-237.
- Britten,K.H., Shadlen,M.N., Newsome,W.T. & Movshon,J.A. (1992) The analysis of visual motion: a comparison of neuronal and psychophysical performance. *J Neurosci*, **12**, 4745-4765.
- Brosch,M. & Scheich,H. (2003) Neural representation of sound patterns in the auditory cortex of monkeys. In Ghazanfar,A.A. (ed), *Primate audition: ethology and neurobiology*. CRC Press, Boca Raton, FL, pp. 151-175.
- Carvell,G.E. & Simons,D.J. (1987) Thalamic and corticocortical connections of the second somatic sensory area of the mouse. *J Comp Neurol*, **265**, 427.
- Casseday,J.H., Ehrlich,D. & Covey,E. (1994) Neural tuning for sound duration: Role of inhibitory mechanisms in the inferior colliculus. *Science*, **264**, 847-850.

- Casseday, J.H., Kobler, J.B., Isbey, S.F. & Covey, E. (1989) Central acoustic tract in an echolocating bat: An extralemiscal auditory pathway to the thalamus. *J Comp Neurol*, **287**, 247-259.
- Chiu, C. & Moss, C.F. (2007) The role of the external ear in vertical sound localization in the free flying bat, *Eptesicus fuscus*. *J Acoust Soc Am*, **121**, 2227-2235.
- Clarey, J.C., Barone, P. & Imig, T.J. (1992) Physiology of thalamus and cortex. In Popper, A.N. & Fay, R.R. (eds), *The Mammalian Auditory Pathway: Neurophysiology*. Springer Handbook of Auditory Research. Springer-Verlag, Berlin, pp. 232-334.
- Clarke, S. & Rivier, F. (1997) Compartments within human primary auditory cortex: Evidence from cytochrome oxidase and acetylcholinesterase staining. *Eur J Neurosci*, **10**, 741-745.
- Clemo, H.R. & Stein, B.E. (1983) Organization of a fourth somatosensory area of cortex in cat. *J Neurophysiol*, **50**, 910-925.
- Covey, E. (2005) Neurobiological specializations in echolocating bats. *Anat Rec A Discov Mol Cell Evol Biol*, **287**, 1103-1116.
- Covey, E. & Casseday, J.H. (1991) The monaural nuclei of the lateral lemniscus in an echolocating bat: Parallel pathways for analyzing temporal features of sound. *J Neurosci*, **11**, 3456-3470.
- Covey, E. & Casseday, J.H. (1986) Connectional basis for frequency representation in the nuclei of the lateral lemniscus of the bat *Eptesicus fuscus*. *J Neurosci*, **6**, 2926-2940.
- Cruikshank, S.J., Killackey, H.P. & Metherate, R. (2001) Parvalbumin and calbindin are differentially distributed within primary and secondary subregions of the mouse auditory forebrain. *Neuroscience*, **105**, 553-569.
- Danscher, G. (1981) Histochemical demonstration of heavy metals. A revised version of the sulphide silver method suitable for both light and electronmicroscopy. *Histochemistry*, **71**, 1-16.
- Dear, S.P., Fritz, J., Haresign, T., Ferragamo, M. & Simmons, J.A. (1993) Tonotopic and functional organization in the auditory cortex of the big brown bat, *Eptesicus fuscus*. *J Neurophysiol*, **70**, 1988-2009.
- Dear, S.P. & Suga, N. (1995) Delay-tuned neurons in the midbrain of the big brown bat. *J Neurophysiol*, **73**, 1084-1100.
- Desimone, R. & Schein, S.J. (1987) Visual properties of neurons in area V4 of the macaque: sensitivity to stimulus form. *J Neurophysiol*, **57**, 835-868.
- Dyck, R., Beaulieu, C. & Cynader, M. (1993) Histochemical localization of synaptic zinc in the developing cat visual cortex. *J Comp Neurol*, **329**, 53-67.
- Ehret, G. (1997) The auditory cortex. *J Comp Physiol A Neuroethol Sens Neural Behav Physiol*, **181**, 547-557.

- Esser, K.H. (1995) Auditory processing in the FM-bat *Phyllostomus discolor*. From behavior to neocortical maps. In Elsner, N. & Menzel, R. (eds), 23rd Goettingen Neurobiology Conference, Learning and Memory, I. Thieme, New York, pp. 193.
- Esser, K.H. & Daucher, A. (1996) Hearing in the FM-bat *Phyllostomus discolor*: A behavioral audiogram. *J Comp Physiol A Neuroethol Sens Neural Behav Physiol*, **178**, 779-785.
- Esser, K.H. & Eiermann, A. (1999) Tonotopic organization and parcellation of auditory cortex in the FM-bat *Carollia perspicillata*. *Eur J Neurosci*, **11**, 3669-3682.
- Esser, K.H. & Eiermann, A. (2004) Processing of Frequency-Modulated Sounds in the *Carollia* Auditory and Frontal Cortex. In Thomas, J.A., Moss, C.F. & Vater, M. (eds), Echolocation in Bats and Dolphins. The University of Chicago Press, Chicago, pp. 190-195.
- Esser, K.H. & Kiefer, R. (1996) Detection of frequency modulation in the FM-bat *Phyllostomus discolor*. *J Comp Physiol A Neuroethol Sens Neural Behav Physiol*, **178**, 787-796.
- Esser, K.H. & Lud, B. (1997) Discrimination of sinusoidally frequency-modulated sound signals mimicking species-specific communication calls in the FM-bat *Phyllostomus discolor*. *J Comp Physiol A Neuroethol Sens Neural Behav Physiol*, **180**, 513-522.
- Esser, K.H. & Schmidt, U. (1990) Behavioral auditory thresholds in neonate lesser spear-nosed bats, *Phyllostomus discolor*. *Naturwissenschaften*, **77**, 292-294.
- Evans, E.E. & Nelson, P.G. (1973) On the functional relationship between the dorsal and ventral divisions of the cochlear nucleus of the cat. *Exp Brain Res*, **17**, 428-442.
- Ewert, S.D. & Dau, T. (2004) External and internal limitations in amplitude-modulation processing. *J Acoust Soc Am*, **116**, 478-490.
- Feng, A.S., Simmons, J.A. & Kick, S.A. (1978) Echo detection and target-ranging neurons in the auditory system of the bat *Eptesicus fuscus*. *Science*, **202**, 645-648.
- Fenzl, T. & Schuller, G. (2005) Echolocation calls and communication calls are controlled differentially in the brainstem of the bat *Phyllostomus discolor*. *BMC Biology*, **3**, 17.
- Firzlaff, U., Schornich, S., Hoffmann, S., Schuller, G. & Wiegrebe, L. (2006) A neural correlate of stochastic echo imaging. *J Neurosci*, **26**, 785-791.
- Firzlaff, U., Schuchmann, M., Grunwald, J.E., Schuller, G. & Wiegrebe, L. (2007) Object-oriented echo perception and cortical representation in echolocating bats. *PLoS Biol*, **5**, e100.
- Firzlaff, U. & Schuller, G. (2001a) Motion processing in the auditory cortex of the rufous horseshoe bat: role of GABAergic inhibition. *Eur J Neurosci*, **14**, 1687-1701.
- Firzlaff, U. & Schuller, G. (2003) Spectral directionality of the external ear of the lesser spear-nosed bat, *Phyllostomus discolor*. *Hear Res*, **181**, 27-39.

- Firzlaff,U. & Schuller,G. (2007) Cortical responses to object size-dependent spectral interference patterns in echolocating bats. *Eur J Neurosci*, **26**, 2747-2755.
- Firzlaff,U. & Schuller,G. (2001b) Cortical representation of acoustic motion in the rufous horseshoe bat, *Rhinolophus rouxi*. *Eur J Neurosci*, **13**, 1209-1220.
- Fitzpatrick,D.C., Kanwal,J.S., Butman,J.A. & Suga,N. (1993) Combination-sensitive neurons in the primary auditory cortex of the mustached bat. *J Neurosci*, **13**, 931-940.
- Fitzpatrick,D.C., Olsen,J.F. & Suga,N. (1998a) Connections among functional areas in the mustached bat auditory cortex. *J Comp Neurol*, **391**, 366-396.
- Fitzpatrick,D.C., Suga,N. & Olsen,J.F. (1998b) Distribution of response types across entire hemispheres of the mustached bat's auditory cortex. *J Comp Neurol*, **391**, 353-365.
- Franco-Pons,N., Casanovas-Aguilar,C., Arroyo,S., Rumia,J., Perez-Clausell,J. & Danscher,G. (2000) Zinc-rich synaptic boutons in human temporal cortex biopsies. *Neuroscience*, **98**, 429-435.
- Frederickson,C.J. (1989) Neurobiology of zinc and zinc-containing neurons. *Int Rev Neurobiol*, **31**, 145-238.
- Frederickson,C.J. & Moncrieff,D.W. (1994) Zinc-containing neurons. *Biol Signals*, **3**, 127-139.
- Fritz,J.B., Elhilali,M. & Shamma,S.A. (2007) Adaptive changes in cortical receptive fields induced by attention to complex sounds. *J Neurophysiol*, **98**, 2337-2346.
- Fuzessery,Z.M. (1996) Monaural and binaural spectral cues created by the external ears of the pallid bat. *Hear Res*, **95**, 1-17.
- Fuzessery,Z.M. & Hall,J.C. (1999) Sound duration selectivity in the pallid bat inferior colliculus. *Hear Res*, **137**, 137-154.
- Fuzessery,Z.M. & Pollak,G.D. (1984) Neural mechanisms of sound localization in an echolocating bat. *Science*, **225**, 725-728.
- Gaese,B.H. & Ostwald,J. (2001) Anesthesia changes frequency tuning of neurons in the rat primary auditory cortex. *J Neurophysiol*, **86**, 1062-1066.
- Gallyas,F. (1979) Silver staining of myelin by means of physical development. *Neurol Res*, **1**, 203-209.
- Garrett,B., Geneser,F.A. & Slomianka,L. (1991) Distribution of acetylcholinesterase and zinc in the visual cortex of the mouse. *Anat Embryol (Berl)*, **184**, 461-468.
- Garrett,B., Osterballe,R., Slomianka,L. & Geneser,F.A. (1994) Cytoarchitecture and staining for acetylcholinesterase and zinc in the visual cortex of the Parma wallaby (*Macropus parma*). *Brain Behav Evol*, **43**, 162-172.

- Geisler, C.D., Rhode, W.S. & Hazelton, D.W. (1969) Responses of inferior colliculus neurons in the cat to binaural acoustic stimuli having wide-band spectra. *J Neurophysiol*, **32**, 960-974.
- Ghose, K. & Moss, C.F. (2003) The sonar beam pattern of a flying bat as it tracks tethered insects. *J Acoust Soc Am*, **114**, 1120-1131.
- Goodwin, G.G. & Greenhall, A.M. (1961) A review of the bats of Trinidad and Tobago: descriptions, rabies infection and ecology. *Bull Am Mus Nat Hist*, **122**, 187-302.
- Green, D.M. & Swets, J.A. (1966) *Signal detection theory and psychophysics*. Wiley, New York.
- Griffin, D.R., Webster, F.A. & Michael, C.R. (1960) The echolocation of flying insects by bats. *Animal Behaviour*, **8**, 141-154.
- Grinnell, A.D. (1970) Comparative auditory neurophysiology of neotropical bats employing different echolocation signals. *Z Vergl Physiol*, **68**, 117-153.
- Grinnell, A.D. & Griffin, D.R. (1958) The sensitivity of echolocation in bats. *Biol Bull*, **114**, 10-22.
- Grothe, B., Covey, E. & Casseday, J.H. (2001) Medial superior olive of the big brown bat: neuronal responses to pure tones, amplitude modulations, and pulse trains. *J Neurophysiol*, **86**, 2219-2230.
- Grunwald, J.E., Schornich, S. & Wiegrebe, L. (2004) Classification of natural textures in echolocation. *Proc Natl Acad Sci USA*, **101**, 5670-5674.
- Hackel, P. & Esser, K.H. (1998) Classification of single units in the high-frequency fields of the *Carollia* auditory cortex. In Elsner, N. & Wehner, R. (eds), Göttingen Neurobiology Report 1998, Proceedings of the 26th Göttingen Neurobiology Conference. Thieme, Stuttgart, pp. 328.
- Hackett, T.A., Preuss, T.M. & Kaas, J.H. (2001) Architectonic identification of the core region in auditory cortex of macaques, chimpanzees, and humans. *J Comp Neurol*, **441**, 197-222.
- Hackett, T.A., Stepniewska, I. & Kaas, J.H. (1998) Subdivisions of auditory cortex and ipsilateral cortical connections of the parabelt auditory cortex in macaque monkeys. *J Comp Neurol*, **394**, 475-495.
- Haplea, S., Covey, E. & Casseday, J.H. (1994) Frequency tuning and response latencies at three levels in the brainstem of the echolocating bat *Eptesicus fuscus*. *J Comp Physiol A Neuroethol Sens Neural Behav Physiol*, **174**, 671-683.
- Hartmann, W.M. & Pumplin, J. (1988) Noise power fluctuations and the masking of sine signals. *J Acoust Soc Am*, **83**, 2277-2289.
- Haug, F.M. (1973) Heavy metals in the brain. A light microscope study of the rat with Timm's sulphide silver method. Methodological considerations and cytological and regional staining patterns. *Adv Anat Embryol Cell Biol*, **47**, 71.

- Heffner,H.E. & Heffner,R.S. (1990) Effect of bilateral auditory cortex lesions on absolute thresholds in Japanese macaques. *J Neurophysiol*, **64**, 191-205.
- Heffner,R.S., Koay,G. & Heffner,H.E. (2003) Hearing in American leaf-nosed bats. III: *Artibeus jamaicensis*. *Hear Res*, **184**, 113-122.
- Heil,P. (1997) Auditory cortical onset responses revisited. II. Response strength. *J Neurophysiol*, **77**, 2642-2660.
- Heil,P. (1998) Neuronal coding of interaural transient envelope disparities. *Eur J Neurosci*, **10**, 2831-2847.
- Heil,P. & Irvine,D.R. (1998) The posterior field P of cat auditory cortex: coding of envelope transients. *Cereb Cortex*, **8**, 125-141.
- Hewitt,M.J. & Meddis,R. (1994) A computer model of amplitude-modulation sensitivity of single units in the inferior colliculus. *J Acoust Soc Am*, **95**, 2145-2159.
- Hoffmann,S., Baier,L., Borina,F., Schuller,G., Wiegrebe,L. & Firzlaff,U. (2008a) Psychophysical and neurophysiological hearing thresholds in the bat *Phyllostomus discolor*. *J Comp Physiol A Neuroethol Sens Neural Behav Physiol*, **194**, 39-47.
- Hoffmann,S., Firzlaff,U., Radtke-Schuller,S., Schweltnus,B. & Schuller,G. (2008b) The auditory cortex of the bat *Phyllostomus discolor*: Localization and organization of basic response properties. *BMC Neurosci*, **9**, 65.
- Horikawa,J., Tanahashi,A. & Suga,N. (1994) After-discharges in the auditory cortex of the mustached bat: No oscillatory discharges for binding auditory information. *Hear Res*, **76**, 45-52.
- Hübner,M. & Wiegrebe,L. (2003) The effect of temporal structure on rustling-sound detection in the gleaning bat, *Megaderma lyra*. *J Comp Physiol A Neuroethol Sens Neural Behav Physiol*, **189**, 337-346.
- Ingham,N.J., Hart,H.C. & McAlpine,D. (2001) Spatial receptive fields of inferior colliculus neurons to auditory apparent motion in free field. *J Neurophysiol*, **85**, 23-33.
- Irvine,D.R.F., Rajan,R. & Aitkin,L.M. (1996) Sensitivity to interaural intensity differences of neurons in primary auditory cortex of the cat. 1. Types of sensitivity and effects of variations in sound pressure level. *J Neurophysiol*, **75**, 75-96.
- Jen,P.H.S., Chen,Q.C. & Wu,F.J. (2003) Interaction between excitation and inhibition affects frequency tuning curve, response size and latency of neurons in the auditory cortex of the big brown bat, *Eptesicus fuscus*. *Hear Res*, **174**, 281-289.
- Jen,P.H.S., Sun,X. & Lin,P.J.J. (1989) Frequency and space representation in the primary auditory cortex of the frequency modulating bat *Eptesicus fuscus*. *J Comp Physiol A Neuroethol Sens Neural Behav Physiol*, **165**, 1-14.
- Joris,P.X., Schreiner,C.E. & Rees,A. (2004) Neural Processing of Amplitude-Modulated Sounds. *Physiol Rev*, **84**, 541-577.

- Kleiser, A. & Schuller, G. (1995) Responses of collicular neurons to acoustic motion in the horseshoe bat *Rhinolophus rouxi*. *Naturwissenschaften*, **82**, 337-340.
- Klug, A., Khan, A., Burger, R.M., Bauer, E.E., Hurley, L.M., Yang, L., Grothe, B., Halvorsen, M.B. & Park, T.J. (2000) Latency as a function of intensity in auditory neurons: influences of central processing. *Hear Res*, **148**, 107-123.
- Koay, G., Bitter, K.S., Heffner, H.E. & Heffner, R.S. (2002) Hearing in American leaf-nosed bats. I: *Phyllostomus hastatus*. *Hear Res*, **171**, 96-102.
- Koay, G., Heffner, R.S., Bitter, K.S. & Heffner, H.E. (2003) Hearing in American leaf-nosed bats. II: *Carollia perspicillata*. *Hear Res*, **178**, 27-34.
- Kössl, M. (1994) Otoacoustic emissions from the cochlea of the 'constant frequency' bats, *Pteronotus parnellii* and *Rhinolophus rouxi*. *Hear Res*, **72**, 59-72.
- Kössl, M. & Vater, M. (1985) The cochlear frequency map of the mustache bat, *Pteronotus parnellii*. *J Comp Physiol A Neuroethol Sens Neural Behav Physiol*, **157**, 687-697.
- Krishna, B.S. & Semple, M.N. (2000) Auditory temporal processing: responses to sinusoidally amplitude-modulated tones in the inferior colliculus. *J Neurophysiol*, **84**, 255-273.
- Krubitzer, L.A., Calford, M.B. & Schmid, L.M. (1993) Connections of somatosensory cortex in megachiropteran bats: The evolution of cortical fields in mammals. *J Comp Neurol*, **327**, 473-506.
- Krubitzer, L.A., Sesma, M.A. & Kaas, J.H. (1986) Microelectrode maps myeloarchitecture and cortical connections of three somatotopically organized representations of the body surface in the parietal cortex of squirrels. *J Comp Neurol*, **250**, 403-430.
- Kvale, M.N. & Schreiner, C.E. (2004) Short-term adaptation of auditory receptive fields to dynamic stimuli. *J Neurophysiol*, **91**, 604-612.
- Langner, G. (1992) Periodicity coding in the auditory system. *Hear Res*, **60**, 115-142.
- Lawrence, B.D. & Simmons, J.A. (1982) Echolocation in bats: The external ear and perception of the vertical position of targets. *Science*, **218**, 481-483.
- Liang, L., Lu, T. & Wang, X. (2002) Neural Representations of Sinusoidal Amplitude and Frequency Modulations in the Primary Auditory Cortex of Awake Primates. *J Neurophysiol*, **87**, 2237-2261.
- Lippe, W.R. (1986) Recent developments in cochlear physiology. *Ear Hear*, **7**, 233-239.
- Long, G.R. & Schnitzler, H.U. (1975) Behavioural audiograms from the bat, *Rhinolophus ferrumequinum*. *J Comp Physiol A Neuroethol Sens Neural Behav Physiol*, **100**, 211-219.
- Lu, T., Liang, L. & Wang, X. (2001) Temporal and rate representations of time-varying signals in the auditory cortex of awake primates. *Nature Neurosci*, **4**, 1131-1138.

- Lu, T. & Wang, X. (2004) Information Content of Auditory Cortical Responses to Time-Varying Acoustic Stimuli. *J Neurophysiol*, **91**, 301-313.
- McDaniel, V.R. (1976) Brain anatomy. In Baker, R.J., Jones, J.K. & Carter, D.C. (eds), *Biology of Bats of the New World Family Phyllostomatidae, Part I*. Texas Tech Press, Lubbock, pp. 147-199.
- Medvedev, A.V. & Kanwal, J.S. (2008) Communication call-evoked gamma-band activity in the auditory cortex of awake bats is modified by complex acoustic features. *Brain Res*, **1188**, 76-86.
- Mendelson, J.R., Schreiner, C.E. & Sutter, M.L. (1997) Functional topography of cat primary auditory cortex: response latencies. *J Comp Physiol A Neuroethol Sens Neural Behav Physiol*, **181**, 615-633.
- Metzner, W. & Radtke-Schuller, S. (1987) The nuclei of the lateral lemniscus in the rufous horseshoe bat, *Rhinolophus rouxi*. *J Comp Physiol A Neuroethol Sens Neural Behav Physiol*, **160**, 395-411.
- Mittmann, D.H. & Wenstrup, J.J. (1995) Combination-sensitive neurons in the inferior colliculus. *Hear Res*, **90**, 185-191.
- Moss, C.F. & Surlykke, A. (2001) Auditory scene analysis by echolocation in bats. *J Acoust Soc Am*, **110**, 2207-2226.
- Movshon, J.A. & Newsome, W.T. (1996) Visual response properties of striate cortical neurons projecting to area MT in macaque monkeys. *J Neurosci*, **16**, 7733-7741.
- Muller, R. & Kuc, R. (2000) Foliage echoes: a probe into the ecological acoustics of bat echolocation. *J Acoust Soc Am*, **108**, 836-845.
- Nataraj, K. & Wenstrup, J.J. (2005) Roles of inhibition in creating complex auditory responses in the inferior colliculus: facilitated combination-sensitive neurons. *J Neurophysiol*, **93**, 3294-3312.
- Nelken, I. (2008) Processing of complex sounds in the auditory system. *Curr Opin Neurobiol*, **18**, 413-417.
- Nelken, I. (2004) Processing of complex stimuli and natural scenes in the auditory cortex. *Curr Opin Neurobiol*, **14**, 474-480.
- Nelken, I. & Bar-Yosef, O. (2008) Neurons and objects: the case of auditory cortex. *Front Neurosci*, **2**, 107-113.
- Neuweiler, G. (1990) Auditory adaptations for prey capture in echolocating bats. *Physiol Rev*, **70**, 615-641.
- O'Neil, W.E. & Suga, N. (1979) Target range-sensitive neurons in the auditory cortex of the mustache bat. *Science*, **203**, 69-73.

- O'Neill, W.E. (1995) The bat auditory cortex. In Popper, A.N. & Fay, R.R. (eds), *Hearing by bats*. Springer-Verlag, New York, pp. 416.
- O'Neill, W.E. & Suga, N. (1982) Encoding of target range and its representation in the auditory cortex of the mustached bat. *J Neurosci*, **2**, 17-31.
- Ohlemiller, K.K. & Siegel, J.H. (1994) Cochlear basal and apical differences reflected in the effects of cooling on responses of single auditory nerve fibers. *Hear Res*, **80**, 174-190.
- Olsen, J.F. & Suga, N. (1991a) Combination-sensitive neurons in the medial geniculate body of the mustached bat: Encoding of relative velocity information. *J Neurophysiol*, **65**, 1254-1274.
- Olsen, J.F. & Suga, N. (1991b) Combination-sensitive neurons in the medial geniculate body of the mustached bat: Encoding of target range information. *J Neurophysiol*, **65**, 1275-1296.
- Ostwald, J. (1984) Tonotopical organization and pure tone response characteristics of single units in the auditory cortex of the greater horseshoe bat. *J Comp Physiol A Neuroethol Sens Neural Behav Physiol*, **155**, 821-834.
- Pandya, D.N. & Sanides, F. (1973) Architectonic parcellation of the temporal operculum in rhesus monkey and its projection pattern. *Z Anat Entwicklungsgesch*, **139**, 127-161.
- Paschal, W.G. & Wong, D. (1994) Frequency organization of delay-sensitive neurons in the auditory cortex of the FM bat *Myotis lucifugus*. *J Neurophysiol*, **72**, 366-379.
- Pearson, J.M., Crocker, W.D. & Fitzpatrick, D.C. (2007) Connections of functional areas in the mustached bat's auditory cortex with the auditory thalamus. *J Comp Neurol*, **500**, 401-418.
- Perez-Clausell, J. (1996) Distribution of terminal fields stained for zinc in the neocortex of the rat. *J Chem Neuroanat*, **11**, 99-111.
- Pollak, G.D. & Schuller, G. (1981) Tonotopic organization and encoding features of single units in inferior colliculus of horseshoe bats: Functional implications for prey identification. *J Neurophysiol*, **45**, 208-226.
- Radtke-Schuller, S. (2001) Neuroarchitecture of the auditory cortex in the rufous horseshoe bat (*Rhinolophus rouxi*). *Anat Embryol (Berl)*, **204**, 81-100.
- Radtke-Schuller, S. (2004) Cytoarchitecture of the medial geniculate body and thalamic projections to the auditory cortex in the rufous horseshoe bat (*Rhinolophus rouxi*). I. Temporal fields. *Anat Embryol (Berl)*, **209**, 59-76.
- Radtke-Schuller, S. & Schuller, G. (1995) Auditory cortex of the rufous horseshoe bat. 1. Physiological response properties to acoustic stimuli and vocalizations and the topographical distribution of neurons. *Eur J Neurosci*, **7**, 570-591.
- Radtke-Schuller, S., Schuller, G. & O'Neill, W.E. (2004) Thalamic projections to the auditory cortex in the rufous horseshoe bat (*Rhinolophus rouxi*). II. Dorsal fields. *Anat Embryol (Berl)*, **209**, 77-91.

- Rauschecker, J.P. & Tian, B. (2000) Mechanisms and streams for processing of "what" and "where" in auditory cortex. *PNAS*, **97**, 11800-11806.
- Rauschecker, J.P., Tian, B., Pons, T. & Mishkin, M. (1997) Serial and parallel processing in rhesus monkey auditory cortex. *J Comp Neurol*, **382**, 89-103.
- Razak, K.A. & Fuzessery, Z.M. (2002) Functional organization of the pallid bat auditory cortex: emphasis on binaural organization. *J Neurophysiol*, **87**, 72-86.
- Razak, K.A., Richardson, M.D. & Fuzessery, Z.M. (2008) Experience is required for the maintenance and refinement of FM sweep selectivity in the developing auditory cortex. *Proc Natl Acad Sci USA*, **105**, 4465-4470.
- Razak, K.A., Shen, W., Zumsteg, T. & Fuzessery, Z.M. (2007) Parallel thalamocortical pathways for echolocation and passive sound localization in a gleaning bat, *Antrozous pallidus*. *J Comp Neurol*, **500**, 322-338.
- Reale, R.A. & Imig, T.J. (1980) Tonotopic organization in auditory cortex of the cat. *J Comp Neurol*, **192**, 265-291.
- Reimer, K. (1991) Auditory properties of the superior colliculus in the horseshoe bat, *Rhinolophus rouxi*. *J Comp Physiol A Neuroethol Sens Neural Behav Physiol*, **169**, 719-728.
- Rennaker, R.L., Carey, H.L., Anderson, S.E., Sloan, A.M. & Kilgard, M.P. (2007) Anesthesia suppresses nonsynchronous responses to repetitive broadband stimuli. *Neuroscience*, **145**, 357-369.
- Rinne, T., Balk, M.H., Koistinen, S., Autti, T., Alho, K. & Sams, M. (2008) Auditory selective attention modulates activation of human inferior colliculus. *J Neurophysiol*, **100**, 3323-3327.
- Riquimaroux, H., Gaioni, S.J. & Suga, N. (1991) Cortical computational maps control auditory perception. *Science*, **251**, 565-568.
- Riquimaroux, H., Gaioni, S.J. & Suga, N. (1992) Inactivation of the DSCF area of the auditory cortex with muscimol disrupts frequency discrimination in the mustached bat. *J Neurophysiol*, **68**, 1613-1623.
- Romanski, L.M., Tian, B., Fritz, J., Mishkin, M., Goldman-Rakic, P.S. & Rauschecker, J.P. (1999) Dual streams of auditory afferents target multiple domains in the primate prefrontal cortex. *Nature Neurosci*, **2**, 1131-1136.
- Ross, L.S., Pollak, G.D. & Zook, J.M. (1988) Origin of ascending projections to an isofrequency region of the mustache bat's inferior colliculus. *J Comp Neurol*, **270**, 488-505.
- Rother, G. & Schmidt, U. (1982) Der Einfluß visueller Information auf die Echoortung bei *Phyllostomus discolor* (Chiroptera). *Säugetierkunde*, **47**, 324-334.

- Rübsamen,R., Neuweiler,G. & Sripathi,K. (1988) Comparative collicular tonotopy in two bat species adapted to movement detection, *Hipposideros speoris* and *Megaderma lyra*. *J Comp Physiol A Neuroethol Sens Neural Behav Physiol*, **163**, 271-285.
- Sanchez,J.T., Gans,D. & Wenstrup,J.J. (2008) Glycinergic "inhibition" mediates selective excitatory responses to combinations of sounds. *J Neurosci*, **28**, 80-90.
- Schlegel,P.A. (2002) Encoding of sound motion by binaural brainstem units in a horseshoe bat. *Neurosci Res*, **43**, 343-362.
- Schreiner,C.E. & Urbas,J.V. (1988) Representation of amplitude modulation in the auditory cortex of the cat. 2. Comparison between cortical fields. *Hear Res*, **32**, 49-64.
- Schuchmann,M., Hübner,M. & Wiegrebe,L. (2006) The absence of spatial echo suppression in the echolocating bats *Megaderma lyra* and *Phyllostomus discolor*. *J Exp Biol*, **209**, 152-157.
- Schuller,G. (1997) A cheap earphone for small animals with good frequency response in the ultrasonic frequency range. *J Neurosci Meth*, **71**, 187-190.
- Schuller,G., O'Neill,W.E. & Radtke-Schuller,S. (1991) Facilitation and delay sensitivity of auditory cortex neurons in CF-FM bats, *Rhinolophus rouxi* and *Pteronotus p. parnellii*. *Eur J Neurosci*, **3**, 1165-1181.
- Schuller,G. & Pollak,G. (1979) Disproportionate frequency representation in the inferior colliculus of Doppler-compensating greater horseshoe bats: Evidence for an acoustic fovea. *J Comp Physiol A Neuroethol Sens Neural Behav Physiol*, **132**, 47-54.
- Schuller,G., Radtke-Schuller,S. & Betz,M. (1986) A stereotaxic method for small animals using experimentally determined reference profiles. *J Neurosci Meth*, **18**, 339-350.
- Schuller,G. (1984) Natural ultrasonic echoes from wing beating insects are encoded by collicular neurons in the CF-FM bat, *Rhinolophus ferrumequinum*. *J Comp Physiol A Neuroethol Sens Neural Behav Physiol*, **155**, 121-128.
- Selezneva,E., Scheich,H. & Brosch,M. (2006) Dual time scales for categorical decision making in auditory cortex. *Curr Biol*, **16**, 2428-2433.
- Sendowski,I., Raffin,F. & Clarencon,D. (2006) Spectrum of neural electrical activity in guinea pig cochlea: effects of anaesthesia regimen, body temperature and ambient noise. *Hear Res*, **211**, 63-73.
- Seshagiri,C.V. & Delgutte,B. (2007) Response properties of neighboring neurons in the auditory midbrain for pure-tone stimulation: a tetrode study. *J Neurophysiol*, **98**, 2058-2073.
- Simmons,J.A., Brock Fenton,M. & O'Farrell,M.J. (1979) Echolocation and pursuit of prey by bats. *Science*, **203**, 16-21.
- Smith,A.L., Parsons,C.H., Lanyon,R.G., Bizley,J.K., Akerman,C.J., Baker,G.E., Dempster,A.C., Thompson,I.D. & King,A.J. (2004) An investigation of the role of auditory

- cortex in sound localization using muscimol-releasing Elvax. *Eur J Neurosci*, **19**, 3059-3072.
- Sovijärvi, A.R.A. & Hyvärinen, J. (1974) Auditory cortical neurons in the cat sensitive to the direction of sound source movement. *Brain Res*, **73**, 455-471.
- Sterbing, S.J., Schmidt, U. & Rübsamen, R. (1994) The postnatal development of frequency-place code and tuning characteristics in the auditory midbrain of the phyllostomid bat, *Carollia perspicillata*. *Hear Res*, **76**, 133-146.
- Stilz, W.P. (2004) *Akustische Untersuchungen zur Echoortung bei Fledermäusen*. PhD Thesis, University of Tuebingen.
- Suga, N. (1989) Principles of auditory information-processing derived from neuroethology. *J Exp Biol*, **146**, 277-286.
- Suga, N. (1990) Cortical computational maps for auditory imaging. *Neural Networks*, **3**, 3-21.
- Suga, N. & Horikawa, J. (1986) Multiple time axes for representation of echo delays in the auditory cortex of the mustached bat. *J Neurophysiol*, **55**, 776-805.
- Suga, N. & Jen, P.H.S. (1976) Disproportionate tonotopic representation for processing CF-FM sonar signals in the mustache bat auditory cortex. *Science*, **194**, 542-544.
- Suga, N., Kawasaki, M. & Burkhard, R.F. (1990) Delay-tuned neurons in auditory cortex of mustached bat are not suited for processing directional information. *J Neurophysiol*, **64**, 225-235.
- Suga, N., Niwa, H., Taniguchi, I. & Margoliash, D. (1987) The personalized auditory cortex of the mustached bat: Adaptation for echolocation. *J Neurophysiol*, **58**, 643-654.
- Suga, N., O'Neill, W.E. & Manabe, T. (1978) Cortical neurons sensitive to combinations of information-bearing elements of biosonar signals in the mustache bat. *Science*, **200**, 778-781.
- Sullivan, W.E. (1982) Neural representation of target distance in auditory cortex of the echolocating bat *Myotis lucifugus*. *J Neurophysiol*, **48**, 1011-1032.
- Sutter, M.L. (2000) Shapes and level tolerances of frequency tuning curves in primary auditory cortex: quantitative measures and population codes. *J Neurophysiol*, **84**, 1012-1025.
- Syka, J., Suta, D. & Popelar, J. (2005) Responses to species-specific vocalizations in the auditory cortex of awake and anesthetized guinea pigs. *Hear Res*, **206**, 177-184.
- Tanaka, H., Wong, D. & Taniguchi, I. (1992) The influence of stimulus duration on the delay tuning of cortical neurons in the FM bat, *Myotis lucifugus*. *J Comp Physiol A Neuroethol Sens Neural Behav Physiol*, **171**, 29-40.

- Thomas,H., Tillein,J., Heil,P. & Scheich,H. (1993) Functional organization of auditory cortex in the Mongolian gerbil (*Meriones unguiculatus*). 1. Electrophysiological mapping of frequency representation and distinction of fields. *Eur J Neurosci*, **5**, 882-897.
- Vallee,B.L. & Falchuk,K.H. (1993) The biochemical basis of zinc physiology. *Physiol Rev*, **73**, 79-118.
- Vater,M., Feng,A.S. & Betz,M. (1985) An HRP-study of the frequency-place map of the horseshoe bat cochlea: morphological correlates of the sharp tuning to a narrow frequency band. *J Comp Physiol A Neuroethol Sens Neural Behav Physiol*, **157**, 671-686.
- von Helversen,D. (2004) Object classification by echolocation in nectar feeding bats: size-independent generalization of shape. *J Comp Physiol A Neuroethol Sens Neural Behav Physiol*, **190**, 515-521.
- Wagner,H. & Takahashi,T. (1990) Neurons in the midbrain of the barn owl are sensitive to the direction of apparent acoustic motion. *Naturwissenschaften*, **77**, 439-442.
- Wakefield,G.H. & Viemeister,N.F. (1990) Discrimination of modulation depth of sinusoidal amplitude modulation (SAM) noise. *J Acoust Soc Am*, **88**, 1367-1373.
- Wallace,M.N., Kitzes,L.M. & Jones,E.G. (1991) Chemoarchitectonic organization of the cat primary auditory cortex. *Exp Brain Res*, **86**, 518-526.
- Washington,S.D. & Kanwal,J.S. (2008) DSCF Neurons Within the Primary Auditory Cortex of the Mustached Bat Process Frequency Modulations Present Within Social Calls. *J Neurophysiol*, **100**, 3285-3304.
- Wehr,M. & Zador,A.M. (2005) Synaptic mechanisms of forward suppression in rat auditory cortex. *Neuron*, **47**, 437-445.
- Wenstrup,J.J. (1999) Frequency organization and responses to complex sounds in the medial geniculate body of the mustached bat. *J Neurophysiol*, 2528-2544.
- Wenstrup,J.J. & Grose,C.D. (1995) Inputs to combination-sensitive neurons in the medial geniculate body of the mustached bat: The missing fundamental. *J Neurosci*, **15**, 4693-4711.
- Wenstrup,J.J., Mittmann,D.H. & Grose,C.D. (1999) Inputs to combination-sensitive neurons of the inferior colliculus. *J Comp Neurol*, **409**, 509-528.
- Wilson,W.W. & O'Neill,W.E. (1998) Auditory motion induces directionally dependent receptive field shifts in inferior colliculus neurons. *J Neurophysiol*, **79**, 2040-2062.
- Winer,J.A., Miller,L.M., Lee,C.C. & Schreiner,C.E. (2005) Auditory thalamocortical transformation: structure and function. *Trends Neurosci*, **28**, 255-263.
- Wittekindt,A., Drexler,M. & Kössl,M. (2005) Cochlear sensitivity in the lesser spear-nosed bat, *Phyllostomus discolor*. *J Comp Physiol A Neuroethol Sens Neural Behav Physiol*, **191**, 31-36.

- Wong,D. & Shannon,S.L. (1988) Functional zones in the auditory cortex of the echolocating bat, *Myotis lucifugus*. *Brain Res*, **453**, 349-352.
- Wotton,J.M., Haresign,T. & Simmons,J.A. (1995) Spatially dependent acoustic cues generated by the external ear of the big brown bat *Eptesicus fuscus*. *J Acoust Soc Am*, **98**, 1423-1445.
- Wotton,J.M. & Simmons,J.A. (2000) Spectral cues and perception of the vertical position of targets by the big brown bat, *Eptesicus fuscus*. *J Acoust Soc Am*, **107**, 1034-1041.
- Wu,M.I. & Jen,P.H.S. (1996) Temporally patterned pulse trains affect directional sensitivity of inferior collicular neurons of the big brown bat, *Eptesicus fuscus*. *J Comp Neurol*, **179**, 385-393.
- Zeki,S. (1983) Colour coding in the cerebral cortex: the reaction of cells in the monkey. *Neurosci*, **9**, 741-765.
- Zhou,X. & Jen,P.H.S. (2002) The effect of sound duration on rate-amplitude functions of inferior collicular neurons in the big brown bat, *Eptesicus fuscus*. *Hear Res*, **166**, 124-135.
- Zilles,K., Wree,A. & Dausch,N.D. (1990) Anatomy of the neocortex: neurochemical organization. In Kolb,B. & Tees,R.C. (eds), *The Cerebral Cortex of the Rat*. The MIT Press, Cambridge (MA), pp. 113.
- Zook,J.M. & Leake,P.A. (1989) Connections and frequency representation in the auditory brainstem of the mustache bat, *Pteronotus parnellii*. *J Comp Neurol*, **290**, 243-261.
- Zook,J.M., Winer,J.A., Pollak,G.D. & Bodenhamer,R.D. (1985) Topology of the central nucleus of the mustache bat's inferior colliculus. *J Comp Neurol*, **231**, 530-546.
- Zwicker,E. & Fastl,A. (1990) *Psychoacoustics. Facts and Models*. Springer, Berlin, Heidelberg, New York.

List of abbreviations

0E	ipsilateral excitation
2-DG	2-deoxy-d-glucose
2AFC	two-alternative forced-choice
3AFC	three-alternative forced-choice
Δ IID	change in interaural intensity difference
A/D	analog/digital
AI	primary auditory cortex
AAF	anterior auditory field
ABI	averaged binaural intensity
AC	auditory cortex
ACHe	acetylcholinesterase
ADF	anterior dorsal field
AFN	Antisedan/Flumazenil/Naloxon
AVF	anterior ventral field
BF	best frequency
CF	constant frequency
D/A	digital/analog
DAP	data acquisition processor
DPOAE	distortion product otoacoustic emission
DR	response to dynamic stimulation
DSCF	doppler-shifted constant frequency
E0	contralateral excitation
EE	excitatory/excitatory
EI	excitatory/inhibitory
FM	frequency modulated
FRA	frequency response area
GABA	gamma-aminobutyric acid
GABA _A	gamma-aminobutyric acid A receptor
HRP	horseradish peroxidase
IC	inferior colliculus
IID	interaural intensity difference
InI	interaction index
IPI	inter pulse interval
IR	impulse response

ISI	inter stimulus interval
M4	fourth moment
MGB	medial geniculate body
MGB _d	dorsal nucleus of the medial geniculate body
MGB _v	ventral nucleus of the medial geniculate body
MMF	Medetomidin/Midazolam/Fentanyl
NaCl	Sodium chloride
PDF	posterior dorsal field
PSTH	peri-stimulus time histogram
PVF	posterior ventral field
PVFBz	border zone of the posterior ventral field
PVFD	dorsal subfield of the posterior ventral field
PVfv	ventral subfield of the posterior ventral field
Q _{10dB}	quality factor 10dB above threshold
Q _{30dB}	quality factor 30dB above threshold
ROC	receiver operating characteristics
SAM	sinusoidal amplitude modulation
SE	standard error
SPL	sound pressure level
SR	response to static stimulation
WGA-HRP	wheat germ agglutinin conjugated to horseradish peroxidase

List of figures

Fig. 1.1 Schematic drawing of the 3AFC setup used for the psychophysical experiments. _____	8
Fig. 1.2 Behavioral audiogram of <i>P. discolor</i> . _____	12
Fig. 1.3 Auditory thresholds of IC and AC units. _____	13
Fig. 1.4 Behavioral audiogram, neural audiogram of cortical units, neural audiogram of collicular units and DPOAE threshold curve of <i>P. discolor</i> . _____	15
Fig. 1.5 Neural audiograms for three species of Phyllostomidae. _____	17
Fig. 1.6 Behavioral audiograms for four species of phyllostomid bats. _____	19
Fig. 2.1 Recording sites and subfields in the auditory cortex of <i>Phyllostomus discolor</i> . _____	24
Fig. 2.2 Frontal sections at two rostro-caudal levels. _____	27
Fig. 2.3 Cut-outs of frontal sections from the centers of the different cortical fields. _____	28
Fig. 2.4 Distribution of response properties of cortical units and examples of PSTHs for different response types. _____	30
Fig. 2.5 Examples of the six different FRA types of cortical units. _____	31
Fig. 2.6 Spatial representation of response properties on the flattened cortical surface and statistical comparison between the four cortical fields. _____	34
Fig. 2.7 Spatial representation of FRA types and binaural response types and distribution in different cortical subfields. _____	35
Fig. 3.1 Results of the psychophysical experiments. _____	52
Fig. 3.2 Electrophysiological results. _____	53
Fig. 3.3 Examples from the stimulus set for the psychophysical and neurophysiological experiments in <i>P. discolor</i> . _____	54
Fig. 3.4 Comparison of the regression lines of response strength calculated for roughness-sensitive units and nonsensitive units. _____	55
Fig. 3.5 Location of recording sites in the auditory cortex of <i>P. discolor</i> . _____	56
Fig. 3.6 Comparison of the psychophysical and neurophysiological roughness discrimination performance. _____	57
Fig. 3.7 Envelope magnitude spectra of echo stimuli presented in the neurophysiological experiments. _____	60
Fig. 3.8 Ideal-observer performance for roughness discrimination as a function of the number of pooled unit responses. _____	61

Fig. 4.1 Schematic of a sequence of three two-tone stimuli representing three different azimuthal movements. _____	67
Fig. 4.2 Schematic of the 9x9 stimulus matrix. _____	69
Fig. 4.3 Schematic representation of the analysis procedure of the responses to two-tone stimulation. _____	72
Fig. 4.4 Distribution of interaction indices. _____	73
Fig. 4.5 PSTHs and dot raster plots of a motion insensitive unit for four different IPI steps. _____	75
Fig. 4.6 Static response area, reference matrix, response matrices of signal 2 and interaction matrices of the motion insensitive unit in Fig. 4.5. _____	76
Fig. 4.7 PSTHs and dot raster plots of a motion sensitive unit for four different IPI steps. _____	79
Fig. 4.8 Static response area, reference matrix, response matrices of signal 2 and interaction matrices of the motion sensitive unit in Fig. 4.7. _____	80
Fig. 4.9 Static response areas, response matrices of signal 2 of three motion sensitive units for different IPI steps. _____	81
Fig. 4.10 Location of recording sites and cortical representation of motion sensitivity. _____	83
Fig. 4.11 Distribution of best frequency, threshold, latency, duration, binaural response type, best IPI and azimuthal start and end position, respectively, of the best stimulus at best IPI for motion sensitive and insensitive units. _____	85

Lebenslauf

Name : Susanne Hoffmann, Dipl. - Biol.

Geburtstag: 19.12.1977

Geburtsort: Havelberg

Staatsangehörigkeit: deutsch

Familienstand: ledig

Werdegang:

1984 – 1992 Sekundarschule, Schollene

1992 – 1996 Pestalozzi-Gymnasium, Havelberg
Abschluss: Abitur (Note: 2,1)

1996 – 1997 Praktikum: Altstädtische Apotheke, Rathenow

SS 97 – WS 98/99 Studium der Pharmazie: Humboldt – Universität zu Berlin,
Exmatrikulation erfolgte auf eigenen Antrag

WS 98/99 – SS 99 Studium der Biologie: Friedrich – Alexander – Universität,
Erlangen

SS 99 – SS 05 Studium der Biologie: Ludwig – Maximilians – Universität,
München
Hauptfach: Neurobiologie
Nebenfächer: systematische Botanik, Psychologie, Zoologie
Diplomarbeit: “The auditory cortex of the neotropical FM-bat
Phyllostomus discolor: Spatial distribution of
neuronal response properties to pure tone stimuli”
Abschluss: Diplom (Note: 1,2)

11.2005 – 11.2007 Doktorandenstipendium, Graduiertenkolleg 1091
Doktorarbeit: „Acoustic scene and its dynamic representation in
neuronal activity in the auditory cortex“, Ludwig – Maximilians
Universität, Department Biologie II, Abteilung Neurobiologie

seit 01.01.2008 angestellt als Doktorandin an der Ludwig – Maximilians
Universität in München, Department Biologie II, Abteilung
Neurobiologie

Studienbegleitende Tätigkeiten:

- 01.09.1997 – 30.09.1997 Famulatur: Goetheplatz – Apotheke, München
20.02.1998 – 27.03.1998 Empfangssekretärin, PPE Personaldienstleistung:
Computer 2000, München
- 01.11.1998 – 31.01.2003 Verkaufskraft, Foto Steinberg OHG, München
01.10.2000 – 31.01.2003 Teamleiterin, Foto Steinberg OHG, München
- 01.05.2003 – 31.09.2004 studentische Hilfskraft, Max-Planck-Institut für Neurobiologie,
München
- 01.11.2004 – 30.04.2005 studentische Hilfskraft, Klinikum der LMU München: Abteilung
neurologische Forschung, München
- 01.04.2005 – 30.04.2005 studentische Hilfskraft, Biozentrum der LMU München,
München

Publikationen:

- Firzlaff,U., Schörnich,S., Hoffmann,S., Schuller,G. and
Wiegrebe,L. (2006) „*A neural correlate of stochastic echo
imaging*” J Neurosci 26(3):785-91
- Hoffmann,S., Baier,L., Borina,F., Schuller,G., Wiegrebe,L.,
Firzlaff,U. (2008) “*Psychophysical and neurophysiological
hearing thresholds in the bat Phyllostomus discolor.*” J Comp
Physiol A: Neuroethology, Sensory, Neural, and Behavioral
Physiology 194:39-47
- Hoffmann,S., Firzlaff,U., Radtke-Schuller,S., Schwellnus,B. and
Schuller,G. (2008) „*The auditory cortex of the bat Phyllostomus
discolor: Localization and organization of basic response
properties.*“ BMC Neurosci 9:65

Lehre:

Betreuung des Fortgeschrittenenpraktikums Neurobiologie:
„Neurophysiologie im Hörsystem von Säugern“

Techniken:

Genotypisierung transgener Mäuse, PCR, Kleintierhaltung,
elektrophysiologische Ableitung von Einzel- und
Summenpotentialen in vivo, invasive Operationsmethoden am
Kleintier, Verwendung von Injektionsanästhetika, Stereotaxie,
histologische Aufarbeitung von Gehirnschnitten,
Versuchstierpflege

EDV – Kenntnisse:

Anwendungssicher: MS Windows 98, 2000, NT und XP,
MS Office, Adobe Photoshop, SigGen Solutions Brainware,
Mathworks MatLab

Sprachkenntnisse:

Englisch fließend in Wort und Schrift,
Grundkenntnisse: Russisch, Französisch

Danksagung

Als erstes möchte ich mich bei Prof. Dr. Gerd Schuller für die freundliche Aufnahme in seine Arbeitsgruppe, die Überlassung des interessanten Themas, die Bereitstellung der experimentellen Geräte, das Korrekturlesen unzähliger Versionen der Veröffentlichungen und das ständige Interesse an meiner Arbeit bedanken.

Nicht weniger dankbar bin ich Dr. Uwe Firzlaff für die Unterstützung während der Planung und Durchführung der Experimente, für die Hilfestellung bei der Programmierung der Auswertprogramme, für das Mitwirken beim Schreiben der Veröffentlichungen und für viele problemlösende Gespräche. Dank ihm wurde mir auch auf wissenschaftlichen Tagungen nie langweilig.

Des Weiteren möchte ich allen Mitgliedern der Arbeitsgruppe von Lutz Wiegrebe für das geduldige Zuhören bei Präsentationen meiner fremdartigen physiologischen Daten und die Lösungsvorschläge bei aufgetretenen Problemen danken. Sven, dir sei besonders für die Hilfe gedankt, meinem Computer seine Macken abzugewöhnen.

Silvana Siebert möchte ich für viele unterhaltsame Gespräche und Tipps im Umgang mit *Phyllostomus* danken.

Als nächstes danke ich den Mitautoren der in dieser Arbeit erwähnten Veröffentlichungen für die gute Zusammenarbeit.

Bei Claudia Aerdker möchte ich mich für die Hilfe im Histologielabor und bei Horst König für die Hilfe bei technischen Problemen bedanken.

Der Deutschen Forschungsgemeinschaft danke ich für die finanzielle Unterstützung dieser Arbeit. Besonderer Dank gilt in der Hinsicht auch Prof. Dr. Ulrich Büttner und Dr. Isolde von Bülow.

Am meisten dankbar bin ich jedoch meiner Familie und meinen Freunden für die jahrelange Unterstützung. Dank gilt allen voran meinem Opa, der mein Interesse für die Biologie schon im zarten Alter von 3 Jahren weckte, meinen Eltern dafür, dass sie immer für mich da sind, und natürlich meinem Freund Udo, der mich ständig daran erinnert, dass es neben der Arbeit auch noch ein Privatleben gibt.

Ehrenwörtliche Erklärung

Diese Arbeit wurde von mir selbständig und nur unter Verwendung der angegebenen Hilfsmittel angefertigt.

Baierbrunn, den _____

Unterschrift